PNNL-14325

Pacific Northwest
National Laboratory
Operated by Battelle for the
U.S. Department of Energy

The Influence of Glass Leachate on the Hydraulic, Physical, Mineralogical and Sorptive Properties of Hanford Sediment

D. I. Kaplan
R. J. Serne
H. T. Schaef
C. W. Lindenmeier
K. E. Parker
A. T. Owen
D. E. McCready
J. S. Young

July 2003

Prepared for CH2M HILL Hanford Group, Inc., and
the U.S. Department of Energy
under Contract DE-AC06-76RL01830

PACIFIC NORTHWEST NATIONAL LABORATORY
operated by
BATTELLE
for the
UNITED STATES DEPARTMENT OF ENERGY
under Contract DE-AC06-76RL01830

The Influence of Glass Leachate on the Hydraulic, Physical, Mineralogical and Sorptive Properties of Hanford Sediment

D. I. Kaplan[(a)]
R. J. Serne[(b)]
H. T. Schaef[(b)]
C. W. Lindenmeier[(b)]
K. E. Parker[(b)]
A. T. Owen[(b)]
D. E. McCready[(b)]
J. S. Young[(b)]

July 2003

Prepared for
the U.S. Department of Energy
under Contract DE-AC06-76RLO 1830

Pacific Northwest National Laboratory
Richland, Washington 99352

(a) Westinghouse Savannah River Company, Aiken, SC 29808.
(b) Pacific Northwest National Laboratory, Richland, WA 99352.

Abstract

The immobilized low activity waste (ILAW) generated from the Hanford Site will be disposed of in a vitrified form. It is expected that leachate from the vitrified waste will have a high pH and high ionic strength. The objective of this study was to determine the influence of glass leachate on the hydraulic, physical, mineralogical, and sorptive properties of Hanford sediments. Our approach was to put solutions of NaOH, a simplified surrogate for glass leachate, in contact with quartz sand, a simplified surrogate for the Hanford subsurface sediment, and Warden soil, an actual Hanford sediment. Following contact with three different concentrations of NaOH solutions, changes in hydraulic conductivity, porosity, moisture retention, mineralogy, aqueous chemistry, and soil-radionuclide distribution coefficients were determined.

Under chemical conditions approaching the most caustic glass leachate conditions predicted in the near field of the ILAW disposal site, approximated by 0.3 M NaOH, significant changes in mineralogy were observed. The clay minerals of the Hanford sediment evidenced the greatest dissolution thereby increasing the relative proportions of the more resistant minerals, e.g., quartz, feldspar, and calcite, in the remaining mass. Some re-precipitation of solids (mostly amorphous gels) was observed after caustic contact with both solids; these precipitates increased the moisture retention in both sediments, likely because of water retained within the gel coatings. The hydraulic conductivities were slightly lower, but because of experimental artifacts, these reductions should not be considered significant. Thus, there does not seem to be large differences in the hydraulic properties of the quartz sand or Warden silt loam soil after 192 days of contact with caustic fluids similar to glass leachate. The long-term projected impact of the increased moisture retention has not been evaluated but likely will not make past simplified performance projections invalid.

Despite the fact that some clay minerals, such as smectites and kaolinite, almost totally dissolved within a year of contact with 3.0 M NaOH (and by inference after longer time frames for 0.3 M NaOH, a more realistic surrogate for ILAW glass leachate) other sorbing minerals such as illite and chlorite do not appreciably react. The net result on sorption of common and risk-relevant mobile radionuclides is not expected to be significant. Specifically, little change in Cs K_d values and a significant increase in Sr K_d values were measured in the simulated glass leachates versus natural groundwater. The difference in the sorptive responses of the radionuclides was attributed to differences in sorption mechanisms (Cs sorbs strongly to high-energy sites, whereas Sr sorbs primarily by cation exchange but also is sensitive to pH-mediated precipitation reactions). Caustic-treated sediments contacted with NaOH solutions radiotraced with Sr exhibited high K_d's likely because of precipitation with $CaCO_3$. In caustic solutions, there was no appreciable adsorption for the three anions I^-, SeO_4^{2-}, or TcO_4^-. In the "far field" vadose zone in past performance projections, some sorption has been allowed for selenate. Even if the caustic glass leachate completely dominates the entire vadose zone below the repository, such that there will be no sorption of selenate, the dilution and pH neutralization that will occur in the upper unconfined aquifer will allow selenate adsorption to occur onto the aquifer sediments. It is recommended that a future performance assessment sensitivity run be performed to address this point.

Executive Summary

The immobilized low activity waste (ILAW) generated from the Hanford Site will be disposed of in a vitrified form. It is expected that leachate from the vitrified waste will have a high pH and high ionic strength. Such solutions dissolve silicate minerals and may have significant effects on radionuclide sorption to subsurface materials. Further, the caustic, high-salt leachate could impact the hydrology, mineralogy, radionuclide geochemistry, and physical properties of the near-field geologic phases surrounding the disposal trench. Collectively, these processes could greatly impact radionuclide mobility and thus the performance assessment of the disposal site.

The objective of this study was to determine the influence of glass leachate on the hydraulic, physical, mineralogical, and sorptive properties of Hanford sediments. Our approach was to put solutions of sodium hydroxide [NaOH], a simplified surrogate for glass leachate, in contact with quartz sand, a simplified surrogate for the Hanford subsurface sediment, and Warden soil, an actual Hanford sediment. Two studies were conducted: a column study consisting of a quartz sand experiment and a Warden soil experiment, and a batch sorption study with Warden soil. Following contact with three NaOH solutions of varying concentration, changes in the hydraulic conductivity, porosity, moisture retention characteristics, mineralogy, aqueous chemistry, and radionuclide distribution coefficients were determined.

After passing 0.3 M and 3.0 M NaOH solutions through quartz sand columns for 194 days, some of the quartz particles became aggregated and brittle, as revealed by wet sieve analysis, and there was an enrichment in darker particles. Scanning electron microscope (SEM) morphologic characterization and EDX chemical analyses suggested that the cemented particles were primarily feldspars; the darker particles had chemistry and morphology similar to the mineral ilmenite ($FeTiO_3$). Ilmenite is largely resistant to dissolution by NaOH; therefore, its increased concentration in the NaOH-treated sand was likely the result of the decreased concentration of other minerals, not the precipitation of additional ilmenite.

The 0.3 M NaOH-treated quartz sand had greater moisture retention than the control (a quartz sand column contacted with 0.03 M $NaClO_4$). The 3.0 M NaOH-treated quartz sand showed the opposite trend, i.e., lower moisture retention than the control. These differing hydrologic responses may be due to the greater amount of aggregation measured in the 3.0 M NaOH-treated quartz sand and to the existence of more precipitated Al-Si gel coatings, which may trap water in their structure, in the 0.3 M NaOH-treated sand. Experimental and analytical problems compromised our ability to draw conclusions about the caustic treatment effects on hydraulic conductivity, but the observed differences before and after caustic treatment were not large and thus likely not a long-term issue for predictive performance assessment modeling.

The NaOH treatments induced much more aggregation in the Warden soil column experiment than in the quartz sand column experiment. The 0.3 M NaOH-treated Warden soil contained very hard aggregates that could not be broken apart with water and manipulation with a rubber stopper. Despite the observation of increased aggregation, however, the particle size distribution was nearly identical to that of the control. The 3.0 M NaOH-treated Warden soil column contained more of these hard aggregates, as well as a gel and several large void spaces, and the particle size distribution was very different from that

of the control. The 3.0 M NaOH-treated soil had almost no clay-sized particles remaining after treatment compared to 4 wt.% clay in the untreated soil. The silt fraction increased by 17% with respect to the control while the percentages of almost all other size fractions, including the various sand fractions, decreased.

The effects of the NaOH treatments on the Warden soil moisture retention characteristics were very similar to those observed for the quartz sand; namely, more moisture was retained by the 0.3 M NaOH-treated Warden soil than the control and less moisture was retained by the 3.0 M NaOH-treated soil than the control. The hydraulic conductivities of both the treated and control soil samples were lower after the 194-day tests than before the tests began. It is not clear, however, if the decreased hydraulic conductivity was caused by reaction with the caustic solutions or by compaction from centrifugation during the measurement of moisture retention. We discovered that our use of the unsaturated flow apparatus (UFA) to perform moisture retention measurements may have compromised the subsequent saturated hydraulic conductivity testing.

The 3.0 M NaOH-treated Warden soil from the column experiment had less kaolinite and essentially no smectite remaining after the 194-day treatment; illite and chlorite did not appear to be impacted by the caustic. Quartz, feldspar and the resistant clays, and calcite concentrations increased. The relative concentrations of quartz, feldspar, illite, and chlorite increased because the proportion of other minerals decreased. The calcite concentrations increased due to the precipitation of calcite in the elevated-pH solutions. SEM images of the treated soil showed that feldspar particles became increasingly pitted as the molar strength of NaOH increased. Significant amounts of Si-Al gel coatings were observed on both quartz and plagioclase particles, and coatings were observed on a few of the K-feldspar particles.

The specific ions in the effluent solution from the Warden soil flow-through column tests were very similar to those in the effluents from the quartz sand columns, presumably because similar minerals (feldspar, quartz, and muscovite/illite) constituted both sediments. Concentrations of the leached ions, however, were generally much higher in the Warden soil column effluents than in the quartz sand effluents. In both experiments, most of the dissolution took place in the first 7 days and aqueous concentrations of Si, Al, Fe, and K then generally decreased over the remaining 187 days.

Appreciably less dissolution but more precipitation took place during the 360-day 3.0 M NaOH Warden soil batch experiment because there is no removal of dissolved material from a closed batch system. Aqueous concentrations of dissolved constituents increase with time as dissolution products accumulate, thus reducing the chemical potential for extensive dissolution while increasing the chemical potential for precipitation to occur. Precipitates in the treated soil included calcite, likely from carbon dioxide diffusing through the plastic containers and reacting with dissolved Ca.

The most significant trend in the particle size distribution in the batch experiment was a tendency for aggregation of particles at all NaOH concentrations, especially at longer treatment times. Aggregation, however, was not the only process causing the apparent increase in average particle size. There was also evidence of certain clay minerals being dissolved by the 3 M NaOH treatment thus eliminating clay-sized (i.e., small) particles.

The NaOH treatments in the Warden soil batch sorption study did not dissolve quartz, Na-feldspar, amphibole, chlorite, or muscovite in the silt and sand fractions. Ca-feldspar, however, showed evidence of dissolution. In the clay fraction, both x-ray diffraction (XRD) and transmission electron microscopy (TEM) analysis suggested that illite and chlorite were not greatly affected by the NaOH treatments. Large unaltered particles of both minerals were observed with TEM after the 360-day treatment. Smectite and kaolinite were severely attacked and almost completely removed from the clay fraction after the 360-day caustic treatment in batch mode. These mineralogical changes in the static tests are quite similar to the changes observed in the flow-through column tests using the same soil.

Sorption tests were conducted with Warden soil from the batch sorption study. Cs, Sr, I, Se, and Tc K_d values were measured in soils treated with caustic solutions for up to 360 days. The Cs K_d values were large in the perchlorate control solutions and did not change significantly over the concentration range of 0.03 to 3 M Na. After 10 days of caustic attack, the Cs K_d values did not change appreciably. After 90 days of caustic treatment, there is still little change in the Cs K_d values, but the K_d did increase as the NaOH concentration increased. After 180 and 360 days of caustic contact, the Cs K_d value dropped noticeably. One plausible explanation is that the complete destruction of the smectite clays removed the most significant and common adsorbent from the soil. In contrast, Sr K_d values dropped significantly as the concentration of NaOH increased; however, the Sr K_d values in the caustic solutions were larger than comparable solutions with neutral pH sodium salts. Based on control samples, in which $NaClO_4$ was used as the background electrolyte, it was shown that most of the reduction in Sr K_d values in the caustic treated batch adsorption tests could be attributed to Na competing for sorption sites and not to dissolution of soil minerals. Neither iodide (I^-), selenate (SeO_4^{2-}), nor pertechnetate (TcO_4^-) sorbed appreciably to soils treated with NaOH. There was some adsorption of selenate in control tests using sodium perchlorate solutions at neutral pH, but after caustic treatment and in high pH solutions, selenate sorption was nil. In the “far field” vadose zone in past performance projections, some sorption has been allowed for selenate. Even if the caustic glass leachate completely dominates the entire vadose zone below the repository, such that there will be no sorption of selenate, the dilution and pH neutralization that will occur in the upper unconfined aquifer will allow selenate adsorption to occur onto the aquifer sediments. It is recommended that a future performance assessment sensitivity run be performed to address this point.

In summary, these studies showed that under chemical conditions approaching the most caustic glass leachate conditions predicted in the near field of the ILAW disposal site, approximated by 0.3 M NaOH, significant changes in mineralogy were observed. The clay minerals of both sediments evidenced the greatest dissolution thereby increasing the relative proportions of the more resistant minerals, e.g., quartz, feldspar, and calcite, in the remaining mass. Some re-precipitation of solids (mostly amorphous gels) was observed; these precipitates increased the moisture retention in both the quartz and Warden soil, likely because of water retained within the gel coatings. The hydraulic conductivities were slightly lower, but because of experimental artifacts, these reductions should not be considered significant.

Little change in Cs K_d values at exposure times < 180 days and a significant increase in Sr K_d values relative to natural groundwater were measured in the simulated glass leachates. Differences in the sorptive responses of the radionuclides were attributed to differences in sorption mechanisms (e.g., Cs sorbs strongly to high-energy sites, whereas Sr sorbs primarily by cation exchange but also is sensitive to pH-mediated precipitation reactions). The drop in Cs K_d values at exposure times ≥ 180 days was

attributed to the dissolution of clay minerals and the accompanying decrease in sorption sites whereas the high K_d values for Sr were likely due to co-precipitation with $CaCO_3$. In caustic solutions, there was no appreciable adsorption of the three anions: I^-, SeO_4^{2-}, or TcO_4^-.

Because a majority of the dissolution and precipitation occurred within 7 days of contact with the caustic solution, future research on the dissolution aspects of caustic attack can be conducted over shorter durations, but the subsequent re-precipitation processes and the re-incorporation of trace contaminants into secondary minerals and gels appear to occur over time periods that do not reach steady state within one year.

Acknowledgments

This work was conducted as part of the Immobilized Low Activity Waste Performance Assessment Project [ILAW-PA] led by CH2M HILL Hanford Group, Inc., in support of the U.S. Department of Energy's Office of River Protection. The authors wish to acknowledge Dr. Fred Mann with CH2M HILL Hanford Group, Inc. (CH2M HILL) for his funding of this work. Further, within the Pacific Northwest National Laboratory (PNNL) portion of the ILAW-PA, Phil Meyer who is charge of near-field hydrology funded portions of the column work that measured moisture retention and saturated hydraulic conductivity.

We would also like to thank Dr. Sherry D. Samson with PNNL for her technical review of this report. The authors also acknowledge the editorial review by Kristin Manke and word processing support by Rose Urbina with Pacific Northwest National Laboratory.

Contents

Figures

Tables

1.0 Introduction

1.1 Background

A performance assessment (PA) is underway to evaluate the suitability of the unsaturated zone of the Hanford Site for immobilized low activity waste (ILAW). This assessment will predict the transport of radionuclides and contaminants from a source to a receptor via pathways that are considered credible. Previous analyses for proposed disposal actions on the Hanford Site (Mann et al. 2001) show that groundwater transport presents the greatest potential for long-term dose uptake by humans.

Although the design of the near-field engineered barriers has not been finalized, it has been decided that the waste will be glassified and that a capillary break will be included among the engineered barriers. It is expected that leachate from the glass will have a high pH and high ionic strength (Mann et al. 2001). Such solutions are known to dissolve silicate minerals (Tardy and Nahon 1985; Holdren and Speyer 1987; Casey et al. 1988; Wieland et al. 1988; Brady and Walther 1989; Casey et al. 1989; Drees et al. 1989). One concern for the ILAW PA is whether the hydraulic properties of near-field materials will change once the plume emanating from the waste-form enters this region. Should dissolution of silicate minerals occur, the hydraulic properties of the near-field could change. The lack of knowledge of how hydraulic properties in the near-field may change when sediments are exposed to caustic effluent could adversely affect the PA by increasing uncertainty and thus requiring unrealistically conservative estimates to be used as input parameters.

Studies were initiated in FY98 to evaluate the effect of high NaOH concentrations on sorptive and hydrological properties of sand-textured sediment collected from the 200-East Area and a commercially available quartz sand (Kaplan et al. 1998). The NaOH solutions were used as a simplified leachate from a low-activity glass waste-form. When the Hanford sediment and quartz sand were put in contact with the NaOH solutions, dissolution was evidenced by a substantial increase in dissolved Si concentrations in the leachates. Incremental increases in NaOH concentration resulted in corresponding increases in leachate Si concentrations. As much as 1944 mg/L Si were measured in NaOH-treated effluents contacting the Hanford sediment, whereas only about 7 mg/L Si were measured in deionized water effluents (i.e., 0 M NaOH treatment) that contacted the Hanford sediment for the same time period. Dissolution of the quartz sand was appreciably less than that observed for the Hanford sediment. After 300 days, the Si concentration in the aqueous phase of batch experiments with quartz sand was 4 mg/L in the 0 M NaOH treatment and 189 mg/L in the 1.0 M NaOH treatment.

A number of physical and hydraulic properties also changed as the NaOH concentration was varied. These changes were especially evident in the dynamic flow experiments; changes were not as systematic in batch experiments. In the flow-through column experiments, wherein the influent NaOH concentration was varied from 0 to 1.0 M, after 10 months of contact the hydraulic conductivity of the Hanford sediment increased from 0.24 to 0.55 cm/min, the porosity increased from 0.34 to 0.44 cm^3/cm^3, and the bulk density decreased from 1.87 to 1.72 g/cm^3. The hydraulic conductivity for quartz sand increased from 8.70 to 10.15 cm/min, the porosity increased from 0.39 to 0.40 cm^3/cm^3, and the bulk density

increased from 1.60 to 1.67 g/cm^3; no significant change occurred in the particle size distribution. These changes were quite moderate, and, in some cases, not statistically significant.

Moisture retention measurements were made on the quartz sand and Hanford sediment. They showed that the 1.0 M NaOH-treated solids consistently retained more water than the 0 M NaOH-treated solids. Since the other chemical, physical and hydraulic measurements suggested that dissolution and not precipitation occurred in the high NaOH treatments, the greater moisture retention of the high NaOH treatments was attributed to a salt effect and not to the formation of small particles. From tests discussed herein, another plausible explanation for the increased moisture retention is the formation of surface gels or coatings that readily retain water. In the Kaplan et al. (1998) studies, no attempt (e.g., by scanning electron microscope [SEM] or transmission electron microscope [TEM] studies) was made to identify surface coatings.

It is clear from this initial study (Kaplan et al. 1998) that the background chemistry of the waste-glass effluent may have a profound effect on hydrology in the near-field environment. This earlier work also identified a number of processes that need additional study. For example, most, if not all, of the changes induced by the NaOH treatments occurred to the < 2-μm particles. Unfortunately, the experimental technique of dry sieving (Gee and Bauder 1986) used in the initial NaOH-aging experiments was not sufficiently sensitive to quantify the clay-sized particles. Consequently, it was not possible to unequivocally define the mechanism responsible for the observed changes in hydraulic conductivity and bulk density. Careful tracking of the changes in particle size distribution of the fine particles in the studies presented herein using wet sieving and the hydrometer method will help predict long-term changes in hydrological behavior. Another aging effect that needs to be determined is changes in mineralogy. The initial NaOH-sediment aging study had problems with algae growing in the batch and column assemblies after 10-month contact times. The presence of algae introduced an experimental artifact that could not be entirely accounted for when interpreting the results. Consequently, many of the Kaplan et al. (1998) measurements made on the samples that were aged 10 months or more with NaOH treatments were not included in the final data set.

Distribution coefficients for Cs and Sr adsorption were also measured on the NaOH-treated sediments. Cs K_d values decreased from about 3,000 to 1,000 mL/g as the NaOH concentration increased from 0.01 to 1.0 M, and were unaffected by the time the sediment was in contact with the NaOH treatment. Similarly, Sr K_d values decreased from about 1,300 to 300 mL/g as the NaOH concentration increased from 0.01 to 1.0 M, and there was no apparent trend with contact time. The lack of a correlation between the K_d values and contact time suggested that the cause for the decrease in K_d values with increased NaOH concentration was not attributable to the dissolution of sediment particles, but to competition for adsorption sites by the added Na.

These adsorption experiments were conducted over a limited contact time relative to the 10,000- to 100,000-year scenarios described in the ILAW PA. Yet, it is clear from these experiments that the background chemistry of the waste-glass leachate is likely to have profound effects on hydrology and radionuclide geochemistry in the near-field environment. These effects may make the ILAW site more or less suitable for waste immobilization than would be estimated based on experiments conducted with un-aged natural sediments. The glass waste-form leachate may make the near-field less suitable for waste immobilization by increasing the hydraulic conductivity via particle dissolution or increasing fluidity, and

decreasing the sorption selectivity of the sediments via the salt effect. Conversely, high pH conditions could also make the system more suitable for waste immobilization by increasing the moisture retention via the salt effect or surface gel coatings, increasing sorption (e.g., of Tc), or inducing precipitation [e.g., of U(VI)].

The studies described in this report were initiated in FY99 and completed in FY01. This report covers the physical, hydraulic, mineralogical, and sorption changes identified for the caustic weathering of both a Hanford fine-grained sediment and a commercially available quartz sand for time periods up to 12 months.

1.2 Objectives

The objectives of these studies were to determine the effect of simulated glass leachate (as approximated by solutions of NaOH) on selected hydrological (saturated hydraulic conductivity and moisture retention), physical (bulk density, porosity, and particle size distribution), mineralogical and sorptive properties of sediment collected from the Hanford Area and a commercially available quartz sand. Particular attention was directed at:

1. supplementing the data collected from the initial NaOH-sediment aging study (Kaplan et al. 1998),

2. understanding and quantifying the fate of small particles (<50-μm diameter) that may be generated or dissolved during the NaOH treatments,

3. measuring the effects of small changes in the concentration of small particles (<50 μm) and mineralogy on Cs, Sr, I, Tc, and Se K_d values, and

4. eliminating experimental artifacts that may have been caused by algae growth in the work conducted in FY98.

The intent of this work was to provide information about the effects of glass leachate on the hydraulic and sorptive properties of backfill materials and natural sediments that may exist in the near-field environment of the proposed ILAW site.

1.3 Scope

Two studies were conducted. The column study was designed to provide primarily hydraulic, physical, and mineralogic data under dynamic flow conditions. The batch sorption study was designed to provide primarily mineralogical and radionuclide sorption information. Details are provided in the next section on methods and materials.

2.0 Materials and Methods

2.1 Column Study

The two solid phase materials used in this study were a fine-grained Hanford sediment (Warden silt loam) and a commercially available sand (#2095 Industrial Quartz, Unimin Corp., Emmett, ID). The air-dried Hanford sediment was passed through a 2-mm sieve to remove gravel particles and the Unimin sand material was washed with deionized water to remove fine particles and then air dried. The two solids, packed in columns, were contacted with 0.03 M $NaClO_4$, 0.3 M NaOH, or 3.0 M NaOH. Sodium perchlorate was used in the control columns instead of the control solution used in the past [0.0 M NaOH (deionized water)] because of experimental and theoretical considerations. If deionized water had been passed through the Warden silt loam columns, the fine particles could have dispersed resulting in column clogging. Although solutions high in Na and low in alkaline earths can also cause dispersion, the total ionic strength in these solutions was adequate to prevent dispersion (more specifically, to prevent collapse of the electrostatic double layer around the clay particles). Furthermore, deionized water is not found under natural conditions; uncontaminated Hanford pore waters and groundwater are generally dominated by bicarbonate and calcium, with a pH of 8.2 ± 0.5. The perchlorate anion was selected for the control because it is largely chemically non-reactive; sodium was selected because it is the dominant cation leached from glass and it is the same cation used in the caustic treatments. The ionic strength of the $NaClO_4$ solution is about three times greater than Hanford groundwater to simulate saltier vadose-zone pore water. Sodium hydroxide was selected as a simplified glass leachate because it consists of the two dominant ions expected in the actual glass leachate (Mann et al. 2001). The 0.3 M solution is likely towards the upper limit of expected glass leachate ionic strength (Mann et al. 2001). The 3.0 M NaOH solution was included as an extreme condition to provide a limit of potential effects of the leachate on the measured soil properties.

The columns were made of poly-ether-ether-ketone (PEEK) and had internal dimensions of 1.91 cm in diameter and 7.62 cm in length, yielding a total volume of 21.72 cm^3. Influent ports in the bottom of each column had a diameter of 0.079 cm and effluent ports on top of each column had a diameter of 0.159 cm. A small piece of Spectramesh was placed in the top portion of the column under the effluent port to retain fine particles. At the start the columns also contained a bubbling plate on the inlet side of the column so that unsaturated flow conditions could have been performed. The columns were to be used in an up-flow configuration. To achieve uniform packing, each column was held on a Vortex-Genie 2 mixer and dry sediment was added to the vibrating column assembly in a continuous stream. Four columns were packed with Unimin sand and eight columns with the Hanford sediment, Warden silt loam (Table 2.1).

Each packed column was placed into the x-ray microfocus tomography (XMT) unit, which produced x-ray images of the intact columns to verify uniform packing (described in detail below). Saturation of the columns was achieved through a multi-step process. First, the columns were partially saturated by connecting each to a micro-burette filled with degassed tap water that was hung above the columns to cause gravity feed for 72 hours. Subsequent XMT scans revealed the column porosity to be approximately 30% air and 70% water. Further attempts at saturating the columns included attaching vacuum lines to the effluent ports while maintaining a 1.25 mL/hr flow of tap water through the influent

Table 2.1. Column-Treatment Descriptions

Column Number	Solid	Solution
1	Unimin Sand[(a)]	0.03 M $NaClO_4$
2	Unimin Sand[(a)]	0.3 M NaOH
3	Unimin Sand[(a)]	3.0 M NaOH
4	Unimin Sand[(a)]	3.0 M NaOH
5	Warden Silt Loam	0.03 M $NaClO_4$
6	Warden Silt Loam	0.03 M $NaClO_4$
7	Warden Silt Loam	0.3 M NaOH
8	Warden Silt Loam	0.3 M NaOH
9	Warden Silt Loam	0.3 M NaOH
10	Warden Silt Loam	3.0 M NaOH
11	Warden Silt Loam	3.0 M NaOH
12	Warden Silt Loam	3.0 M NaOH

(a) A commercial sand (#2095 Industrial Quartz, Unimin Corp., Emmett, ID).

ports, and placing the columns in a vacuum desiccator filled with water to approximately 0.32 cm from the top of the columns while pulling a vacuum for 48 hours. XMT scans conducted after both processes revealed little change. The air inside the columns was finally reduced by removing the bubbler plate and gently tapping the side of the columns, causing the air to move up and out of the sediment. Columns 9 and 12 appeared to compact slightly and each required the addition of 1.5 g of soil to re-fill. Final XMT scans verified that most of the air had been removed.

Following the initial column saturation with degassed tap water, the saturated hydraulic conductivity and moisture retention values were determined. After these measurements, treatment solutions were pumped up-flow through the columns using syringe pumps at a rate of 1.25 mL/hr. This slow flow rate was selected to approximate the expected saturated flow rate at the disposal site. The pumps were turned off once clogging of any one of the columns was detected, which was 194 days after initiating treatment.

Once the tests were stopped, the columns were disconnected from the pumps, capped, weighed, and scanned by XMT. Each column was then flushed with approximately three pore-water volumes of deionized water and the hydraulic conductivity and moisture retention measurements were repeated using tap water. Upon completion of the non-destructive testing, the solids in the columns were removed using a syringe plunger and spatula. The treated solids were placed onto white paper and visually inspected. Sub-samples were collected for SEM analysis. Material from similar cores was combined and wet-sieved using deionized water following Pacific Northwest National Laboratory procedure PNL-MA-567, SA-3 (Table 2.2). The solids collected on the sieves were oven-dried at 105°C. Sub-samples of the dried material were collected for bulk x-ray diffraction (XRD) analysis.

The silt-clay fraction that passed through the stack of sieves was kept in suspension and separated using Stoke's settling law described in Jackson (1969). The lower limit of the silt fraction was taken at

Table 2.2. Procedures Used in Study

Parameter	PNNL Procedure	Procedure/Comments
Particle Size Distribution	PNL-MA-567, SA-3	Particle-Size Analysis (Pipette or Hydrometer Method) (Gee and Bauder 1986; ASTM 1985); Wet-sieve analysis used to remove sand-sized particles
Hydraulic Conductivity	PNL-MA-567, SA-5	Falling Head Hydraulic Conductivity (Klute and Dirksen 1986)
Water Retention	UFA-SK-01	Determination of Water Retention as a Function of Water Content Using Open-Flow Centrifugation Techniques
Water Content	PNL-MA-567, SA-7	Water Content
Bulk Density	PNL-MA-567, SA-8	Clod Density/Bulk Density (Blake and Hartge 1986)
Particle Density	PNL-MA-567, SA-9	Determining Particle Density
Column Packing	WHC-IP-0635, GEL-3 Rev. 3	Moisture-Density Relationship of Soils (see Section 2.5 for packing column)
Cation Concentrations	University of Georgia	Determination of Elements by Inductively Coupled Argon Plasma Optical Emission Spectrometry
XRD Mineralogy	JEA-3	Mineralogical Analysis of Soil Samples by X-Ray Diffraction (XRD) (Whittig and Allardice 1986; Moore and Reynolds 1989; Amonette 1994)
Alkalinity	ASTM 1067-92	Test Methods for Acidity and Alkalinity
pH/EC	PNL-G-5-pH/EC	Measuring pH/EC of Low-Level Radioactive Solutions
Dissolved Inorganic and Organic Carbon	D4129-88	Standard Test Method for Total and Organic Carbon in Water by High Temperature Oxidation and by Coulometric Detection (ASTM 1988)—**used for batch tests only**
Rad counting (Cs, Sr, Se, I)	PNL-G-10-DE	Procedure for Calibrating and Operating a Detector for Radionuclide Determination
Rad Counting (Tc)	PNL-F-11-ABE	Alpha and Beta Analysis of Aqueous Solutions using a Liquid Scintillation Detector

>2 microns. Both the silt and clay fractions were oven-dried at 105°C. Silt fractions were submitted for XRD analysis and clay fractions were submitted for XRD and TEM analysis. Procedures and methods used in this study are provided in Table 2.2.

2.2 Batch Sorption Study

In the batch experiment, 200 g of Warden silt loam soil were combined with 900 mL of treatment solution and placed in dark plastic containers in the hope of minimizing the algal growth problems encountered in previous work (Kaplan et al. 1998). The treatment solutions were 0.03 M NaOH, 0.3 M NaOH, and 3 M NaOH. The batch containers were stored at 4°C in a refrigerator and periodically hand shaken throughout the treatment period. After four contact times (10, 90, 180 and 360 days), the aqueous solutions were separated from the solid phases by vacuum transferring the liquid into another container. At each sampling, the pH, electrical conductivity, inorganic carbon and organic carbon and elemental composition of the effluent were measured following standard procedures listed in Table 2.2. Approximately 120 mL of the contact solution were filtered using a syringe and 0.45-μm filter, and submitted for metals characterization. A small sub-sample of the sediment was taken for moisture

determination. Particle size determination was conducted with approximately 60 g of treated sediment using wet sieving and the hydrometer method (Gee and Bauder 1986). Characterization using XRD, TEM, and SEM was conducted on a select few of the treated materials after sieving.

The batch K_d tests were performed on the treated sediment (hydroxide contact times 10, 90, 180, 360 days) using radiotraced solutions with the same composition as used during the extended caustic treatment step. The contaminants studied were iodide [I^-], selenate [SeO_4^{2-}], pertechnetate [TcO_4^-], strontium [Sr^{2+}], and cesium [Cs^+]. The radiotraced solutions were allowed to equilibrate with each treated sediment for 14 days. In addition, K_d values for the same ions were determined in untreated soils with 0.03, 0.3, and 3.0 M $NaClO_4$ solutions. The untreated-sediment K_d values were determined over the standard 14-day contact period with spiked $NaClO_4$ solutions and enabled us to differentiate changes in sorption due to competition from Na for sorption sites from those changes induced by mineral dissolution, caustic attack, or high pH. In order to minimize the formation of evaporites and the fragmentation of fragile precipitates and surface coatings, the soils (both untreated and treated) were never dried. Moisture content of the treated soils was determined gravimetrically. All analytical results, including K_d values, were reported on a dry-weight basis. K_d values were determined using the method described in Kaplan et al. (1998). Iodide (I^-) and selenate (SeO_4^{2-}) K_d values were measured in one set of tubes, Tc as pertechnetate (TcO_4^-) was measured in a second set of tubes, and Cs and Sr K_d values were measured in a third set of tubes. For the I/Se, and Sr/Cs pairs, Kaplan et al. (1998) showed that their respective K_d values can be measured in the same test tubes without analytical interference or competitive adsorption.

2.3 Solid and Aqueous Phase Characterization

The solid phases and effluents from the column tests on quartz sand and Warden silt loam, and the batch contact solutions from the Warden silt loam tests, were characterized for the parameters listed in Table 2.2.

2.3.1 Hydraulic Properties

The Unimin quartz sand and the Hanford soil (Warden silt loam) were characterized for the following hydraulic parameters both before and after treatment:

- Saturated hydraulic conductivity (K_{sat}) as determined by the falling head method (Klute and Dirksen 1986), and
- Moisture retention as measured with the unsaturated flow apparatus (UFA).

Hydraulic conductivity was measured on all columns using the same parameters of time, temperature, and volume of infusion solution (tap water). A small piece of 105-μm Spectra/Mesh fluorocarbon filter screen (Spectrum Medical Industries, Laguna Hills, CA) was used to reduce the loss of sediment from the column. The columns and burettes were mounted on individual stands and height measurements were taken.

Baseline moisture retention curves were measured on all columns using the UFA method (Table 2.2). The saturation levels from the hydraulic conductivity measurements were used as the starting point for the

moisture retention measurements. The columns were weighed, then mounted two at a time into the UFA rotor head. Moisture retention data were collected over a period of ~7 hr. For this test, 1-hr runs were conducted at 300, 600, 900, 1250, 1750, 2500, and 2570 rpm, giving pressures of -0.06, -0.24, -0.54, -1.04, -2.05, -4.18, and -4.98 bars, respectively. After each rpm run, the motion of the UFA was stopped and residual moisture contents were determined through gravimetric (i.e., weighing) methods.

2.3.2 Physical Properties

The Unimin sand and the Warden silt loam soil were characterized before and after treatment for the following physical parameters:

- grain morphology and pore structure by XMT,
- particle size distribution by the wet-sieve (sand and silt fractions) and hydrometer (clay fraction) methods (Gee and Bauder 1986), and
- dry bulk density by weighing the sediment mass in a packed column of known volume and moisture content (Blake and Hartge 1986).

XMT scans of the packed columns were conducted after equilibration with degassed tap water, prior to NaOH treatment, and after NaOH treatment for ~194 days. The scans were generated using the XMT system (ACTIS 200/160 KXR, Bio-Imaging Research, Chicago, IL). The instrument is housed in a lead-lined, near zero-emission enclosure, and is capable of achieving a resolution in the focal plane of one one-thousandth of the object's diameter. A microfocus x-ray source allows variable slice widths over a nominal range of 10 to 250 μm. Two-dimensional images generated by computer tomography (CT) are displayed using 256^2, 512^2, or 1024^2 pixels, each at 12 bits (4096 contrast levels). The instrument can also be used to obtain digital radiographs. The system is composed of a Kevex model KM16010E-A x-ray tube with spot sizes of 10, 20, 65, 250 μm at power levels 5, 10, 50, and 160 watts, respectively. The x-ray source uses a tungsten target and the x-rays are emitted through a 0.01-inch thick beryllium window. The RLS-2048/100 CCD detector is a cesium iodide scintillation phosphor screen optically coupled to a linear photodiode array through a fiber optic taper. The diode array is an EG&G Reticon RL2048S, monolithic self-scanning linear photodiode array with 2048 photodiode sensor elements having 25-μm center-to-center spacing. A computer-controlled sample manipulator with a 75-mm diameter turntable allows 365° of continuous rotation and a maximum vertical travel of 150 mm. Large objects (up to 150 mm) may be placed on the table using jigs. A computer data acquisition, instrument control, and image reconstruction system with the ACTIS+ software provides x-ray and sample manipulation control in addition to CT and CT Multi-Planer (MPR-3D) image reconstruction. The computer system is an EISA (enhanced industry standard architecture) bus system running SCO UNIX.

Each column scan was done in two XMT modes: digital radiography (DR), which produces an image similar in appearance to film x-rays, and CT, which produces an image of a thin cross-sectional slice of an object. Each column was initially scanned using a large focal spot size of 250 μm, target power of 160.0 keV, and a current of 1.0 mA. DR scans were done starting 5.0 mm from the bottom of the column moving up ~70 mm to the top of the column. CT images were then reconstructed with high resolution

(2000 scans/CT image) and a field size of 28 mm. Five CT scans per column were generated at 16.2, 31.2, 46.2, 61.2, and 76.2 mm from the bottom of the column.

2.3.3 Mineralogical Properties

The Warden silt loam soil and Unimin quartz sand were characterized before and after treatment by the following analytical techniques:

- XRD to identify minerals and provide semi-quantitative estimates of mineral concentrations (Whittig and Allardice 1986),
- SEM to provide information on morphology and chemistry, and
- TEM (used on Warden silt loam only), to provide information about particle morphology, chemistry, and crystallinity.

Sediment samples were characterized by XRD on a Philips PW3040/00 X'Pert MPD system with a vertical θ-θ goniometer (220-mm radius). The X-ray source was a long fine-focus, ceramic X-ray tube (Cu anode) operated at 2000 W. The scan range was 2°-75° 2θ, or, in some cases, 2°-65° 2θ. In all cases, the scan rate was 0.04°/s. As needed, samples were ground to powder in an agate mortar and pestle and mounted into a shallow cavity of a single-crystal quartz plate. Data analysis was accomplished using Jade 5 (Materials Data Inc., Livermore, CA). Semi-quantification of crystalline phase content was based on the ratio of the peak height above background for each identified phase to the combined peak heights of all phases present. The XRD work described above was performed at the Environmental Molecular Sciences Laboratory, a national scientific user facility sponsored by the U.S. Department of Energy's Office of Biological and Environmental Research and located at Pacific Northwest National Laboratory in Richland, WA.

The clay-sized fraction of the sediments was analyzed by XRD on a Scintag XRD automated powder diffraction unit equipped with a Cu-Kα radiation tube and a Peltier thermoelectrically cooled detector. Mineral identification was conducted by a modification of the method proposed by Whittig and Allardice (1986) outlined in procedure JEA-3 (Table 2). The clay fraction was mounted on an aluminum slide by the filter-membrane peel technique of Drever (1973). Four XRD analyses were conducted for each clay sample: Mg-saturated, Mg-saturated and ethylene glycol-solvated, K-saturated, and K-saturated plus heated to 550°C. Illite was assigned to the fraction that gave a 10Å spacing in Mg-saturated subsamples and did not expand with glycol treatment. Kaolinite was assigned to the fraction that gave a 7.2Å and 3.58Å spacing that disappeared upon heating to 550°C. Smectite was assigned to the fraction of the Mg-saturated sub-sample that gave 12Å to 15Å spacings at 30 to 54% relative humidity, expanded to 17Å to 20Å upon saturation with glycol, and collapsed to 9.0Å to 10Å upon heating to 550°C. Chlorite was assigned to the fraction that gave 14.2Å, 7.1Å, and 3.54Å spacings that did not change with either glycol or heat treatments. Semi-quantitative estimates of the mineral composition of the clay fractions were calculated using the attenuation coefficients of the unknown sample and of pure mineral phases. The absolute intensity values of these standard materials were compared to the same peaks in the natural sediment samples and the NEWMOD computer program. See Moore and Reynolds (1989) for a

description of the theory behind the technique or http://www.angelfire.com/md/newmod/ for more current information or how to purchase NEWMOD. There was an insufficient amount of clay-sized particles in 3.0 M NaOH treatments in the column study to permit running both oriented and un-oriented samples. Consequently, no quantification of the mineralogy from this clay fraction was possible.

TEM samples were prepared by permitting 7 μL of a dilute sample suspension to dry on a Formvar carbon-coated 3-mm copper grid, and were analyzed on a JEOL 1200 analytical electron microscope equipped with a LINKS EDS system (energy dispersive spectrometer for elemental analysis).

2.3.4 Aqueous Effluent Chemistry

Effluent from the Unimin quartz sand and Warden silt loam sediment columns, and supernatants from the batch studies, was characterized for the following parameters:

- electrical conductivity: a conductivity bridge was used to provide an indirect measure of the solution ionic strength (Rhoades 1996),
- free hydroxide, by the titration method,
- total alkalinity, by a titration method used to calculate carbonate concentration,
- for the batch tests with Warden silt loam the dissolved inorganic carbon and organic carbon were also determined using a total carbon analyzer
- cation concentrations, by inductively coupled plasma-optical emission spectrometer (ICP-OES), and
- pH, by solid state electrode.

Effluent samples of ~30 mL per column were collected 0, 7, 14, 21, 28, 61, 95, 122, 150, and 180 days after initiating column treatment. At the flow rate of 1.25 mL/hr this required ~28 to 30 hr. The samples were stored in a 4°C refrigerator, but no attempt was made to maintain the samples in a CO_2-free environment or to acidify the samples to preserve the metals in the aqueous phase. The aliquots used for metals analysis were, however, acidified prior to ICP-OES analysis. Between sampling events, all effluent was collected in separate column-specific containers for the time intervals 0 to 28 days, 29 to 60 days, 61 to 95 days, 96 to 120 days, 121 to 150 days, and 151 to 180 days. Aqueous chemistry including pH, alkalinity (both free hydroxide and carbonate), and electrical conductivity was analyzed at Pacific Northwest National Laboratory. ICP-OES analysis was conducted at a commercial service lab at the University of Georgia. At least one set of the composite samples for each solid-treatment condition (see Table 1) was analyzed as noted above to allow complete mass balance for dissolution of material from each solid-solution treatment.

Radiological measurements on the effluent samples from the batch K_d tests were performed using two methods. Analysis for ^{99}Tc was conducted by liquid scintillation counting (LSC), using a quench-

calibrated Wallac® 1415 LCS and Packard® Opti-fluor™ LCS cocktail (Wallac Instruments, Inc., and Packard instrument, Meriden, CT). Analysis for ^{137}Cs, ^{85}Sr, ^{75}Se, and ^{125}I was conducted using a Wallac® 1480 Wizard™ 3-inch NaI automatic gamma detector.

3.0 Results

3.1 Column Study

3.1.1 Quartz Sand Column Experiment

At the end of the flow-through column testing phase (194 days) and after the measurements requiring intact cores were completed, the column contents were poured onto a piece of white paper and observations were recorded. The purpose of these observations was to note the qualitative changes caused by the caustic treatments. The top of the column was the effluent end and the bottom of the column was the influent end.

0.03 M $NaClO_4$ –Column #1: No visible difference between this treatment and the as-received quartz sand was observed. This is an important conclusion insofar as it indicates that this treatment provides a reasonable control for detecting physical changes to the quartz sand caused by the NaOH treatments.

0.3 M NaOH – Column #2: When still wet, the top 2-3 cm of the column had a reddish-pink tint on all of the grains. After drying, the sand became progressively more pink from the bottom (influent end) to the top of the column. The top ~5 cm of sand grains appeared pocked like Swiss cheese. Other than the pink tint, the bottom grains did not appear to have any changes.

3.0 M NaOH – Columns #3 and #4: As in column #2, there were several particles that were full of holes. No changes, however, were observed in the color of the grains. Particles appeared to be uniform in color and shape throughout the column. Small black particles, both free and stuck on the grains of sand, were perhaps twice as abundant as in the as-received samples. Many of the particles were aggregated.

3.1.1.1 Physical Properties of the Sand Column Experiment

The particle-size range, based on technical data sheets provided by the vendor (Unimin Corporation, Emmett, ID, Table 3.1), was 0.210 mm to > 2.38 mm, and particle density was 2.65 g/cm^3. A scanning electron micrograph of the untreated Unimin sand is presented in Figure 3.1. At this scale, the micrograph shows that the sand particles have rounded edges. The average width and length of the sand particles were 0.710 ± 0.106 mm and 0.723 ± 0.198 mm (n = 20), respectively. These values are somewhat smaller than expected based on the vendor's specifications. Our SEM data may not be representative of the bulk particles or the vendor's dry-sieving data in Table 3.1 may have been biased high by agglomeration.

As mentioned in the Materials and Methods Section, the 0.03 M $NaClO_4$ treatment was included in the experimental design to provide a control wherein minimal mineral dissolution and clay dispersion would occur. Upon spreading the treated quartz onto white paper after the experiment, the 0.03 M $NaClO_4$-treated sand, as expected, looked identical to the as-received Unimin sand. Based on wet-sieving methods, 86% of the 0.03 M $NaClO_4$-treated sand existed in the 1 to 2 mm size fraction (Table 3.2). This is consistent with the vendor's data shown in Table 3.1.

Table 3.1. Technical Specification Provided by Vendor of Unimin Sand

Particle Size (mm)	wt.%
> 2.4	3.5
1.2 to 2.4	70.5
0.8 to 1.2	22.8
0.6 to 0.8	2.1
0.4 to 0.6	0.8
0.3 to 0.6	0.2
0.2 to 0.3	0.1
0.1 to 0.2	0

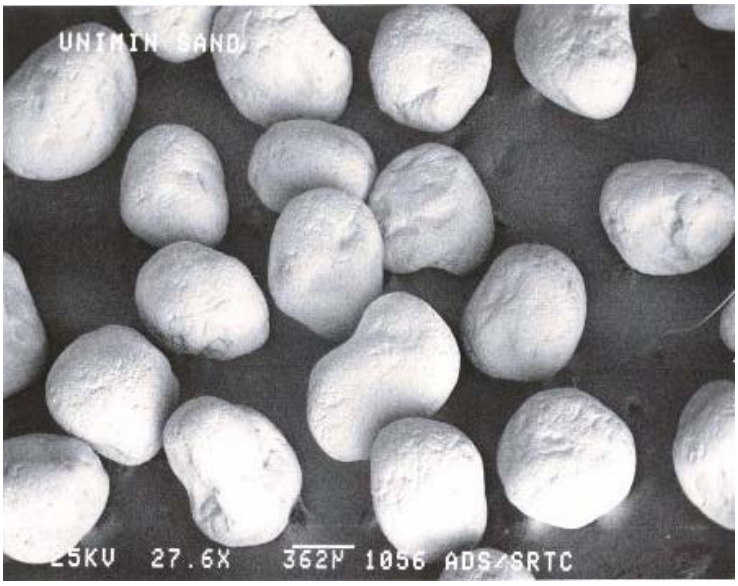

Figure 3.1. Scanning Electron Micrograph of Untreated Unimin Sand (Average Width = 710 ± 106 μm and Average Length = 723 ± 198 μm; n = 20)

The 0.3 M NaOH-treated quartz sand had slightly fewer 0.5- to 1-mm particles and more 1- to 2-mm particles than the 0.03 M $NaClO_4$ control (see Table 3.2). This result may be attributed to:

1. some of the finer particles aggregating to form larger particles, or

2. some of the finer particles dissolving, resulting in a proportionate increase in the two remaining size-fractions (> 2 mm and 1-2 mm fractions).

The 3.0 M NaOH-treated quartz sand also had less of the 0.5- to 1-mm fraction than the control; a corresponding increase, however, was observed in the > 2 mm fraction. Based on the visual observations made of the columns after the experiment, it is likely that the increase in the > 2 mm fraction can be attributed to aggregation.

Table 3.2. Particle Size Distribution of Quartz Sand After Treatment

Sieve #	Particle Size Fraction (mm)	Treatment		
		0.03 M $NaClO_4$	0.3 M NaOH	3 M NaOH[(a)]
		wt.%	wt.%	wt.%
10	> 2	3	4	7 ± 3
18	1 to 2	86	90	87 ± 2
35	0.5 to 1	11	6	6 ± 1
60	0.25 to 0.5	0	0	0 ± 0
140	0.106 to 0.25	0	0	0 ± 0
200	0.075 to 0.106	0	0	0 ± 0
270	0.05 to 0.75	0	0	0 ± 0
Silt	0.002 to 0.05	0	0	0 ± 0
Clay	< 0.002	0	0	0 ± 0

(a) Average ± standard deviation of 2 replicates. No replicates were conducted for the 0.03 M $NaClO_4$ and the 0.3 M NaOH treatments.

In summary, the NaOH treatments caused changes in the quartz sand particle size distribution: the percentage of the smallest fraction decreased, resulting in a corresponding increase in the two larger size fractions. If this shift was the result of dissolution of the smaller fraction, then increased hydraulic conductivity is expected. If it was the result of increased aggregation, perhaps because of an increase in carbonate or other cementing caused by the NaOH treatment, then a small increase or no change in hydraulic conductivity is expected.

XMT scans in both DR and CT modes were conducted on only the 3.0 M NaOH treatment replicate 2 column (column #4; see Table 1.1). Each scanning event included one DR and 5 CT slices typically at 20 mm, 35 mm, 50 mm, 65 mm, and 80 mm from the base of the holder (x-3.8 mm from the inlet of the column). In all, a total of five scanning events were performed on each column during the 194-day test. The first event was done immediately after packing the columns under dry conditions. The columns were scanned again after saturation with degassed tap water. The columns were presumed to still be saturated during the third scanning event, conducted following the base-line (before-treatment) hydraulic conductivity test. The fourth measurement was made after the base-line moisture retention curve was performed using the UFA, when the columns had very little water left in the pores. The fifth and final event was performed at the completion of the 194-day caustic treatment test, prior to measuring the final hydraulic conductivity and moisture retention curves.

Figure 3.2 presents three DR images of the quartz sand for the 3.0 M NaOH, replicate 2 column (column #4). The left image is of the column packed dry. The middle image is of the column after saturation with degassed tap water and prior to conducting the hydraulic conductivity test and treatment. The right image is of the column after the 194-day 3.0 M NaOH treatment. In these images, the darker the coloration, the greater the amount of absorbed x-rays, whose absorption is generally attributed to contact with a denser material. Some compaction or subsidence appears to have occurred in the treated column. This observation is based on the appearance of an air-filled space at the top of the column. The compaction could be an experimental artifact caused either by the introduction of flowing liquid into a

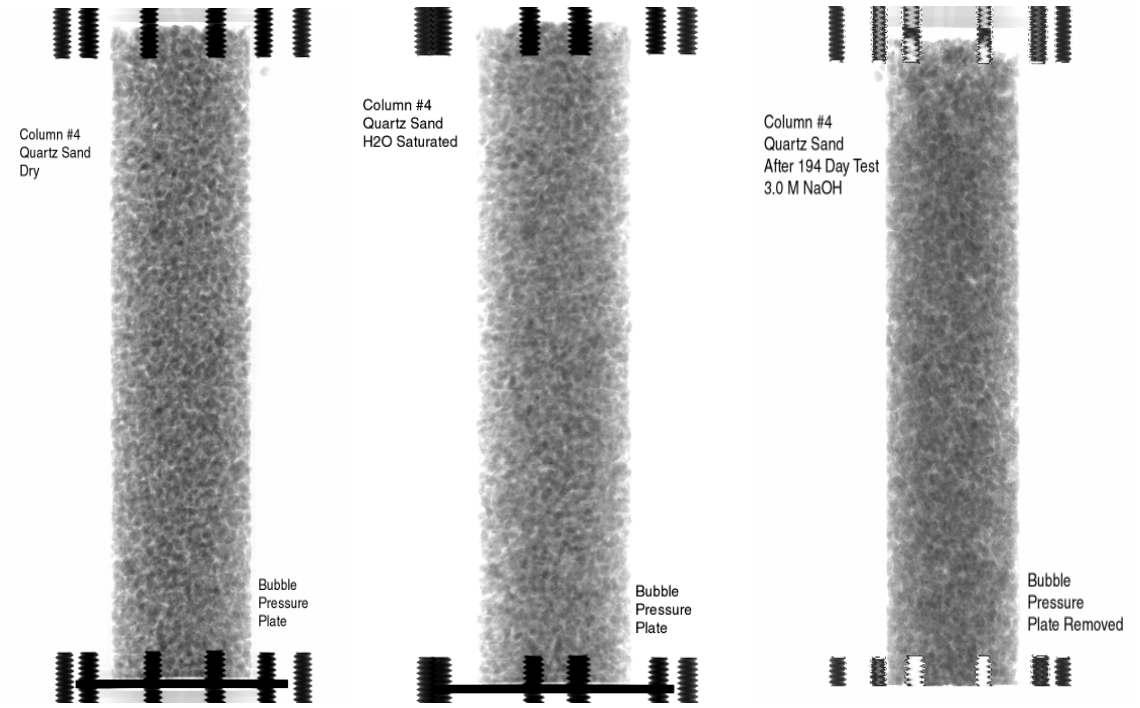

Figure 3.2. Digital Radiography (DR) Scans of a 3.0 M NaOH Column: the Left Image Is of the Column Prior to Treatment in a Dry State, the Middle Image Is of the Column Prior to Caustic Treatment but in a Water-Saturated State, and the Right Image Is of the Column After the 194-Day Treatment Period

loosely packed column or by placing the column in the UFA, a centrifuge, to gather moisture retention data. Alternatively, the subsidence could be the result of mineral dissolution caused by the treatment solution.

Two examples of CT scans are presented in Figure 3.3. The image on the left is of the 3.0 M NaOH Rep. 2 column immediately after saturation with degassed tap water. The image on the right is of the same column after the 194-day caustic treatment period. Both images were taken at 35 mm from the base of the column holder (at ~31.2 mm from the column inlet). The CT scan on the left was taken with a 250-µm spot focus at 160 keV. The CT scan on the right was taken with a 65-µm spot focus at 160 keV. Appreciably better resolution was obtained using the smaller spot focus size. Unlike DR images, CT images represent denser materials as lighter colors. Thus, individual quartz grains are white or very light gray, the surrounding water is gray, and air-filled void spaces are black. A simple visual comparison between the before and after treatment scans in Figure 3.3 shows that significantly more air was present in the column after treatment. Similar results were also observed at the 20 mm, 50 mm, 65 mm, and 80 mm depths (data not shown).

A new digitizing software called Clemex (Clemex Inc. 800 Guimond, Longueuil Quebec Canada J4G 1T5) was used for quantifying pixel shades in the CT scans. By processing Figure 3.3 with this software, it was possible to estimate the proportions of air, water, and solid phases in the images (see Figure 3.4).

Results from the image analysis show that the 3.0 M NaOH treatment caused the air-filled area of the column to increase from 3.69% to 7.18%, the water-filled area to decrease from 35.4% to 30.3%, and the solid particle area remained about the same, 61 to 62%. In other words, the air-filled

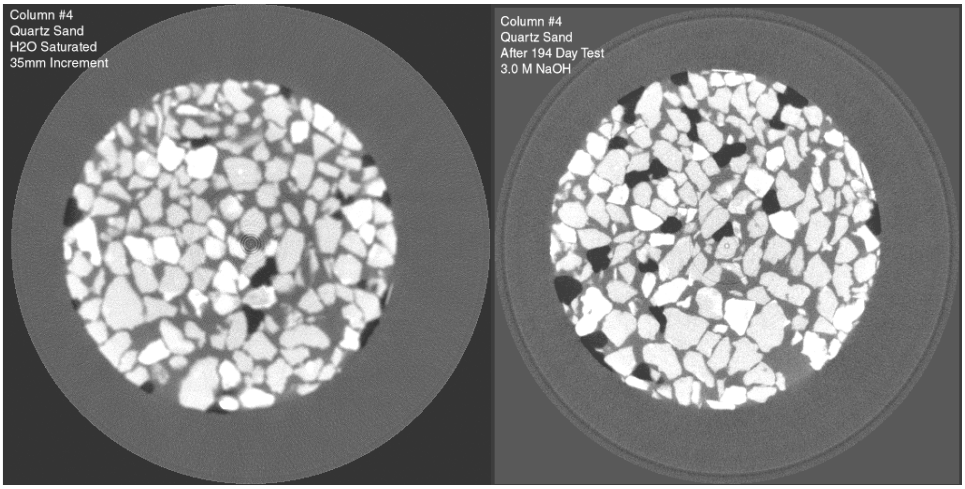

Figure 3.3. Computer Tomography (CT) Scans Before (Left) and After (Right) Treatment With 3.0 M NaOH

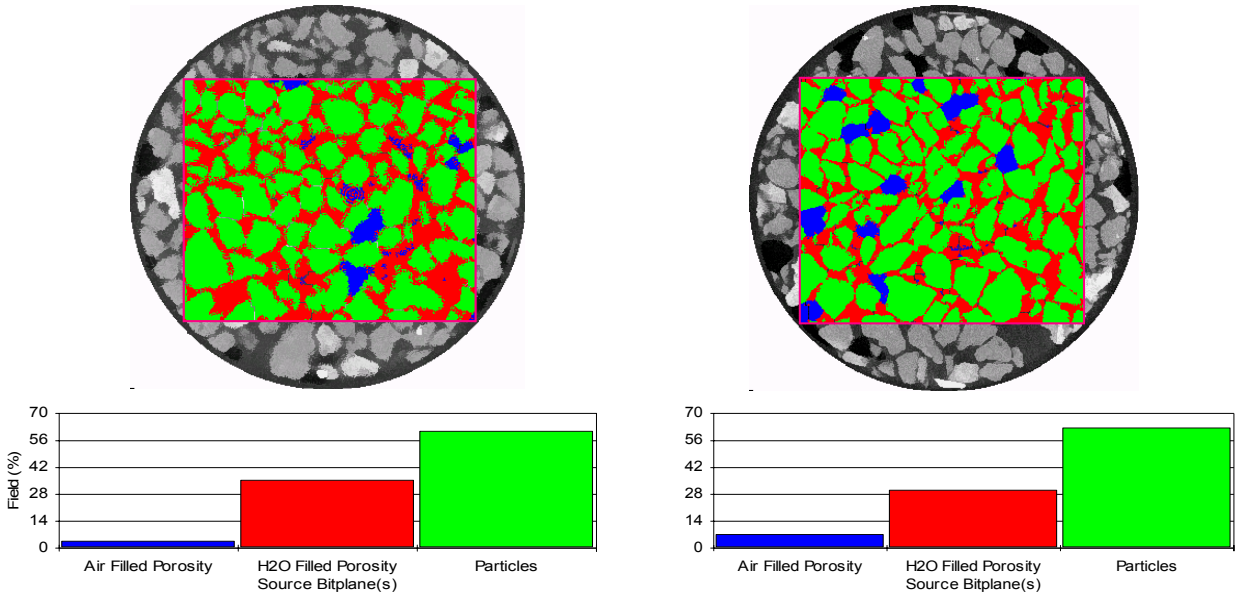

	Field (%)		Field (%)
Air-Filled Porosity	4	Air-Filled Porosity	7
Water-Filled Porosity	35	Water-Filled Porosity	30
Particles	61	Particles	62

Figure 3.4. Digitization of Computer Tomography Images Taken Before (Left) and After (Right) Treatment with 3.0 M NaOH

volume increased, the water-filled volume decreased, and the quartz sand volume remained about the same despite the fact that some solid dissolved as evidenced from the higher mass in the effluent than the influent. The apparent constancy in solid cross sectional area in the CT image, likely occurs from two opposing phenomena; mass dissolution and compaction of the remaining particles. There was an obvious decrease in the overall height of the quartz sand packed zone as evidenced by a larger void area at the top of the column (see right-hand image in Figure 3.2). Application of this digitizing technique was used on only a few images (slices from within the middle of the column and thus little quantified data for the entire packed column is available to do a total column analysis of changes in air-, water-, and solid-filled volumes.

3.1.1.2 Hydraulic Properties of the Sand Column Experiment

The hydraulic conductivity of the quartz sand was measured both before and after treatment by the falling head method (results are shown in Table 3.3). We have since discovered that this is not the best method for measuring high hydraulic conductivity values; the constant head method would have been more appropriate. Furthermore, it was discovered that the inlet and outlet ports on the columns restricted the flow rates such that the measured hydraulic conductivities were partially controlled by the columns. Consequently, the analytical accuracy of our measurements was compromised. Another important issue regarding the hydraulic conductivity methodology is that tap water, not the treatment solution, was used. Tap water was used to eliminate the confounding effect that the varying salt solutions would have on solution density. Solution density and viscosity influence fluidity, which is the aspect of hydraulic conductivity controlled by the aqueous phase. By using the same solution for all treatments, differences in fluidity were minimized and differences in the measured hydraulic conductivity could be attributed to changes in intrinsic permeability, the aspect of the hydraulic conductivity attributed to the solid phase. To accomplish this, the treated columns were repeatedly flushed with tap water to rinse the interstitial salt solutions from the columns prior to making the hydraulic conductivity measurements.

Table 3.3. Saturated Hydraulic Conductivity (K) of Sand Columns

	Before Treatment					After Treatment		
	K	K Avg.	K Stdev.	Bulk Density	Porosity	K	K Avg.	K Stdev.
Treatment	(cm/min)			(g/cm^3)	(cm^3/cm^3)	(cm/min)		
0.03 M $NaClO_4$	0.83	0.83	0.00	1.58	0.41	0.60	0.53	0.09
	0.83					0.43		
	0.83					0.56		
0.3 M NaOH	0.91	0.81	0.08	1.55	0.41	0.41	0.44	0.10
	0.77					0.37		
	0.77					0.56		
3 M NaOH-1	0.66	0.63	0.04	1.57	0.41	0.46	0.43	0.07
	0.59					0.35		
	0.63					0.49		
3 M NaOH-2	0.69	0.54	0.13	1.55	0.41	0.46	0.41	0.06
	0.48					0.34		
	0.44					0.43		

Hydraulic conductivity in the columns decreased with time in a systematic manner *prior* to the caustic treatments. This can only be a consequence of differences in how the columns were packed, and underscores the importance of measuring the condition of a column prior to treatment and not assuming that multiple columns can be packed identically. The effects of caustic treatment on this parameter can be assessed by evaluating the difference between the hydraulic conductivity before and after caustic treatment, i.e., $\Delta K = K_{\text{after trt.}} - K_{\text{before trt.}}$:

ΔK for the 0.03 M $NaClO_4$ column was –0.30 cm/min,

ΔK for the 0.3 M NaOH column was –0.37 cm/min,

ΔK for the 3.0 M NaOH – Rep. 1 column was –0.20 cm/min, and

ΔK for the 3.0 M NaOH – Rep. 2 column was –0.13 cm/min.

The ΔK data show that for all treatments, including the 0.03 M $NaClO_4$ control, there was a reduction in hydraulic conductivity after treatment. A change in the hydraulic conductivity in the control was not expected and it is not clear why the proportion of air-filled pores increased as a result of introducing the 0.03 M $NaClO_4$ treatment solution. The likely explanation is the centrifugation during the initial determination of moisture retention properties before the treatments were begun allowed the quartz particles to compact. The reduction in conductivity in the control was not attributable to precipitation, gel formation, or dissolution with compaction of the solid phase; it was caused by changes in the physical structure of the column. XMT data show that compaction and subsidence (length of solid filled portion of the packed column decreased) occurred during the ultracentrifugation that lead to a slight increase in the proportion of air-filled pores (Section 3.1.1.1), changes that should result in reduced hydraulic conductivity. The 0.3 M NaOH-treated column had a slightly greater reduction in hydraulic conductivity than the control. This observation suggests that more fine-grained particles might be present after caustic treatment but the data in Table 3.2 show just the opposite. Alternatively, as discussed below, the moisture retention data from the quartz sand from this column suggested that surface gels may have formed thus causing more drag on the solutions flowing through the pores.

The 3.0 M NaOH-treated quartz sand columns had less reduction in hydraulic conductivity than the control. The smaller reduction in hydraulic conductivity (or increased hydraulic conductivity with respect to the control) is likely attributable to the greater aggregation directly observed in the 3.0 M NaOH-treated sand columns. The larger aggregates would be expected to create larger pores. This smaller decrease in hydraulic conductivity versus the control, however, is barely larger than the variance in the individual determinations in the replicate analyses for the before- and after-treatment measurements (see Table 3.3 for details). During column dismantling after treatment, we realized it was impossible to accurately measure the volume of the columns that remained filled with sand and that some grains were inevitably lost during dismantling and the subsequent particle size measurements. Thus to get a final weight of sediment and final volume to determine the post-treatment bulk density and porosity was impossible. This total column dismantling approach to measuring bulk density and porosity is obviously less accurate than the XMT techniques discussed and shown in Figures 3.2, 3.3, and 3.4.

Moisture retention of the quartz sand before and after treatment was determined using tap water (see Figures 3.5, 3.6, and 3.7). Tap water was used instead of the caustic treatment solutions to minimize the influence the varying solutions would have on fluidity and, perhaps more important, surface tension. The intent of the moisture retention measurements was to quantify changes in the ability of the treated sediments to retain water, not to determine the influence of these solutions AND the treated sediment on moisture retention. Moisture retention in the 0 to 1 bar (0 to 1020 cm) pressure range is generally controlled by sediment structure, pore size distribution, and the sand-sized fraction. Moisture retention at pressures > 1 bar is typically associated with mineral surface characteristics and the clay-sized fraction (Hillel 1971).

There was no change in moisture retention characteristics before and after treatment with the 0.03 M $NaClO_4$ solution (Figure 3.5). For the 0.3 M NaOH treatment, there was more water retained for a given pressure (i.e., suction) in the after-treatment samples than in the before-treatment state (Figure 3.6). Greater moisture retention was especially evident at pressures > 1020 cm, suggesting there may have been more fine-grained materials. The particle size data in Table 3.2, however, do not support this premise. An alternative explanation for the change in moisture retention is based on possible changes in the mineral surface properties. Based on simple unaided visual inspection of the treated sand, it was clear that a great deal of change in the appearance of the quartz sand had occurred as a result of the 0.3 M NaOH treatment. Chemical polishing of the particle surfaces and the formation of gel coatings, resulting from mineral dissolution, are among the changes in surface properties that could result in increased moisture retention. Chemical polishing of the surface would remove rough edges, causing an increase in the surface potential, which in turn would increase the "wetability" of the surfaces (see Rafal et al. 1994). These changes in surface properties would lead to greater water retention. Gel coatings, likely composed of Al and Si, could trap water in their amorphous structure, again leading to greater water retention. Although the visual descriptions of the treated quartz sand suggest some surface coatings, only one SEM image was taken of these treated quartz sand samples, that shows mostly dissolution features not surface

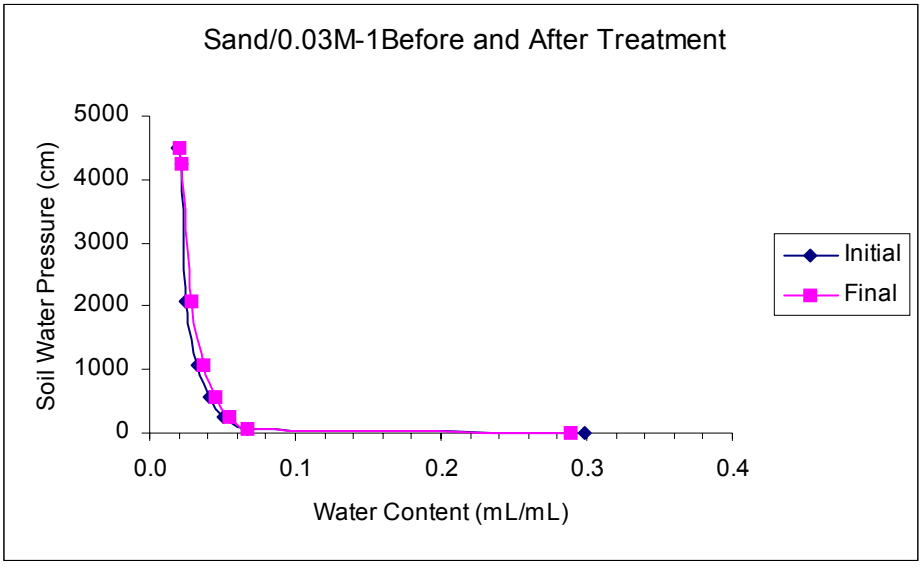

Figure 3.5. Moisture Retention Curve Before and After 0.03 M $NaClO_4$ Treatment of Sand

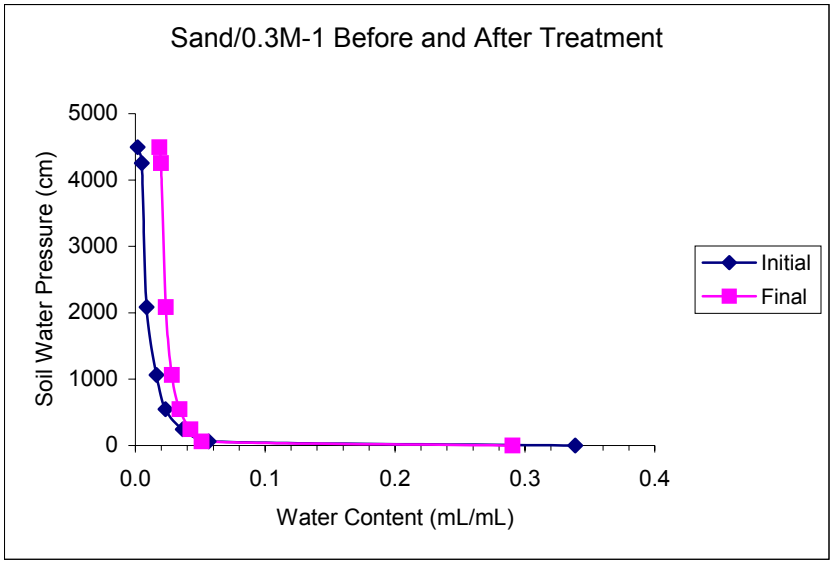

Figure 3.6. Moisture Retention Curve Before and After 0.3 M NaOH Treatment of Sand

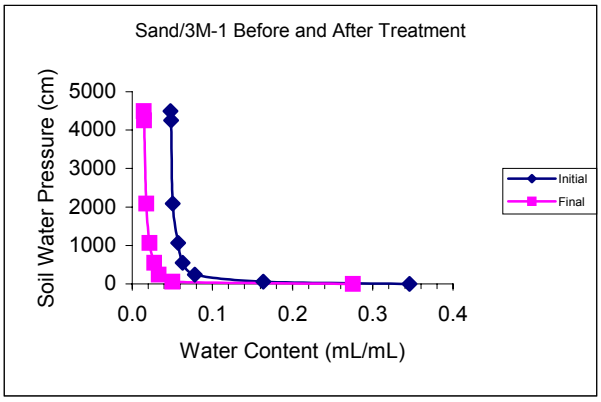

(a)

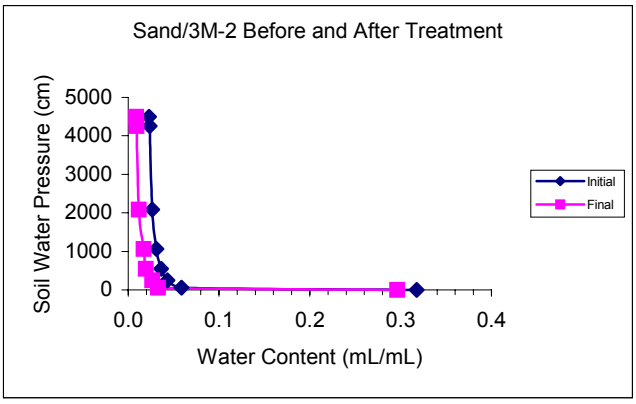

(b)

Figure 3.7. Moisture Retention Curve Before and After 3 M NaOH Treatment of Sand (2 Replicates)

coatings. Based on more numerous SEM images of quartz particles from the Warden Soil columns treated with the same solutions (for example Appendix A, Figure A.1), there appear to be more coatings in the 0.3 M NaOH treatment, than in either the 0.03 M $NaClO_4$ or the 3.0 M NaOH treatments. Other SEM images of the Warden silt loam not presented in this report also support this observation. Furthermore, there is no evidence of chemical polishing in the 0.3 M NaOH solutions. Additional SEM images of the 0.3 M NaOH treated quartz sand would be required to substantiate these observations and to ascertain whether they were biased by our expectations.

Additional discussion of the influence of these treatments on particle morphology is presented in Section 3.1.1.3.

For the 3.0 M NaOH-treated quartz sand, less water was retained for a given pressure in the after-treatment than in the before-treatment samples (Figure 3.7). This suggests that there was a coarsening in particle size and some agglomeration but little gel formation. The visual observations discussed above support these suggestions.

3.1.1.3 Mineralogy of the Sand Column Experiment

An XRD spectrum of the untreated Unimin sand is presented in Figure 3.8. Also included are library spectra for quartz (SiO_2), plagioclase feldspar, K-feldspar, and muscovite ($KAl_2(AlSi_3O_{10}(OH)_2$) used to facilitate identification of the peaks in the Unimin quartz sand spectrum. Semi-quantitative estimates of the mineralogy of the untreated Unimin sand based on this spectrum suggested the following composition:

90 wt.%	quartz
9 wt.%	feldspar
< 1 wt.%	muscovite.

Based on x-ray fluorescence analysis of the untreated Unimin sand (Table 3.4), a ranking of the elements by their concentration is:

$$Si >> Al > K = Mg = Na > Ca > Fe >> Ti = Cl > Mn = Cu.$$

An important conclusion drawn from these data is that the sand is not composed exclusively of quartz because it contains more than just oxygen and silicon; perhaps most important are the large concentrations of Al and K indicating that other mineral phases or amorphous impurities are likely present. For example, the Al and K concentrations could not be as large as found if the sample had less than 10% feldspar and muscovite.

In excess of 30 SEM images were taken of the untreated Unimin sand. As suggested by the XRD data, most of the particles were quartz. An example of the SEM images taken of the untreated Unimin sand is presented in Figure 3.9. The zircon inclusions, although not common, are shown as examples of the various types of inclusions (Cu-, Ti-, and Zr-phases) present in the sand.

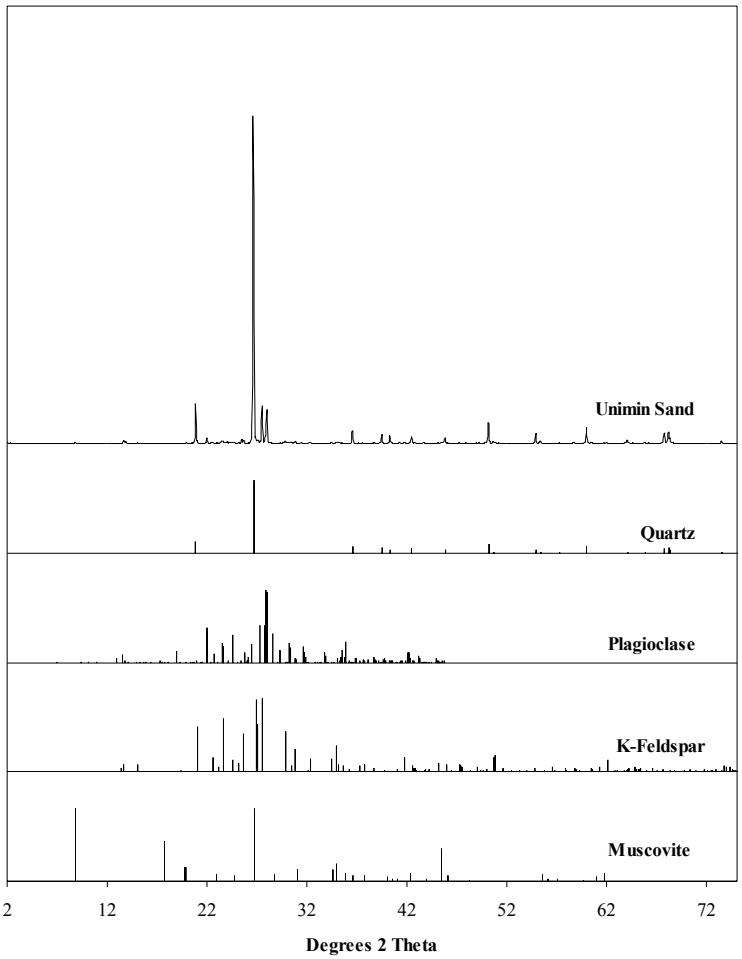

Figure 3.8. XRD Spectrum of the Untreated Unimin Sand and Reference Spectra for Quartz, Plagioclase, K-feldspar, and Muscovite

Table 3.4. X-ray Fluorescence Analysis Results for the Untreated Unimin Sand

Element[(a)]	Unit	Concentration	Standard Deviation	Concentration as Oxides wt.%
Al	%	2.73	0.25	5.158
Si	%	40	2	85.57
Cl	%	0.051	0.008	0.051
K	%	2.07	0.1	2.493
Ca	%	0.12	0.008	0.168
Na	%	1.94	0.002	2.62
Mg	%	2.09	0.001	3.46
Ti	%	0.072	0.004	0.120
Mn	ppm	36.8	7.2	0.005
Fe	%	0.108	0.006	0.154
Cu	ppm	7.8	1.6	0.001
Total				99.80
(a) Below detection limit concentrations were measured of P, S, V, Cr, Co, Ni, Hg, Se, As and Br.				

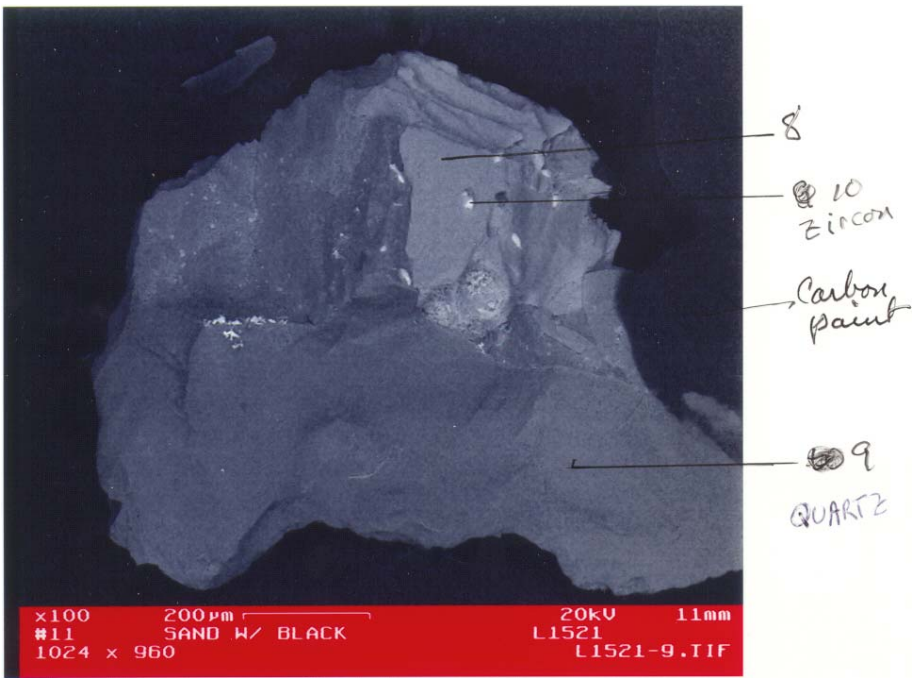

Figure 3.9. SEM Image of a Unimin Sand Particle; Spots 8 and 9 Were Identified by EDX as Quartz; Spot 10 as Zircon

Upon treatment with NaOH, the minerals became hole-ridden (Section 3.1.1). SEM images of particles with and without 0.3 M NaOH treatment are shown in Figure 3.10. The morphology of the particles is strikingly different: the untreated surface is smooth, whereas the treated surface is greatly undulated. The other observation made during examination of the column sand after the 194-day treatment was that there was an increase in the occurrence of black particles (Section 3.1.1). Based on energy dispersive x-ray (EDX) analyses, these particles have a chemical composition similar to ilmenite, $FeTiO_3$. Ilmenite is largely resistant to dissolution by NaOH (see Amer 2002; de Andrade et al. 1997; McKinley et al. 1986 for example), and its increase in concentration in the NaOH-treated quartz sand is the result of dissolution of other particles, not the precipitation of additional ilmenite.

3.1.1.4 Effluent Chemistry of the Sand Column Experiment

The effluent of one quartz-sand column from each treatment (three columns total) was chemically characterized as a function of time. Approximately 30 mL of effluent sample were collected from each column on days 0, 7, 14, 21, 28, 61, 95, 122, 150, and 180. These samples, typically collected over a 30-hr period, provided elemental compositions for distinct times throughout the experiment. Additionally, as described in the Materials and Methods Section, the effluent between each sampling episode was collected from the individual columns, resulting in six composite samples for each column (0-28, 28-60, 61-90, 95-120, 121-150, and 151-180 days). These composite samples provided average elemental concentrations over the range of days in which the sample was collected. Measurements including pH, free hydroxide concentration, carbonate content, and cation concentrations were conducted on the samples collected at distinct times. The composite samples were characterized for metals. Data representing the various measurements on both types of samples are presented in Figures 3.11 through 3.17.

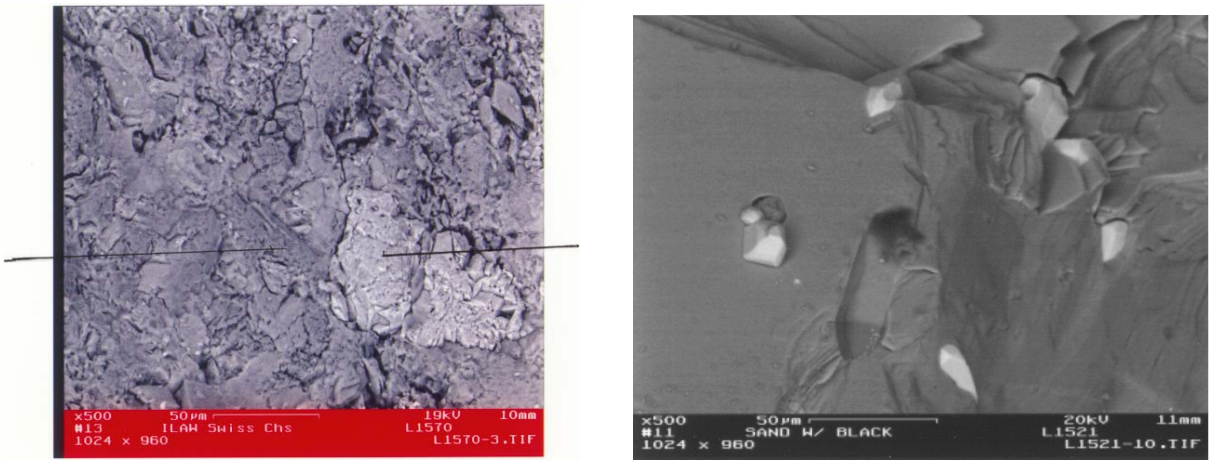

Figure 3.10. Top - SEM Image (500x magnification) of Hole-Ridden Quartz Particle Recovered After 0.3 M NaOH Treatment; Bottom – SEM Image (500x magnification) of Untreated Quartz Particle

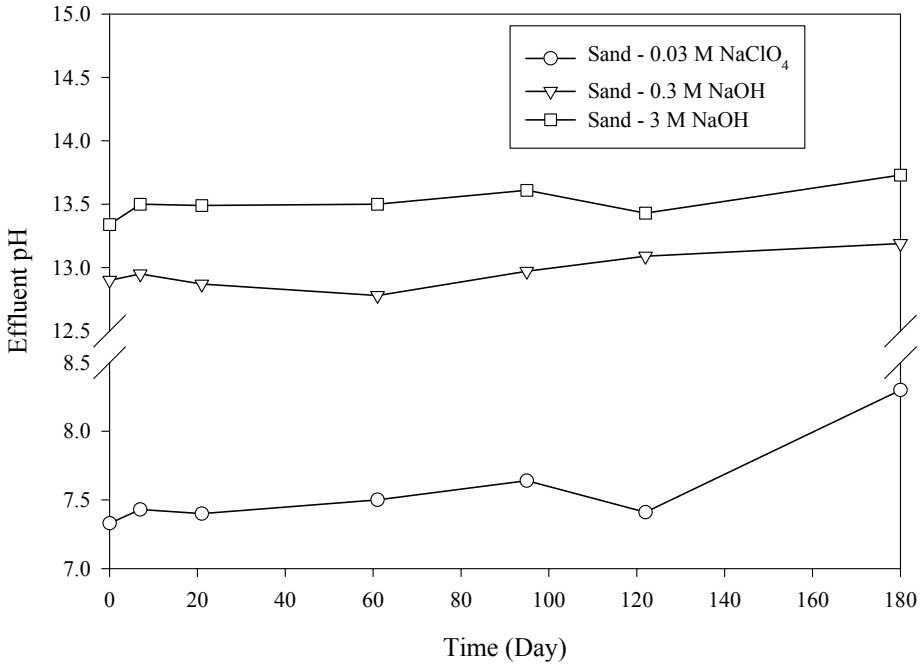

Figure 3.11. Effluent pH From the Control and NaOH-Treated Quartz Sand Columns

Overall, the pH measurements of the effluent from the quartz columns on sampling days 0, 7, 21, 61, 95, 122, and 180 did not vary greatly during the study (Figure 3.11). The 0.03 M $NaClO_4$ treatment had a pH of about 7.5 for most of the duration. At the 180-day sampling, however, the pH had increased to 8.30. This increase cannot be explained. The 0.3 M NaOH treatment had a starting pH of 12.90 and slowly increased to a pH of 13.20 at the 180-day sampling. Columns #3 and #4, the 3 M NaOH treatment, had an initial pH of 13.34 and steadily increased to a pH of 13.74 (Figure 3.11).

Concentrations of Si, Al, Fe, and K in the effluent solutions were measured and are presented in Figures 3.12, 3.13, 3.14, and 3.15. The individual data points represent the samples collected on distinct days whereas the data points with the horizontal bars represent the samples collected as composites over each ~30-day interval. Generally, the effluent from the NaOH-treated columns showed an initial increase in metal concentrations within the first seven days of starting the experiment. Figure 3.12 shows Si concentrations were highest at the 7-day sampling for both NaOH treatments. After this initial spike, the Si concentrations gradually decreased during the remainder of the study. The Si concentrations from the composite samples match well with the individual data points in both NaOH-treated columns. Effluent from the sodium perchlorate control remained low in Si throughout the experiment.

As with Si, the Al and Fe effluent concentrations from the NaOH treatments increased dramatically during the first 7 days (see Figures 3.13 and 3.14). After this initial spike, the Al concentration tended to decrease, with the exception of the 90-day Al concentration in the 0.3 M NaOH treatment, which is probably a bad data point. As will be discussed in more detail in Section 3.1.2.4, the Si:Al ratio in the effluents remained nearly constant at 4:1 throughout the Warden silt loam column study. This same ratio is also observed in the quartz sand columns' effluents, except for the 90-day sample from the 0.3 M NaOH treatment, thus this data point is suspect. The Al concentration in the control remained low throughout the experiment. As discussed in Section 3.1.1.3, feldspar impurities and trace levels of mica in the quartz sand are the most likely source of the dissolved Al in these caustic attack tests. The source of the Fe is likely ferric oxide particle coatings or other iron impurities in the quartz sand.

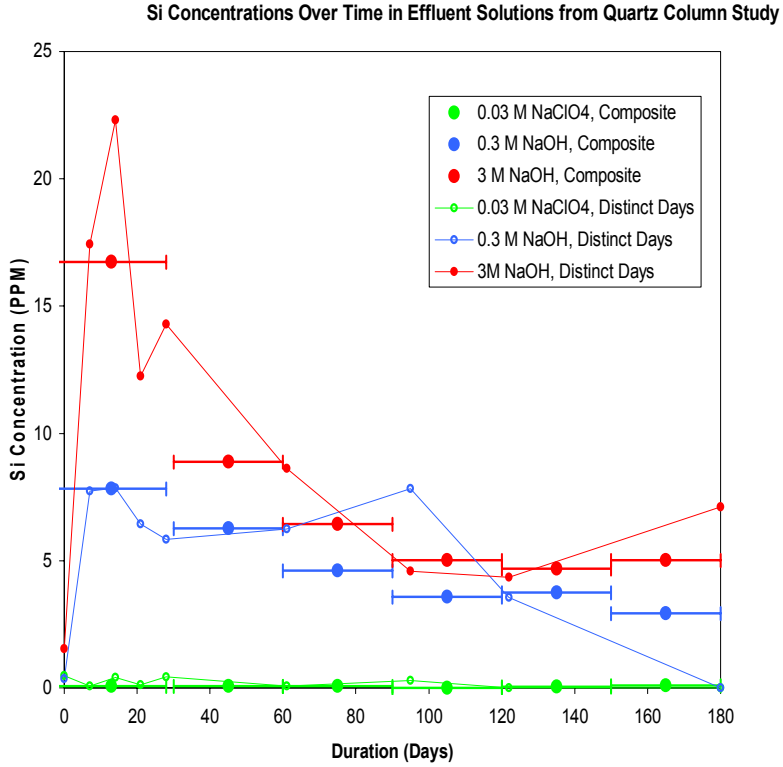

Figure 3.12. Effluent Si Concentrations in the Control and NaOH-Treated Quartz Sand Columns

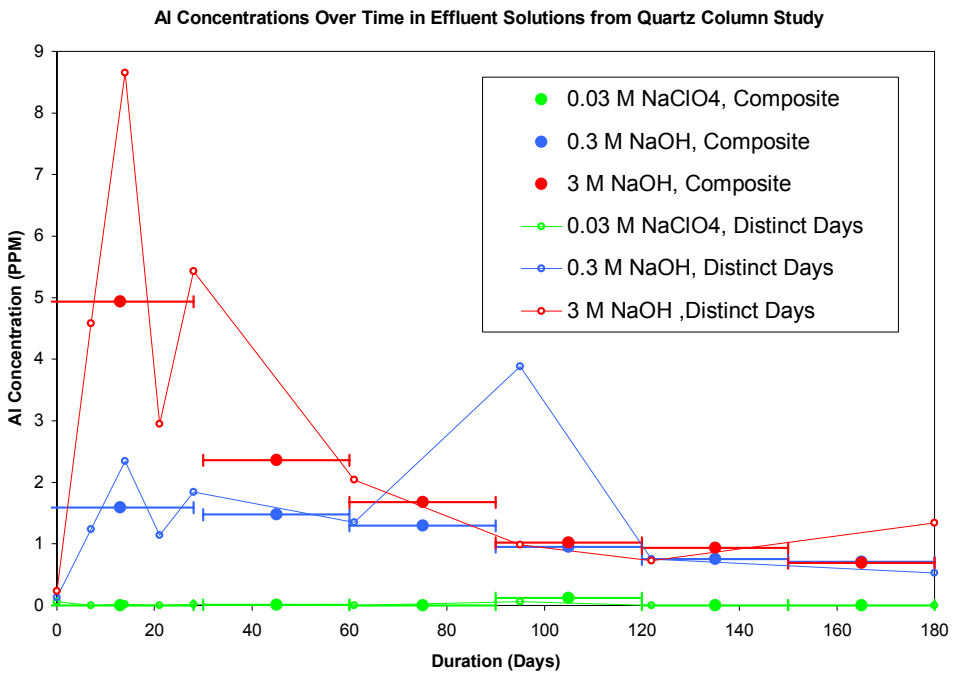

Figure 3.13. Effluent Al Concentrations in the Control and NaOH-treated Quartz Sand Columns

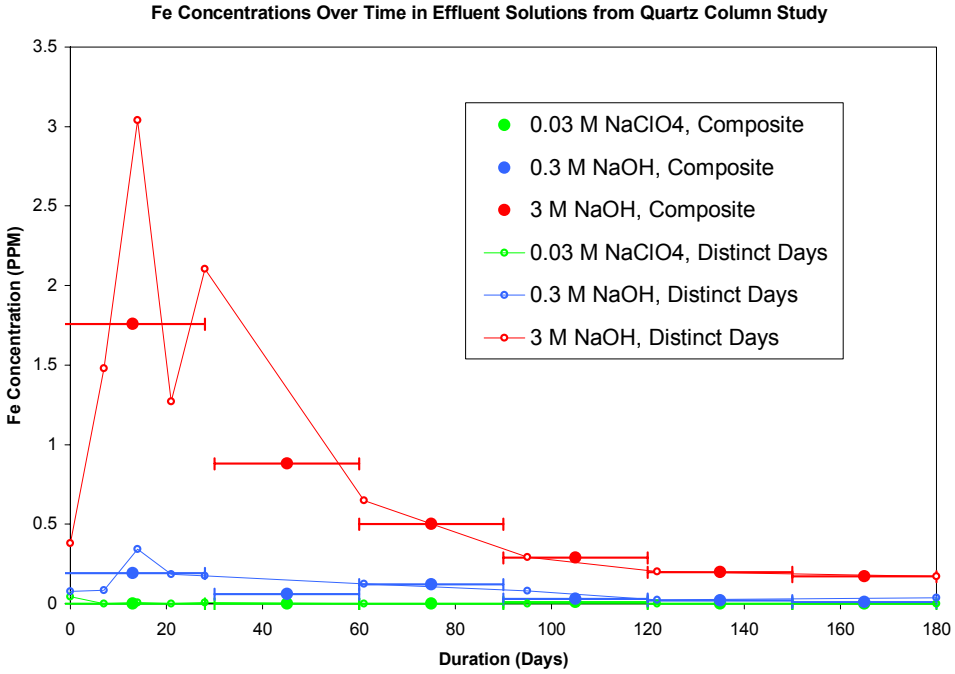

Figure 3.14. Effluent Fe Concentrations in the Control and NaOH-treated Quartz Sand Columns

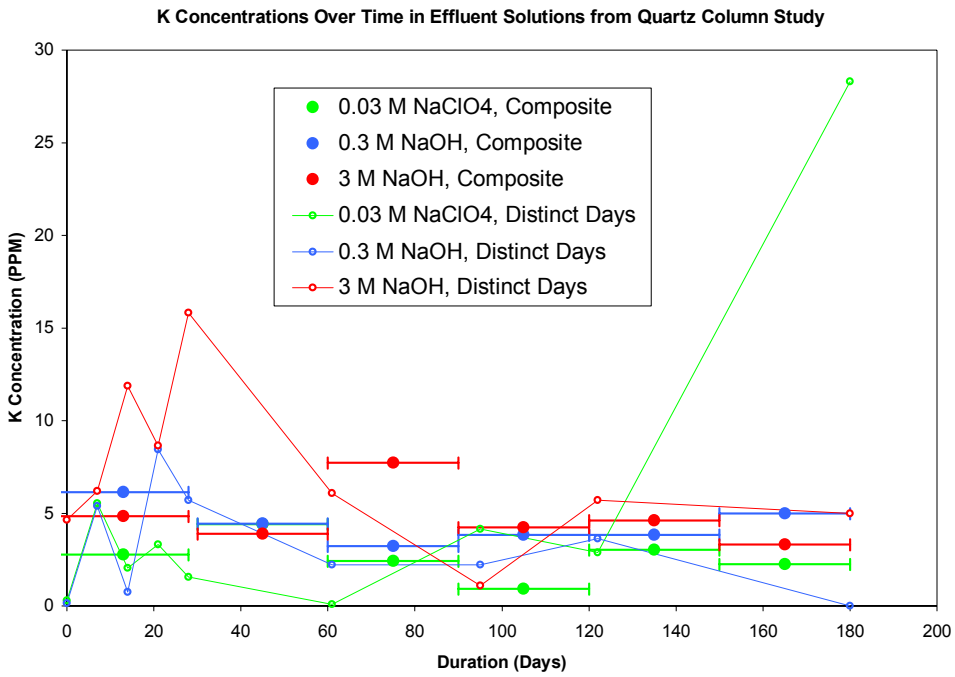

Figure 3.15. Effluent K Concentrations in the Control and NaOH-treated Quartz Sand Columns

Potassium concentrations in the NaOH treatment effluents are slightly higher than the control between 20 and 60 days of treatment but before and after this time period the caustic experiments do not appear to dissolve much K (see Figure 3.15). It is difficult, however, to analyze K in high salt solutions with ICP-OES, and the high detection limit on these effluent samples impacts any conclusions that might be drawn from the data. The most probable source of the K is likely caustic attack on the feldspar minerals and, to some degree, the mica.

The effluent carbonate concentrations from the 3.0 M NaOH treatment increased to about 40,000 mg/L after only 7 days, and then decreased over the remainder of the study (see Figure 3.16). This increase in carbonate concentration occurred even though the pH increased only moderately from pH 13.4 to 13.5. The carbonate concentration of the 0.3 M NaOH treatment was greater than that of the control (0.03 M $NaClO_4$ treatment) and the concentration in both these treatments did not change greatly over the whole test period. As expected, the free hydroxide concentrations in the 3.0 M NaOH treatment were greater than in the 0.3 M NaOH treatment, which in turn were greater than the control column tests (see Figure 3.17). This trend is consistent with the pH data. The free hydroxide concentrations were generally about an order of magnitude greater in the 3.0 M NaOH treatment than in the 0.3 M NaOH treatment, consistent with the difference in the amount of hydroxide in the influent (the low free hydroxide value measured in the 3.0 M NaOH treatment at 7 days is suspect and likely an analytical error). As discussed in more detail in Section 3.1.2.4, the free-hydroxide concentrations remained largely constant during the Warden silt loam soil column study. Based on the large number of similar trends between the effluent chemical composition of the quartz sand and Warden silt loam columns, it is likely this free-hydroxide value for the 7-day 3.0 M NaOH treatment is incorrect.

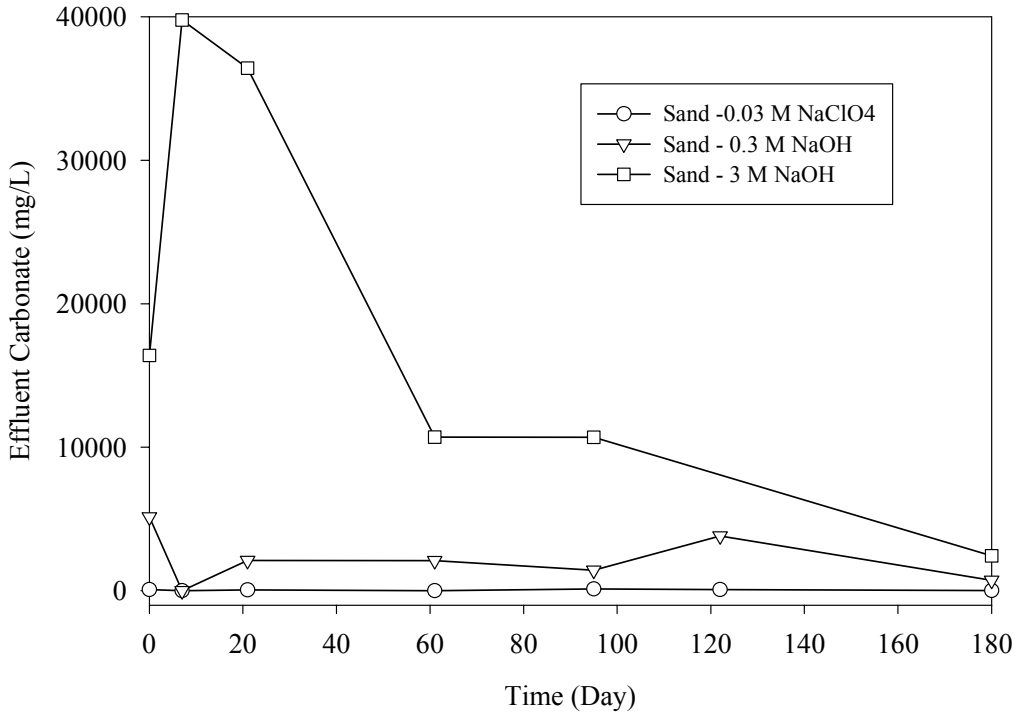

Figure 3.16. Effluent Carbonate Concentrations [as mg/L $CaCO_3$] in the Control and NaOH-treated Quartz Sand Columns

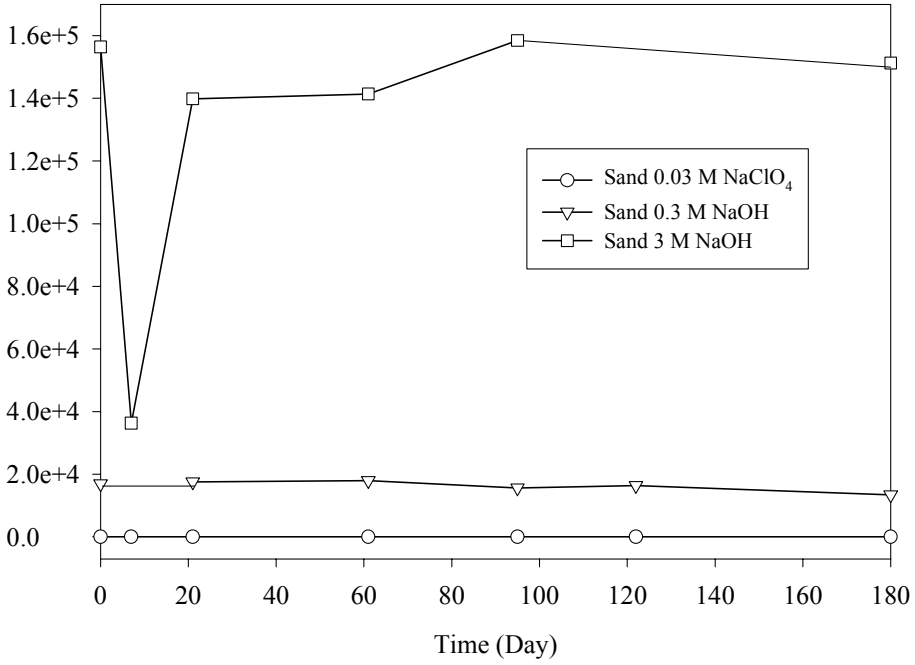

Figure 3.17. Free-hydroxide Concentrations [as mg/L $CaCO_3$] in the Control and NaOH-treated Quartz Sand Column Effluents

We had the dry starting and ending masses of sediment and the complete mass of major constituents in the starting treatment solutions and effluents such that mass balance calculations were possible. In general, the mass of quartz sand left over after about one year of treatment with caustic or the neutral control solutions ranged between 98.3 and 99.4 % of the starting mass. When we add in the small amount of material leached (based on Al, Si, Fe, Ca, K, and excess Na leached) and assume no back reactions (such as precipitation of calcite) the unaccounted mass is less than 0.4 g out of ~35 g starting mass in each quartz sand column. Very little mass (~0.07 g) was lost by dissolution reactions. Most of the missing mass was lost during the column dismantling and particle size distribution activities.

In summary, caustic treatment of the quartz sand caused small but measurable changes in the hydraulic conductivity and moisture retention properties, likely due to dissolution of solids with concomitant formation of gels (in the 0.3 M NaOH treatment) and particle agglomeration (in the 3 M NaOH treatment). The effluent cation concentrations suggest that the 3 M NaOH treatment dissolves more solid but does not necessarily cause the formation of more gel within the remaining particles. The hydraulic conductivity of all the quartz columns, including the controls, decreased because of compaction. The compaction may have been an artifact of using the UFA centrifuge technique to perform the moisture retention measurements. The hydraulic conductivity of the 3 M NaOH treatment decreased the least and these columns showed the largest increase in void space because of mass dissolution. On the other hand, the 3 M NaOH treatment seems to cause less change in moisture retention than the 0.3 M NaOH treatment suggesting that stronger hydroxide treatment may lower the amount of gel that coats grain surfaces.

3.1.2 Warden Soil Column Experiment

Once the soil columns were treated and the measurements requiring intact cores were completed, the contents from each column were poured onto an individual piece of white paper and observations were recorded. The purpose of these observations was to note the qualitative changes caused by the treatments.

0.03 M $NaClO_4$ – Columns #5 and #6: Some large voids were observed and appeared to be caused by water channeling. No color differences were observed between treated and untreated soil samples.

0.3 M NaOH – Columns #7, #8, and #9: Many more aggregates existed in these treated soils than in the controls (0.03 M $NaClO_4$). These aggregates were very hard and did not break apart when treated with water and pressed with a rubber stopper suggesting cementation had occurred. As with the 0.03 M $NaClO_4$ treatments, there were voids in the columns of soil, perhaps the result of flow channeling. In replicate #8, some reddish-brown coloration appeared in the bottom half of the column (the influent end of the column).

3.0 M NaOH – Columns #10, #11, and #12: Very large voids existed; e.g., in #10, a 0.5-cm-diameter void existed between 6.8 and 7.5 cm in depth. In #11, a 0.2 cm-diameter void existed between 4.2 and 5.4 cm in depth and a second void of ~1-cm diameter existed between 6.8 and 7.2 cm in depth. The soil was very soft; during wet sieving, it turned to a jelly-like slime making sieving difficult and requiring additional deionized water.

After the visual observations were completed, the replicate column material from each treatment was combined to form three treated-sediment samples for the particle size and mineralogy work described below.

3.1.2.1 Physical Properties of the Warden Soil Column Experiment

Particle size distribution of the Warden soil was measured after treatment by the combined wet-sieve and hydrometer methods and the results are shown in Table 3.5. Compared to the 0.03 M $NaClO_4$ treatment (the control), the 0.3 M NaOH particle size distribution had a very slightly greater silt (0.002 to 0.05 mm) fraction, with concomitant decreases in the percentage of particles in the larger size fractions. The silt-sized fraction also increased in the 3.0 M NaOH-treated soils. Concomitant decreases occurred in almost all other size classes for the 3.0 M NaOH-treated soil. The silt-sized fraction of the 3.0 M NaOH-treated soil was 17% greater than that in the control. Of particular interest was that very little clay-sized material remained in the 3.0 M NaOH-treated soil after treatment. We are not confident, however, that the suspensions used to disperse the individual particles were completely effective and some clay-sized particles may have agglomerated and settled with the larger silt particles. As mentioned, the 3 M NaOH soil particles turned slimey during the wet sieving.

3.1.2.2 Hydraulic Properties of the Warden Soil Column Experiment

The hydraulic conductivity of each of the eight Warden silt loam soil columns was measured both prior to and after treatment (Table 3.6). The initial hydraulic conductivities were measured three times over a period of several days. Differences in hydraulic conductivity caused by variations in column packing can best be seen in column #3 of Table 3.6, which lists the average hydraulic conductivity of the columns prior to caustic treatment. The hydraulic conductivity ranged from 5.96e-3 to 16.8e-3 cm/min. This range is typical for natural fine-grained Hanford sediments (Meyer and Serne 1999; Khaleel 1999; Khaleel and Freeman 1995; Rockhold et al. 1993). Nevertheless, because the sediment samples were homogeneous, the hydraulic conductivities should all have been the same if the columns were all packed

Table 3.5. Particle Size Distribution (wt.%) of the Warden Soil After Treatment with $NaClO_4$ or NaOH

Sieve #	Particle Size Fraction (mm)	Treatment[(a)], wt.%		
		0.03 M $NaClO_4$	0.3 M NaOH	3.0 M NaOH
10	> 2	0 ± 0	0 ± 0	0 ± 0
18	1 to 2	1 ± 0	1 ± 0	1 ± 0
35	0.5 to 1	2 ± 0	3 ± 1	1 ± 0
60	0.25 to 0.5	2 ± 0	3 ± 1	1 ± 0
140	0.106 to 0.25	9 ± 0	8 ± 1	7 ± 1
200	0.075 to 0.106	14 ± 0	12 ± 1	12 ± 1
270	0.05 to 0.075	15 ± 0	13 ± 1	14 ± 1
Silt	0.002 to 0.05	54 ± 1	56 ± 2	63 ± 2
Clay	< 0.002	4 ± 1	3 ± 2	<1 ± 0

(a) Average ± standard deviation of 2 replicates for 0.03 M $NaClO_4$, and 3 replicates for 0.3 M NaOH and 3.0 M NaOH.

Table 3.6. Hydraulic Conductivity (K), Porosity, and Bulk Density of the Warden Soil

Before Treatment						After Treatment	
Treatment	K	K Avg.	K Stdev.	Bulk Density	Porosity	K	$\Delta K = K_{aft} - K_{before}$
	(cm/min)			(g/cm^3)	(cm^3/cm^3)	(cm/min)	
#5; 0.03 M $NaClO_4$	1.08E-02	9.47E-03	1.12E-03	1.64	0.41	4.62E-05	-9.42E-03
	8.76E-03						
	8.89E-03						
#6; 0.03 M $NaClO_4$	1.97E-02	1.56E-02	3.54E-03	1.64	0.41	4.22E-04	-1.52E-02
	1.37E-02						
	1.34E-02						
#7; 0.3 M NaOH	7.56E-03	7.55E-03	2.52E-04	1.61	0.42	4.99E-03	-2.56E-03
	7.29E-03						
	7.80E-03						
#8; 0.3 M NaOH	1.70E-02	1.68E-02	5.37E-04	1.59	0.43	3.01E-03	-1.38E-02
	1.62E-02						
	1.72E-02						
#9; 0.3 M NaOH	1.02E-02	8.82E-03	1.34E-03	1.63	0.41	1.93E-04	-8.63E-03
	8.61E-03						
	7.59E-03						
#10; 3 M NaOH	7.07E-03	6.88E-03	3.62E-04	1.61	0.42	9.91E-03	+3.03E-03
	6.46E-03						
	7.10E-03						
#11; 3 M NaOH	1.70E-02	1.51E-02	1.86E-03	1.60	0.42	5.45E-05	-1.50E-02
	1.49E-02						
	1.33E-02						
#12; 3 M NaOH	7.01E-03	5.96E-03	9.26E-04	1.65	0.40	3.18E-04	-5.64E-03
	5.24E-03						
	5.64E-03						

identically. After treatment, the hydraulic conductivity values for all the treatments, including the control (0.03 M $NaClO_4$ treatment), decreased with respect to their pre-treatment values as shown by the ΔK values in Tables 3.6 and 3.7. Given that the control columns showed the greatest change (decrease) in hydraulic conductivity, the changes in this parameter cannot be attributed solely to NaOH treatment. This is surprising in light of the gross differences in the appearance of the soil after treatment (Section 3.1.2). Upon further review we found that some flow limitations occurred because the column apparatus itself limited flow (data not shown). This is of course undesirable in that the objective was to measure the

Table 3.7. Treatment Averages of Hydraulic Conductivity Values (cm/min) of the Warden Soil

		Before		After		ΔK, Before K – After K	
	# Rep	K Avg.	K Stdev.	K Avg.	K Stdev.	ΔK Avg.	ΔK Stdev.
Soil/0.03 M $NaClO_4$	2	1.26E-02	4.09E-03	2.00E-04	2.83E-04	-1.23E-02	4.10E-03
Soil/0.3 M NaOH	3	1.11E-02	4.40E-03	2.73E-03	2.41E-03	-8.33E-03	5.60E-03
Soil/3.0 M NaOH	3	9.30E-03	4.47E-03	3.43E-03	5.60E-03	-5.87E-03	9.00E-03

hydraulic conductivity of the soil, not that of the apparatus and the soil as a unit. Thus the data in Tables 3.6 and 3.7 should not be used in a quantitative sense.

There were several impediments to measuring the total weight and volume of the solids in the column after treatment. Thus we could not get an accurate final measure of the weight or volume of the soil. As noted above, however, void spaces were observed in the treated columns upon dismantling so volume was obviously reduced. Further, as discussed below, there were significant quantities of Al, Si, Ca, and other constituents leached out of the soil so indeed mass was lost during the NaOH treatments.

Moisture retention for each column was measured before and after caustic treatment (see Figures 3.18 through 3.25). The overall trends, although not the absolute values, in moisture retention for the Warden silt soil were similar in many respects to those for the quartz sand after treatment (Section 3.1.1.2). The most important similarities between the sand and soil columns were that moisture retention increased after the 0.3 M NaOH treatment and decreased after the 3.0 M NaOH treatment. Another important finding for the soil columns was that there was little difference in the moisture retention curves between treatment replicates.

For the 0.03 M $NaClO_4$ tests (i.e., the controls), a 2-3% increase in moisture retention was measured after treatment, compared to the before-treatment samples (see Figures 3.18 and 3.19). Ideally, there should be no change in the moisture retention capacity for the control before and after treatment, as was observed in the quartz sand columns. Thus this was an unexpected result. Compaction during centrifugation, as qualitatively measured by XMT, may be responsible for the increase in moisture retention rather than the 0.03 M $NaClO_4$ treatment.

Similarly, the soil retained more moisture after treatment with 0.3 M NaOH than prior to treatment (see Figures 3.20 through 3.22), thus some of the change in moisture retention can be attributed to an experimental artifact, likely compaction during centrifugation. The increase in moisture retention, however, is appreciably greater in the 0.3 M NaOH-treated columns than in the 0.03 M $NaClO_4$ control columns. This suggests that the caustic treatment had some influence on moisture retention. Greater moisture retention is characteristic of soils containing more small-grained particles or soils with gel coatings. The latter explanation was our hypothesis.

The soil retained less moisture after treatment with 3.0 M NaOH than prior to treatment (see Figures 3.23 through 3.25). This trend was consistent in all three replicates. Less moisture retention is characteristic of soils containing fewer small-grained particles, a finding reported for this treatment (see Table 3.5). Upon visual inspection of the 3 M NaOH columns during wet sieving, it was observed that

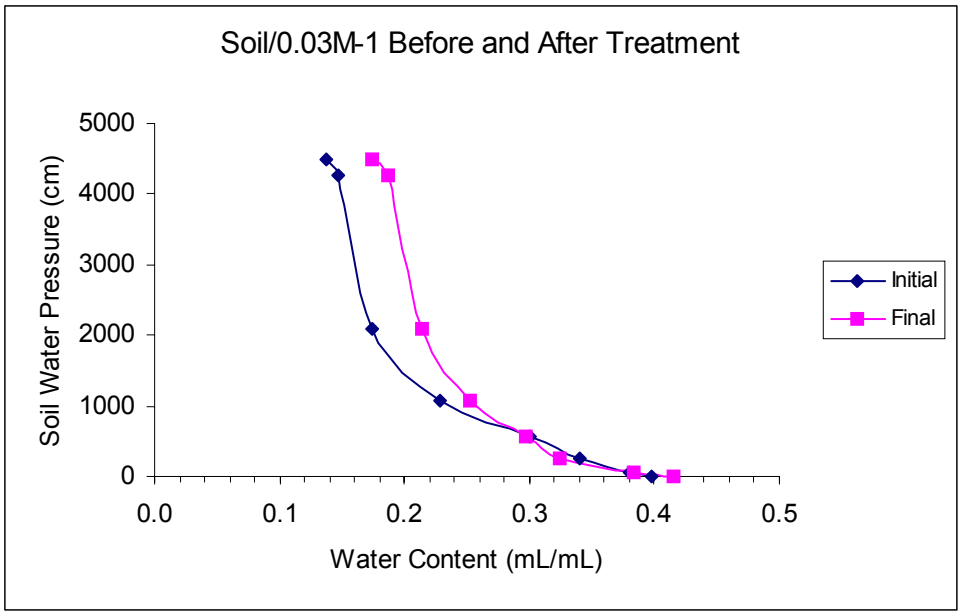

Figure 3.18. Moisture Retention Curve of the Warden Soil Before and After 0.03 M $NaClO_4$ Treatment, Column 5

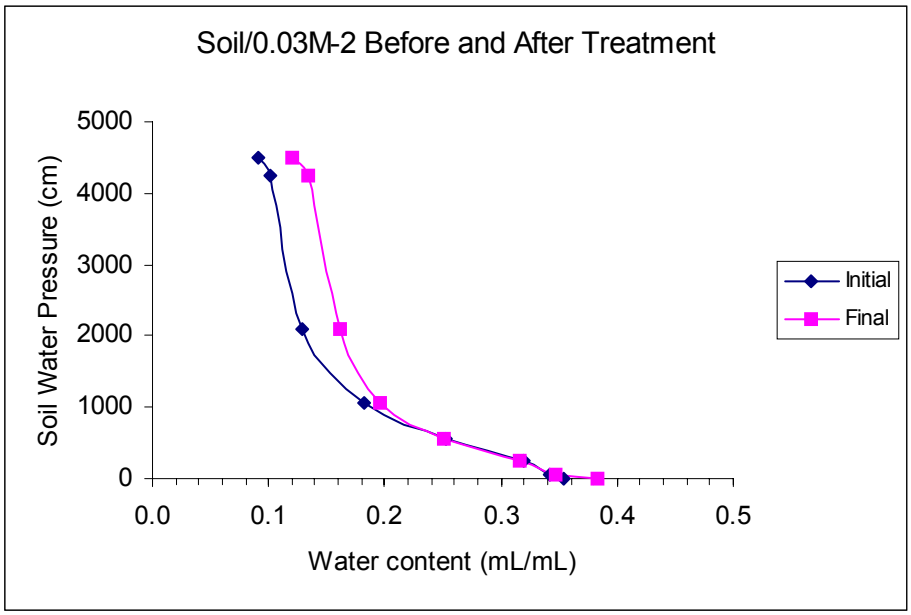

Figure 3.19. Moisture Retention Curve of the Warden Soil Before and After 0.03 M $NaClO_4$ Treatment, Column 6

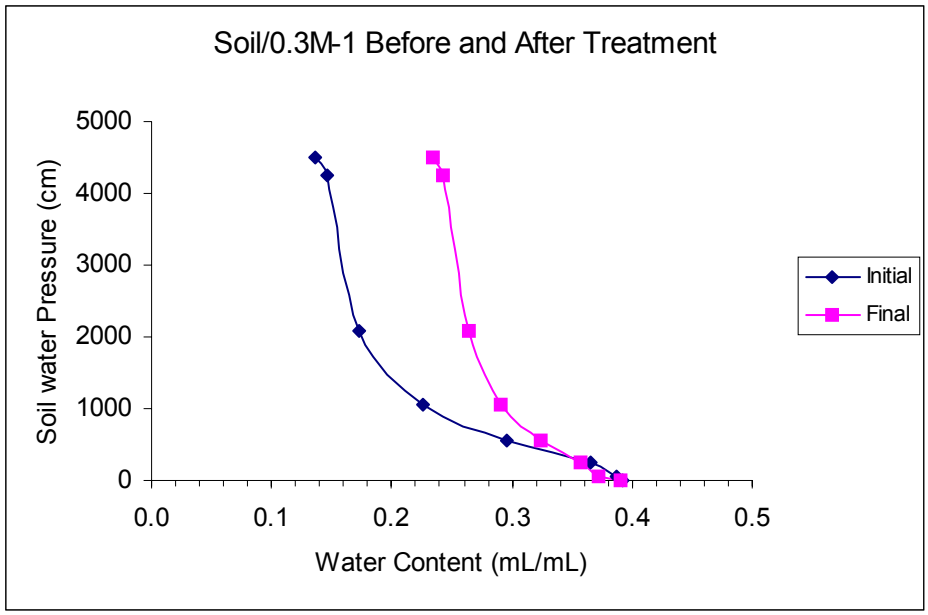

Figure 3.20. Moisture Retention Curve of the Warden Soil Before and After 0.3 M NaOH Treatment, Column 7

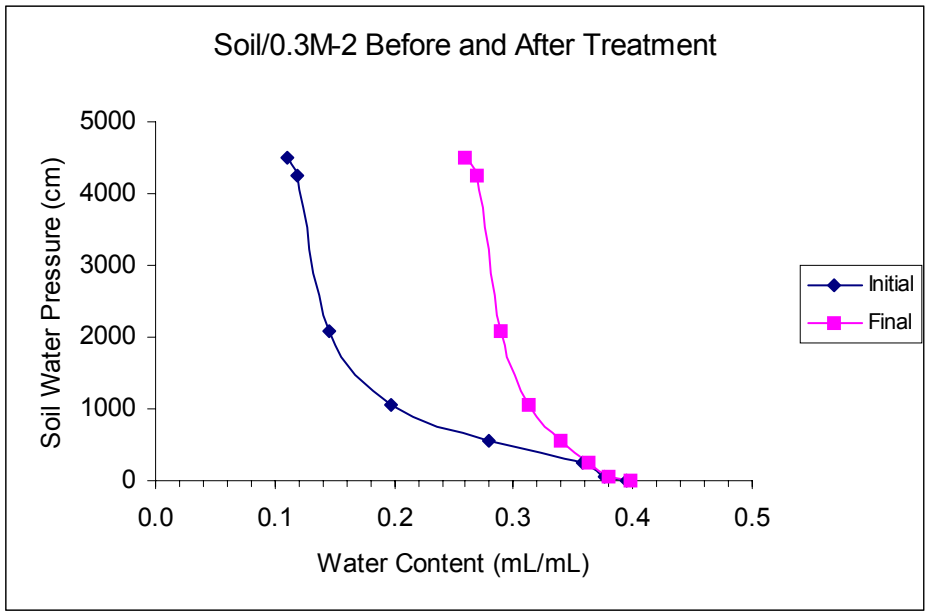

Figure 3.21. Moisture Retention Curve of the Warden Soil Before and After 0.3 M NaOH Treatment, Column 8

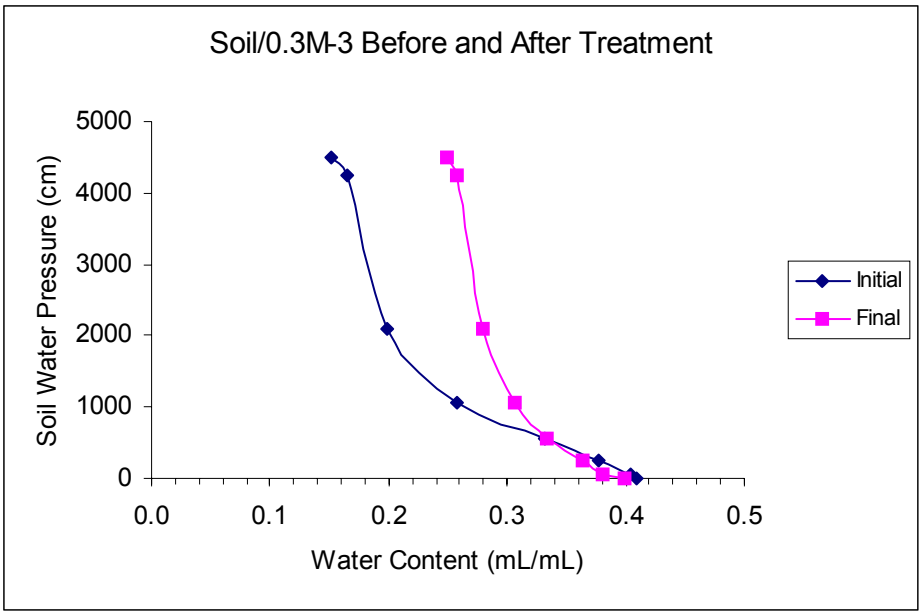

Figure 3.22. Moisture Retention Curve of the Warden Soil Before and After 0.3 M NaOH Treatment, Column 9

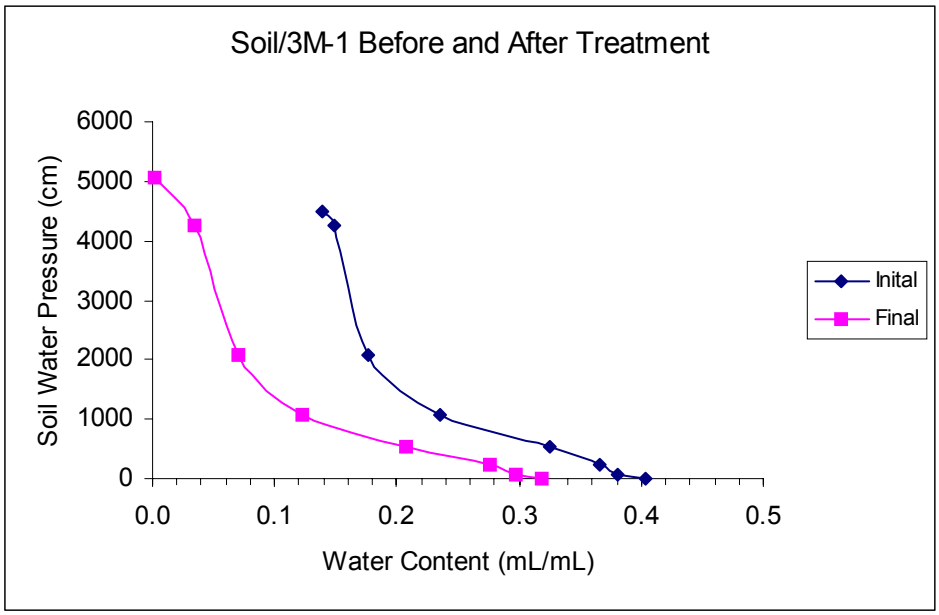

Figure 3.23. Moisture Retention Curve of the Warden Soil Before and After 3 M NaOH Treatment, Column 10

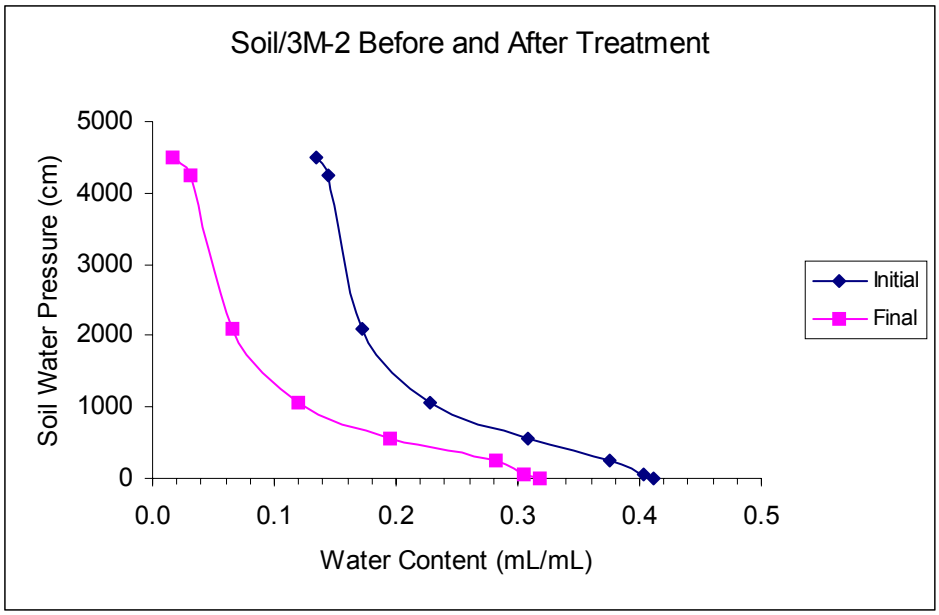

Figure 3.24. Moisture Retention Curve of the Warden Soil Before and After 3 M NaOH Treatment, Column 11

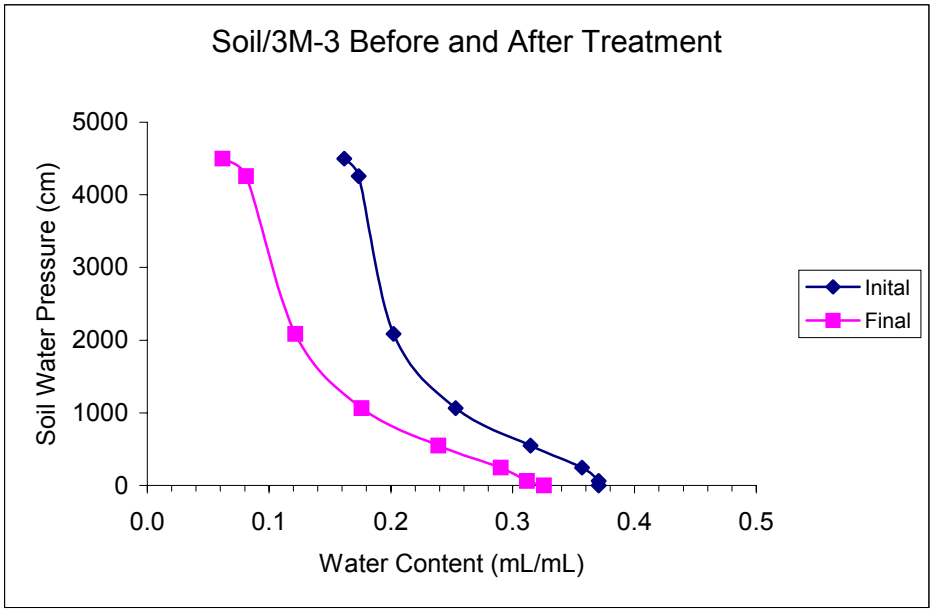

Figure 3.25. Moisture Retention Curve of the Warden Soil Before and After 3 M NaOH Treatment, Column 12

the soil cores had become a gelatinous jelly-like "mush" (Section 3.1.2). The particle size distribution data for the 3 M NaOH-treated soil showed an increase in silt concentrations whereas nearly all of the clay, which constitutes ~4 wt % of the untreated soil, had disappeared, either as a result of dissolution or aggregation into silt-sized particles.

3.1.2.3 Mineralogy of the Warden Soil Column Experiment

XRD analysis of the clay (< 2 μm) fraction from the Warden silt loam soil column experiments is presented in Figure 3.26 (random mounts) and Figure 3.27 (oriented mounts). The top four patterns in Figure 3.26 are the clay fractions from the untreated sediment and the following treatments: 0.03 M $NaClO_4$, 0.3 M NaOH, and 3.0 M NaOH. The bottom five patterns in Figure 3.26 were generated from the designated reference minerals and can be used for mineral identification. Patterns in Figure 3.27 are

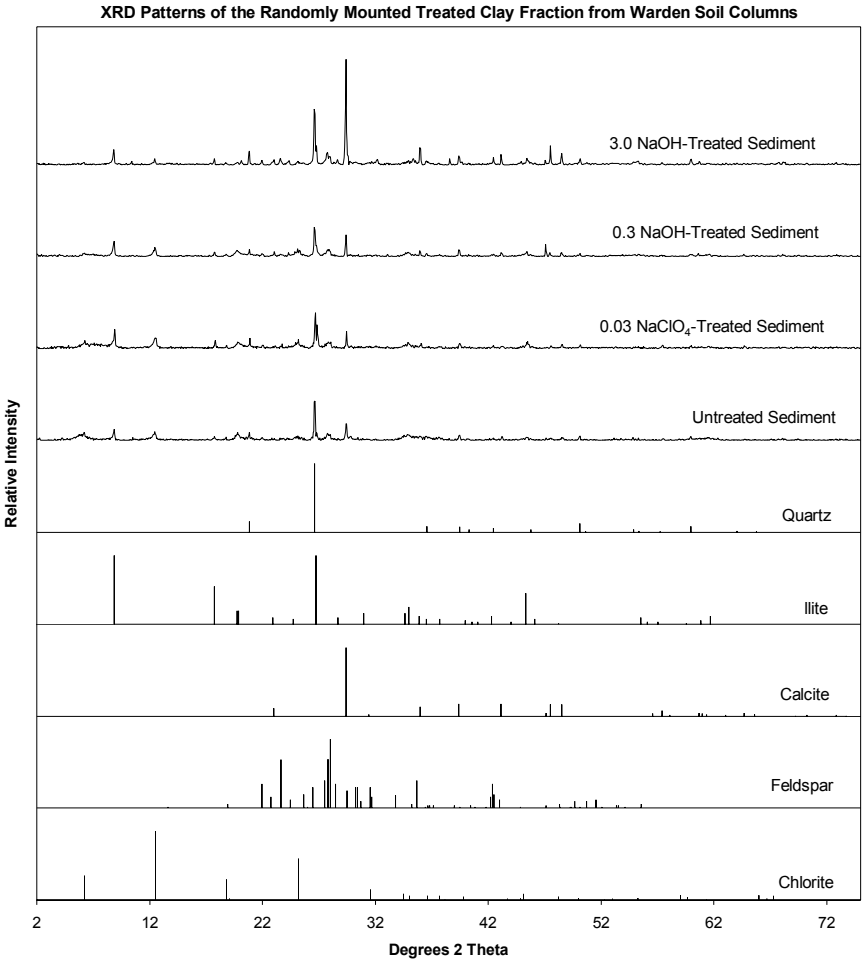

Figure 3.26. XRD Patterns of Randomly Mounted Clay Fractions Scanned From 2 to 75° 2θ Using Cu K_α Radiation (Bottom Five Patterns Are Reference Spectra)

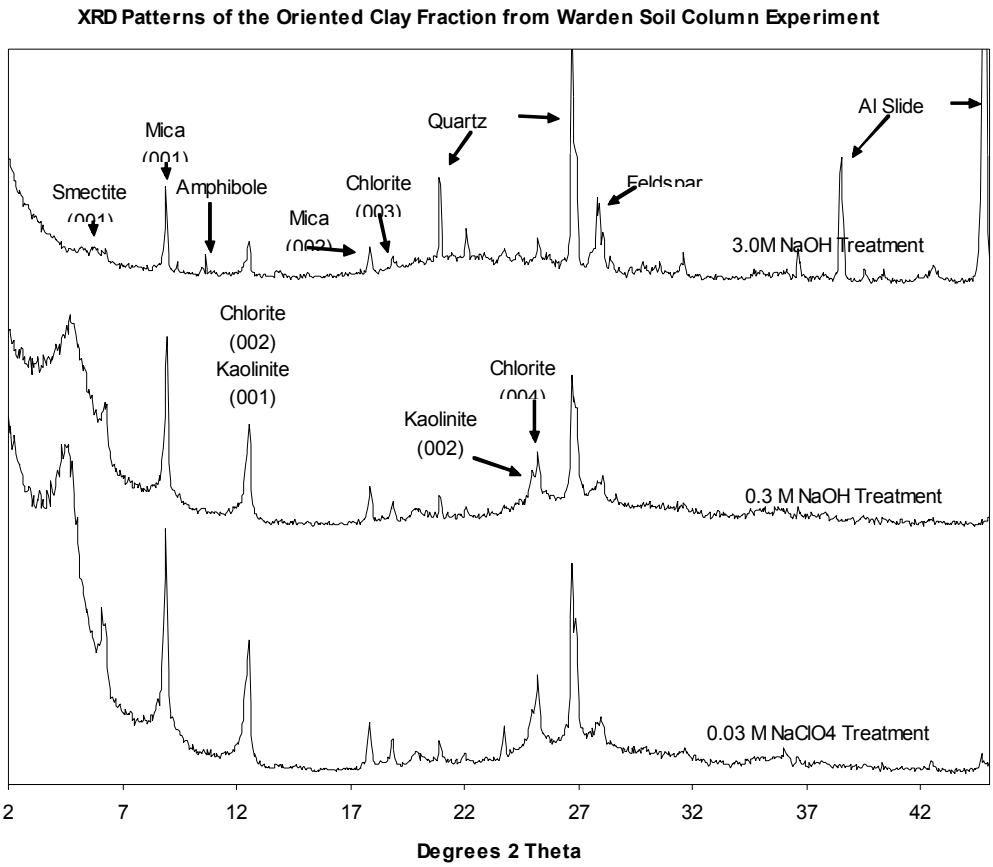

Figure 3.27. XRD Patterns of the Oriented Clay Fractions from the Column Experiments Scanned From 2 to 45° 2θ Using Cu K_α Radiation

from Mg^{2+}-saturated, ethylene glycol-solvated samples of the 0.03 $NaClO_4$, 0.3 M NaOH, and 3.0 M NaOH treatments. The clay fraction was preferentially oriented on an aluminum slide to enhance the 001 basal reflection of the clay minerals.

Prior to preparation of the oriented slide, the samples were treated to remove calcite using dilute acetic acid-sodium acetate (pH = 5). This process left an amount of the 3.0 M NaOH-treated clay-sized fraction that was inadequate for semi-quantitative XRD analysis. Furthermore, large amounts of non-clay minerals (e.g., quartz, amphibole, and plagioclase) in the samples disturbed the orientation of the clays resulting in lower peak intensities. Therefore, in Figures 26 and 27, the XRD tracings of the 3.0 M NaOH sediment should not be directly compared to the clay-fraction XRD tracings for the other treatments.

Based on semi-quantitative XRD measurements of the < 2 μm fraction of the untreated Warden silt-loam, calcite (3.03 Å d-spacing) was present at about 10 wt.%, with quartz (3.34 Å) and a feldspar (3.18 Å) present at less than 5 wt.% each. Clays dominating the < 2 μm fraction (see Figure 3.27) were smectite (17.1 Å) and illite (10.0 Å) at 40 wt. % and 25 wt. %, respectively. Chlorite (14.1 Å) made up about 10 wt. % and kaolinite (7.1 Å) was present at < 5 wt. %.

XRD analysis of the 0.03 M $NaClO_4$- and 0.3 M NaOH-treated clay fractions did not reveal any significant differences in mineral concentrations from the untreated soil. Examination of the 3.0 M NaOH XRD tracing, however, showed evidence of extreme caustic attack on selected minerals. Smectites were the most severely attacked of the clays in the 3.0 M NaOH treatment (Figure 3.27). Characterization of the 3.0 M NaOH-treated sediment by TEM showed no smectite particles, whereas the untreated soil contained an abundant number. Instead, amorphous gel-like material rich in Si, Al, and Fe was observed in the TEM studies of the 3.0 M NaOH-treated clay-sized particles. Figures 3.28 and 3.29 also show feldspar crystals exfoliating and smectites becoming amorphous gel. Observations based on XRD and TEM analysis showed that illite was generally unaffected by the NaOH treatments. XRD patterns (see Figure 3.27) show a slight decrease of the illite (002) reflection with the 3.0 M NaOH treatment relative to the 0.3 M NaOH treatment, which is probably a result of the limited amount of sample and poor particle orientation for the 3.0 M NaOH sample. TEM analysis of 3.0 M NaOH-treated illites showed clean, unaltered particles, much as in the untreated sediment (Figure 3.30). The effect of the caustic treatment on chlorite and kaolinite is more difficult to determine based on XRD patterns. Peak interferences produced by the kaolinite reflections (001, 002), and chlorite reflections (002, 004) require the use of less intense reflections. It appears that the 3.0 M NaOH treatment caused a slight decrease in the 003 chlorite (4.75 Å) reflection (Figure 3.27). Chlorites examined by TEM, however, were intact and abundant in the 3.0 M NaOH-treated sample. The kaolinite reflection (3.58 Å) that is resolved from the chlorite (3.54 Å) reflection in the untreated clay fraction is absent in the 3.0 M NaOH-treated sediment. Kaolinite particles were not observed during TEM analysis supporting the XRD interpretation that caustic attack dissolves kaolinite. The resistant minerals, e.g., quartz, feldspar, and amphibole (Figure 27), account for a greater percentage of the mineral assemblage in the 3.0 M NaOH-treated soil than in the untreated soil because of the dissolution of less-resistant minerals, e.g., smectite minerals. Calcite, present in the original sample in minor amounts, also precipitated as a result of increased hydroxide concentrations in the NaOH-treated systems (Figure 26). The increased hydroxide concentrations in solution absorbed CO_2 from the atmosphere, which in turn precipitated with dissolved Ca to form calcite, $CaCO_3$.

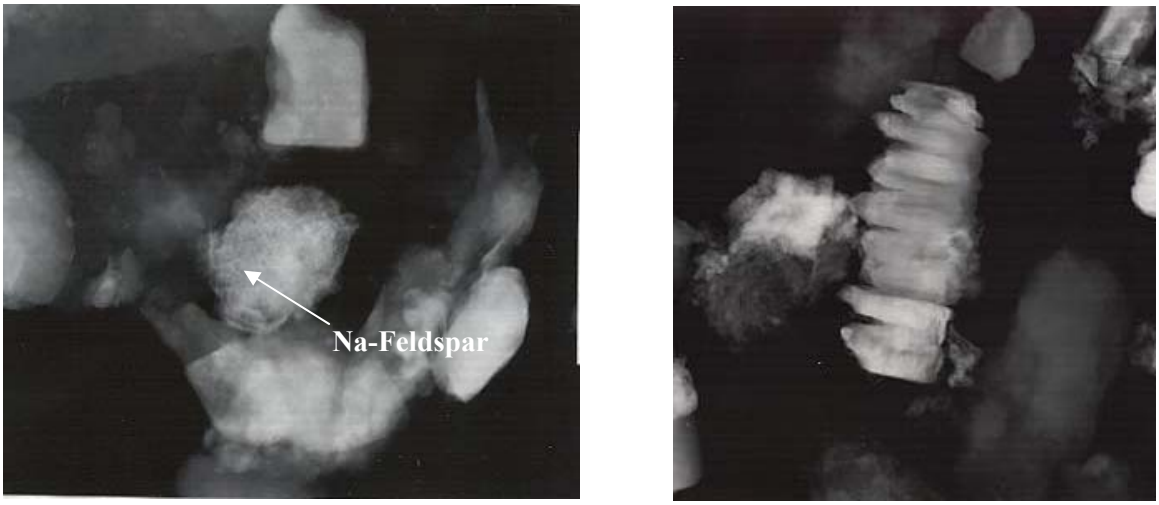

Figure 3.28. TEM Images of Nontreated (Top) and 3 M NaOH-treated (Bottom) Warden Soil (Note that the Treated Na-Feldspar Is Starting to Pry Apart)

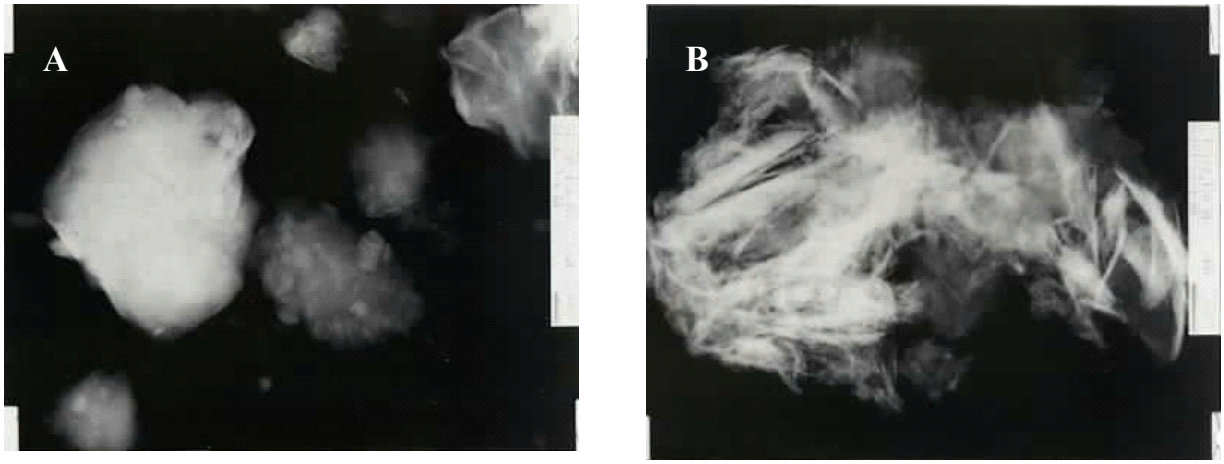

Figure 3.29. TEM Image of (A) Untreated Smectite Particle and (B) 3.0 M NaOH-treated Smectite Particle (the Small Platelets and Ribbons Visible in the Structure Are Crystalline; Areas Without These Types of Morphologies Are Amorphous)

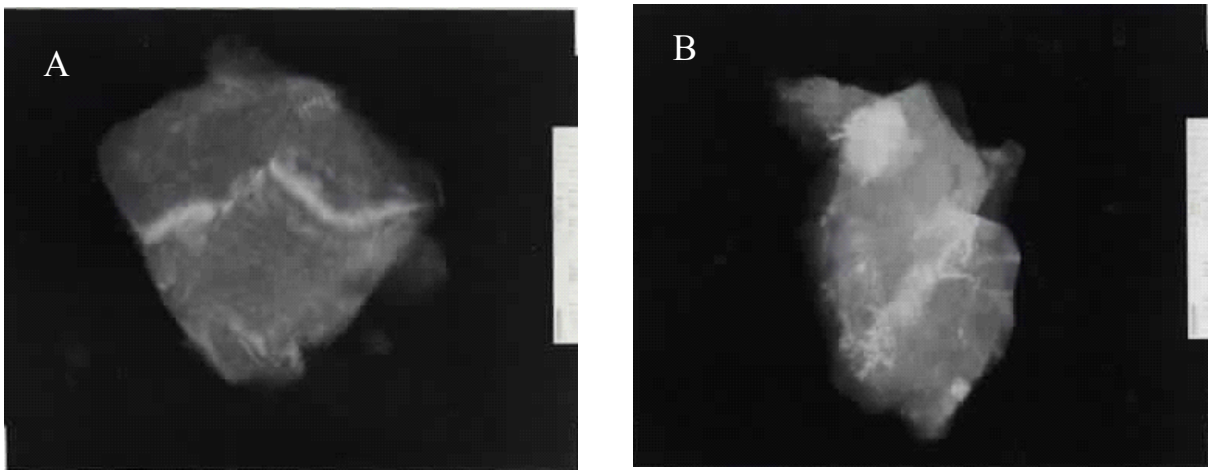

Figure 3.30. TEM Images of Illite Particles (A) Before and (B) After Treatment with 3.0 M NaOH for 360 Days

More than 100 SEM and EDX analyses were done of the column sediments after the 194-day treatments. Some examples of the SEM images are provided in Appendix A, Figures A.1 through A.5. These analyses identified two dominant minerals: quartz, a crystalline silicate, and feldspars (K-, Na-, and Na-Ca-feldspars). The quartz and feldspars were identified in XRD and are shown in Figure 3.26. Based on SEM images of the 194-day-treated Warden silt loam, there was little difference between the untreated and the 0.03 M $NaClO_4$-treated Na-feldspar particles (Appendix A, Figure A.2). In the two NaOH treatments, however, an appreciable amount of mineral deposition of unknown composition can be observed on the Na-feldspar. There was no evidence of Na-feldspar degradation in the SEM images in Appendix A and others not presented. It would not have been easy, however, to observe Na-feldspar degradation because of the presence of these depositions.

K-feldspar was not altered in the 0.03 M $NaClO_4$ treatment (Appendix A, Figure A.3). For the NaOH treatments, some deposition of smaller particles was observed on the K-feldspar, but the extent of deposition appeared to be less than that on the Na-feldspar. The quartz particles within the Warden silt loam in the untreated and 0.03 M $NaClO_4$ tests looked similar in that they both contained an appreciable amount of fine particles on their surfaces (Appendix A, Figure A.4). The 0.3 M NaOH-treated quartz had more surface coatings than the untreated quartz, and the 3.0 M NaOH-treated quartz had even more surface coatings than quartz subjected to either of the other two treatments. In addition, many quartz surfaces from the 3.0 M treatment appeared to have corrugated surfaces, an indication of significant dissolution. An example of this corrugation is captured in the photograph in Appendix A, Figure A.4.

3.1.2.4 Effluent Chemistry of the Warden Soil Column Experiment

Effluents from three Warden silt loam soil columns (one from each treatment) were characterized chemically as a function of time. Approximately 30 mL of effluent were collected from each column on days 0, 7, 14, 21, 28, 61, 95, 122, 150, and 180. These samples, typically collected over a 30-hour period, provided elemental compositions for distinct times throughout the experiment. Additionally, as described in the Materials and Methods section, between each sampling episode effluent was collected from the individual columns, resulting in six composite samples for each column (0-28, 28-60, 61-90, 95-120, 121-150, and 151-180 days). These composite samples provided average elemental concentrations over the range of days during which the sample was collected. Measurements including pH, free hydroxide, carbonate content, and cation concentrations were made on the samples collected at distinct times. The composite samples were characterized for cations only. Data representing the effluent chemistry for both types of samples is presented in Figures 3.31 through 3.37.

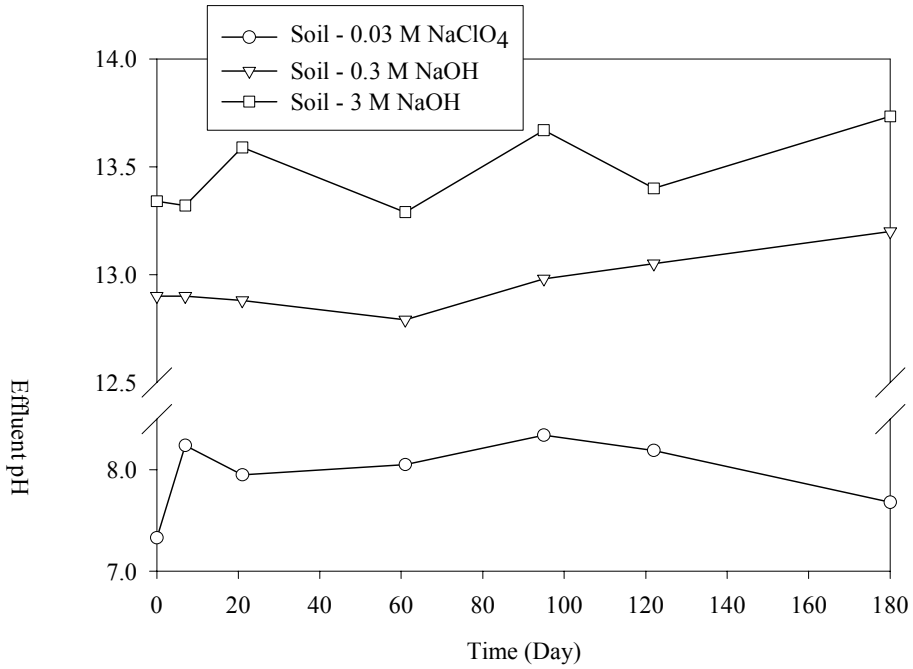

Figure 3.31. Effluent pH Exiting the Control and NaOH-treated Columns of Warden Silt Loam Soil

The effluent pH for all treatments is presented in Figure 3.31. The pH of the 3.0 M NaOH system was ~13.5, the pH of the 0.3 M NaOH system was ~13.0, and the pH of the 0.03 M $NaClO_4$ system was ~8.0. A large change in pH was recorded between 0 and 7 days in the 0.03 M $NaClO_4$ treatment wherein the pH increased ~1 pH unit. This reflects the difference in the pH in the influent (time = 0 days) and the effluent after the perchlorate solution exited the soil, which had a 1:1 soil:water extract pH of ~8.2. The fact that the effluent pH remained closer to 8.2 than 7.2, the pH of the 0.03 M $NaClO_4$ influent, suggests that the effluent pH was controlled by reactions with the soil. In contrast, the 0.03 M $NaClO_4$ effluent of the quartz sand column was closer to pH 7.4 indicating that the sodium perchlorate effluent pH will remain stable when the solid is essentially inert (see Figure 3.11).

Concentrations of Si, Al, Fe, and K in the effluent solutions were measured and are presented in Figures 3.32, 3.33, 3.34, and 3.35, respectively. The individual data points represent the samples collected on distinct days whereas the data points with horizontal bars represent the samples collected as composites over ~ 30 day intervals. A significant change in effluent Si and Al concentrations occurred within the first 7 days of contact with both NaOH solutions for the Warden silt loam column tests. The Si concentrations in the caustic-treated soil columns rapidly rose (Figure 3.32) to 150 and 600 ppm for the 0.3 and 3 M NaOH treatments, respectively. The effluent Al concentrations also rose rapidly (Figure 3.33), to 40 and 155 ppm for the 0.3 and 3 M NaOH treatments, respectively. Similar early spikes in the effluent Si and Al concentrations were observed in the quartz sand experiments. Of particular interest is the near constant Si:Al ratio of 4:1 in the effluents from both the quartz sand and Hanford soil column tests; indeed the two sets of figures have nearly identical patterns of Si and Al concentrations versus time. The fact that the quartz sand and the Warden silt loam soil columns had the same Si:Al ratio suggests that the same mineral phase may be controlling the release of Si and Al from the two solids. If both systems were in equilibrium with the same mineral, the concentrations of Si and Al would be similar. The concentrations are not the same, however, only the ratios are. Thus, the reaction must be kinetically controlled. In fact, the Warden silt loam is releasing Al and Si about 35 times faster than the quartz sand. We do have not determined what mineral or minerals would control the release of Si and Al with a near constant ratio of 4.

As was the case with Si and Al, carbonate, free hydroxide, and changes in the shape of the effluent Fe concentration curve versus time (Figure 3.34) were very similar in the quartz sand and Warden soil columns. The mass of Fe released at early times varied by a factor of about 4, with release from the Warden silt loam soil greater than release from the quartz sand. The maximum Fe concentration in the quartz sand effluents for the 3 M NaOH treatment was 1.5 mg/L, and for the Warden silt loam soil, it was 6.3 mg/L. The smectite clays in the Warden silt loam soil contain Fe and, based on XRD and SEM characterization, the smectites are readily attacked and dissolved in the caustic treatments, thus the higher release of Fe may be due to this reaction, resulting in a trend similar to that observed in the soil column effluents for the 0.03 M $NaClO_4$ and 0.3 M NaOH treatments.

Effluent carbonate concentrations remain constant over time for the 0.03 M $NaClO_4$ and 0.3 M NaOH treatments. In contrast, the effluent carbonate concentrations for the 3.0 M NaOH treatments peaked at 21 days and slowly decreased during the remainder of the study. The final carbonate concentrations were similar for all three treatments, ~2000 mg/L as calcium carbonate. This is essentially the identical trend

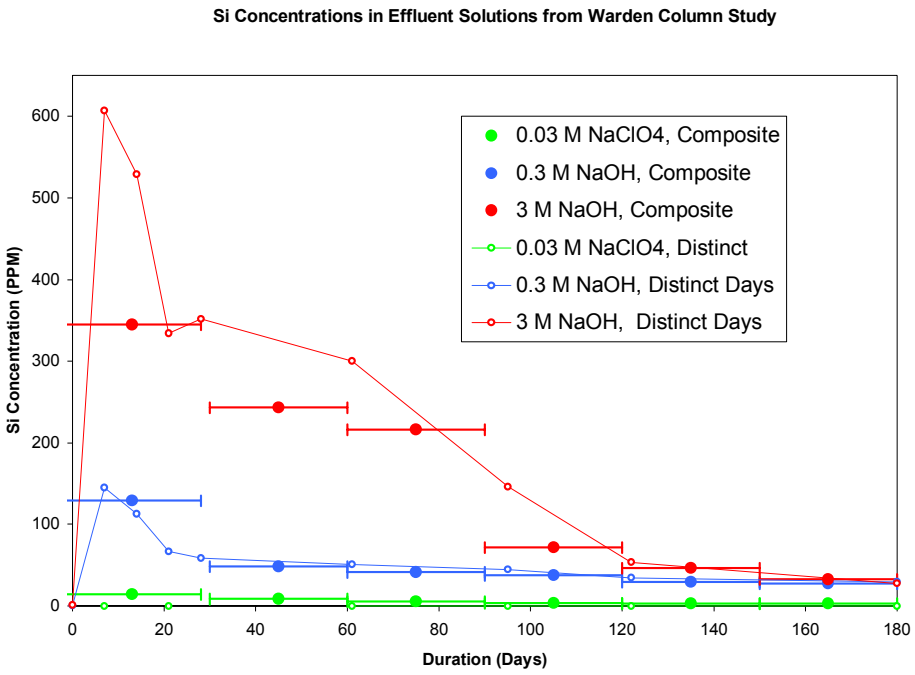

Figure 3.32. Effluent Si Concentrations Exiting the Control and NaOH-treated Columns of Warden Silt Loam Soil

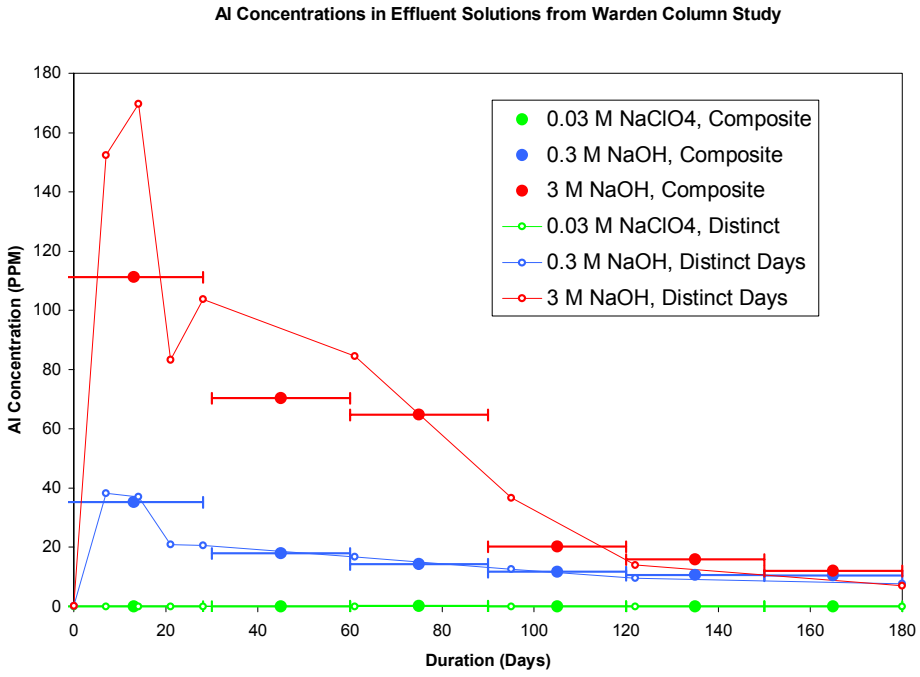

Figure 3.33. Effluent Al Concentrations Exiting the Control and NaOH-treated Columns of Warden Silt Loam Soil

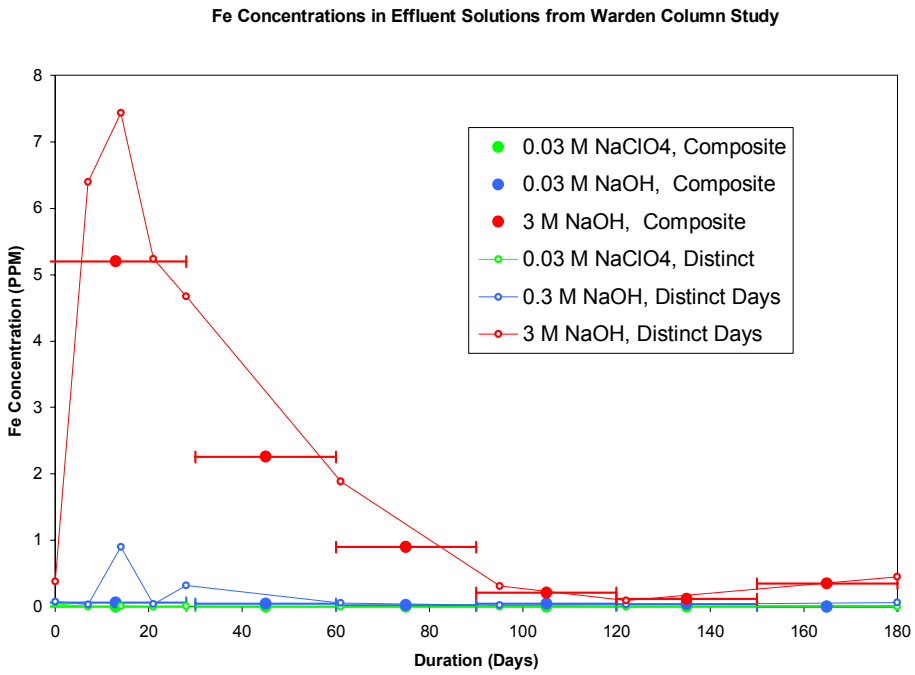

Figure 3.34. Effluent Fe Concentrations Exiting the Control and NaOH-treated Columns of Warden Silt Loam Soil

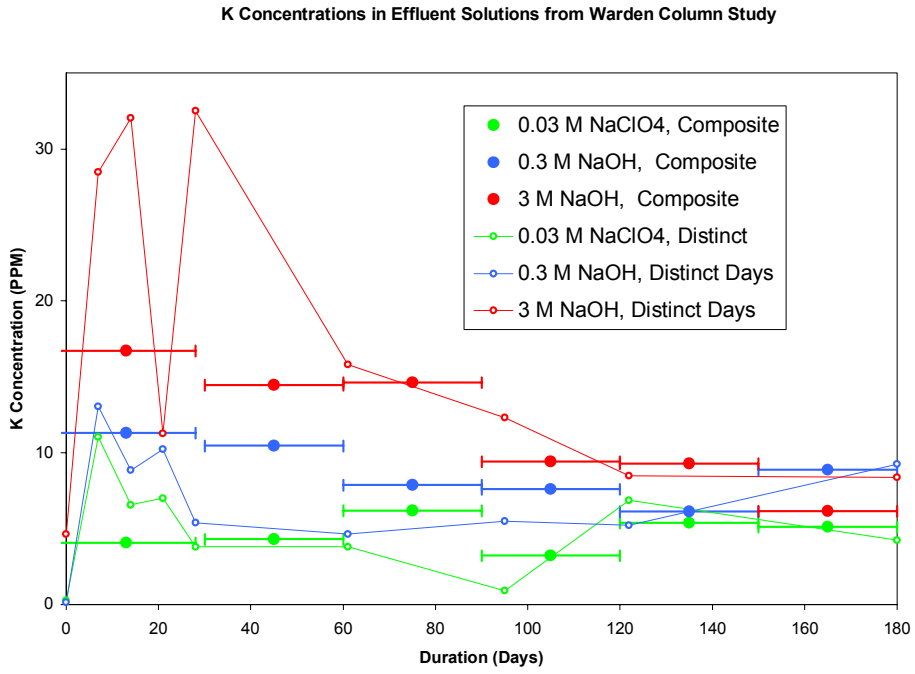

Figure 3.35. Effluent K Concentrations Exiting the Control and NaOH-treated Columns of Warden Silt Loam Soil

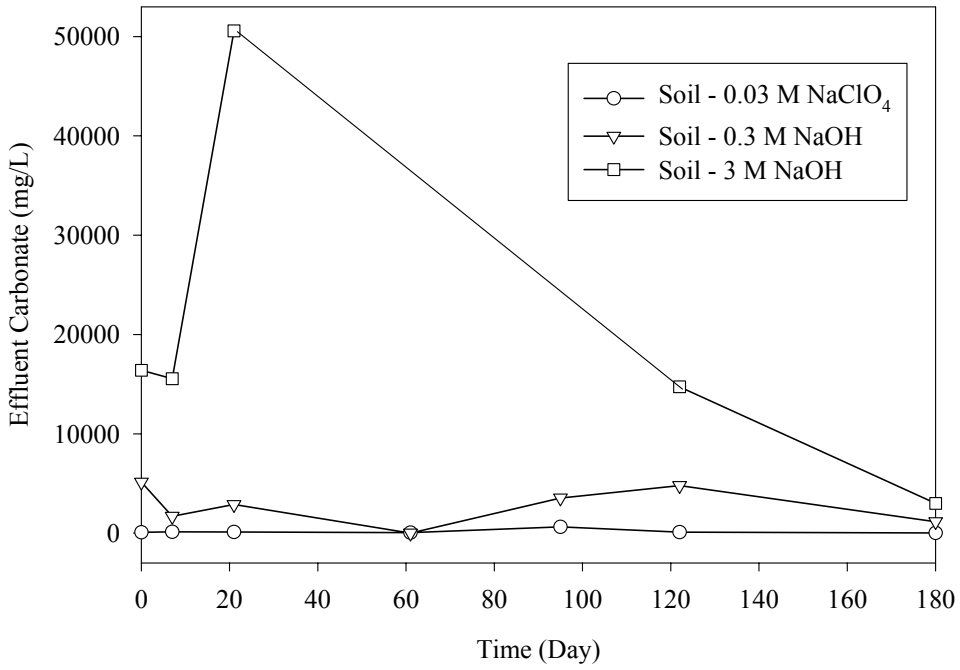

Figure 3.36. Effluent Carbonate Concentrations (as mg/L $CaCO_3$) Exiting the Control and NaOH-treated Columns of Warden Silt Loam Soil

observed in the quartz sand columns (Figure 3.16), indicating that the solid phase had little impact on effluent carbonate concentrations and that carbonate concentrations may be controlled primarily by the absorption of CO_2 from air within the influent reservoir.

The free hydroxide concentrations also remained constant throughout the experiments, and, as expected, the free hydroxide concentrations in the 3.0 M NaOH system were about an order of magnitude greater than for the 0.3 M NaOH system (Figure 3.37). The free hydroxide concentrations and the trends are nearly identical to those in the quartz sand columns (except for one outlier at 7 days for the 3.0 M NaOH sample; Figure 3.17).

The mass of Warden silt loam remaining after the 180-day treatments was significantly less than the starting mass, which supports observations that caustic attack on the sediment was much greater than on the commercial quartz dominated sand. Up to 6 g of mass (out of ~35 g starting mass was lost to dissolution and inadvertent losses during the particle size determinations and sample preparations for mineralogical characterization. However, almost as much mass was lost in the control tests that used 0.03 M sodium perchlorate. The sum of excess Al, Si, Fe, K, Ca, and Na leached out of the Warden silt loam columns that were treated with sodium hydroxide ranged from 0.7 g for the 0.3 M NaOH tests to 1.8 g for the 3 M NaOH tests. Thus most of the missing mass can not be attributed to dissolution. However, the mass attributable to dissolution for the Warden silt loam sediment (0.7 to 1.8 g) is much larger than the mass attributed to dissolution in the quartz sand columns (0.07 to 0.7 g). All the columns started with ~35 g of solid material.

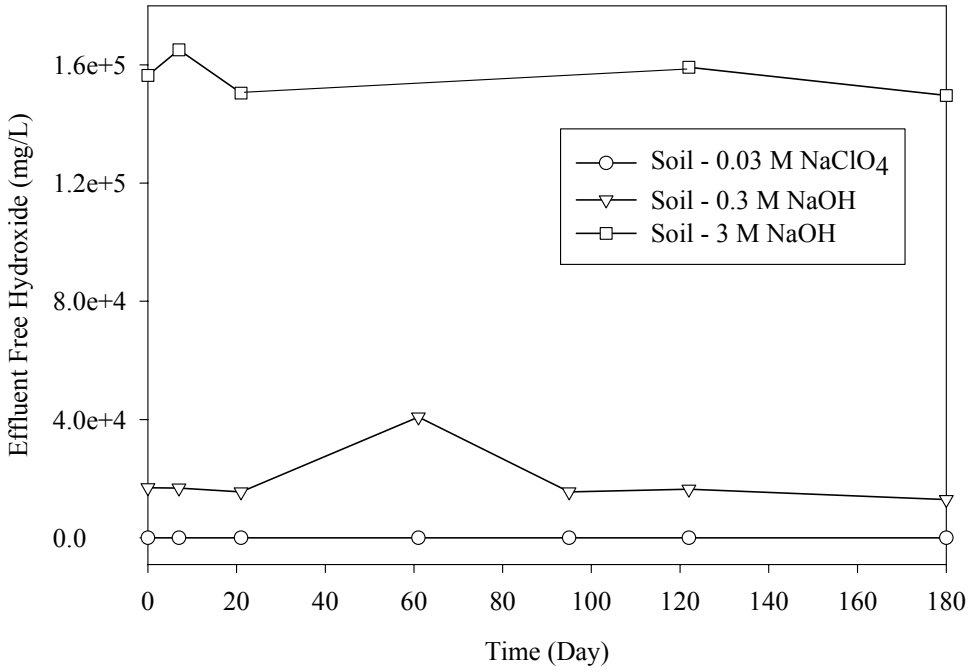

Figure 3.37. Effluent Free Hydroxide (as mg/L $CaCO_3$) Exiting the Control and NaOH-treated Columns of Warden Silt Loam Soil

3.2 Batch Sorption Study

Batch experiments consisting of 200 g of Warden silt loam soil in contact with 900 mL of treatment solution were performed for several contact times. The treatment solutions consisted of 0.03 M NaOH, 0.3 M NaOH or 3.0 M NaOH. At 10, 90, 180, and 360 days, the caustic attack portion of the experiments was stopped and the solid and liquid phases were characterized. Aliquots of the solids from these experiments were then used to measure iodide, selenate, pertechnetate, cesium, and strontium K_d values using fresh aliquots of the caustic solutions spiked with radiotracers and a 14-day contact time. The intent of these tests was to evaluate under non-flow conditions the influence of NaOH, a simplified simulant for glass leachate, on radionuclide sorption. These experiments, unlike the column experiments, permitted direct evaluation of the effects of NaOH on the solid phase as a function of time. In the column tests solids were available for mineralogical characterization only before and after 180 days of treatment. The solution-to-solid ratio also differed significantly between the two tests. Extensive characterization of the liquids from these tests was conducted to provide supplemental information for understanding the chemical and mineralogical processes influencing radionuclide sorption.

To differentiate the effects of caustic attack and high pH from Na-cation competition, similar batch K_d tests were performed on untreated Warden silt loam with a contact time of 14 days with 0.03, 0.3 and 3 M $NaClO_4$ solutions that had a neutral pH. The difference in K_d's between the perchlorate- and hydroxide-treated sediments should thus be caused by caustic attack or high pH as opposed to sodium competition or ionic strength.

3.2.1 Soil Physical Properties of the Batch Sorption Study

The NaOH aqueous treatments impacted the particle size distribution of the treated soils as shown in Tables 3.8, 3.9, and 3.10. The particle size distribution in the 0-day sample provides the reference for evaluating treatment effects. This sample consists of soil that was washed for 10 minutes with sodium

Table 3.8. Particle Size Distribution (wt. %) of Warden Soil As a Function of Contact Time with 0.03 M NaOH

Days of Treatment	2 to 1 mm (wt.%)	1 to 0.5 mm (wt.%)	0.5 to 0.25 mm (wt.%)	0.25 to 0.106 mm (wt.%)	0.106 to 0.075 mm (wt.%)	0.075 to 0.05 mm (wt.%)	0.05 to 0.002 mm silt (wt.%)	< 0.002 mm clay (wt.%)
0[(a)]	0	0	0	14.7	18	13.5	50.4	3.4
10	0	0	0	7.6	15.2	13.1	59.2	4.9
90	0	0	0	14	17.6	13.8	50.7	3.9
180	1	1.7	1.6	7.9	13.2	14.4	53	7.2
360	0.7	1.4	1.4	8	12	15	56.6	4.9

(a) The 0-day sample consists of soil that was washed for 10 minutes with the 0.03 M $NaClO_4$ solution, centrifuged, phase-separated, and then subjected to particle size distribution by wet sieving. Yellow highlight signifies an increase versus the control and blue highlight signifies a decrease versus the control.

Table 3.9. Particle Size Distribution (wt.%) of Warden Soil As a Function of Contact Time with 0.3 M NaOH

Days of Treatment	2 to 1 mm (wt.%)	1 to 0.5 mm (wt.%)	0.5 to 0.25 mm (wt.%)	0.25 to 0.106 mm (wt.%)	0.106 to 0.075 mm (wt.%)	0.075 to 0.05 mm (wt.%)	0.05 to 0.002 mm silt (wt.%)	< 0.002 mm clay (wt.%)
0[(a)]	0	0	0	12.6	18.9	12.6	52.4	3.5
10	0	0	0	13	9.7	14.6	58.5	4.2
90	0	0	0	15.1	17.8	14.1	49.7	3.4
180	0	0	0	15.1	17.8	14.1	49.7	3.4
360	0.7	1.8	2	7.6	11.9	14.4	55.8	5.7

(a) The 0-day sample consists of soil that was washed for 10 minutes with 0.3 M $NaClO_4$ solution, centrifuged, phase-separated, and then subjected to particle size distribution by wet sieving. Yellow highlight signifies an increase versus the control and blue highlight signifies a decrease versus the control.

Table 3.10. Particle Size Distribution (wt.%) of Warden Soil As a Function of Contact Time with 3.0 M NaOH

Days of Treatment	2 to 1 mm (wt.%)	1 to 0.5 mm (wt.%)	0.5 to 0.25 mm (wt.%)	0.25 to 0.106 mm (wt.%)	0.106 to 0.075 mm (wt.%)	0.075 to 0.05 mm (wt.%)	0.05 to 0.002 mm silt (wt.%)	< 0.002 mm clay (wt.%)
0[(a)]	0	0	0	11.9	17.3	10.8	56.8	3.2
10	0	0	0	20.7	19.4	15.5	43.3	1
90	0	0	0	22.5	20.7	15.8	38.5	2.6
180	1.6	3	3.5	10.5	16.3	15.2	49.3	0.6
360	1.2	2.5	2.6	8.5	14.3	13.9	54.9	2

(a) The 0-day sample consists of soil that was washed for 10 minutes with 3.0 M $NaClO_4$ solution, centrifuged, phase-separated, and then subjected to particle size distribution by wet sieving. Yellow highlight signifies an increase versus the control and blue highlight signifies a decrease versus the control.

perchlorate solution at the same ionic strength as the three NaOH treatments. The slurry was then centrifuged and the excess solution decanted. The wet soil was then subjected to wet sieving to determine the particle size distribution.

In the 0.03 M NaOH treatment, a small degree of aggregation occurred to create particles in the size range > 0.25 mm to < 2 mm after 90 days of contact with the caustic solution. Conversely, some of the original particles in the size range 0.075 to 0.25 mm must have been broken down or disaggregated to form particles between 0.002 and 0.05 mm after contact times of 10 days or longer (Table 3.8). Thus it appears that both aggregation (perhaps cementation) and disaggregation (either dispersion of recalcitrant agglomerates with time or actual dissolution of surfaces to form smaller particles) occurred when the Warden silt loam was contacted with 0.03 M NaOH. This same trend was also observed in the 0.3 M NaOH treatment (Table 3.9). The formation of the > 0.25 mm particles occurred only after 180 days but there are signs of increased numbers of silt-sized particles (2 to 50 microns) at 10 days and after 180 days of caustic attack. The 3 M NaOH treatment shows more evidence of aggregation in all of the sand fractions (see Table 3.10). The particle aggregation tends to create large particles (> 0.25 mm) after 90 days of contact. At earlier contact times the very fine and fine sands (> 0.075 to 0.25 mm) show increased masses. At the longer time periods these particles further agglomerate to make larger particles. Conversely, the silt and clay particles within the Warden silt loam are either incorporated into the agglomerates or some are dissolved to form the cementing agent that holds the agglomerates together.

Unlike the column studies, where the clay fraction of the Warden soil was almost completely dissolved, not all the clay fraction of the 3.0 M NaOH-treated Warden soil dissolved in the batch study. In the column studies, reaction products were constantly removed by the flow of liquid through the columns. In contrast, there was a finite volume of liquid in the batch experiments. As reaction products accumulated in solution, dissolution rates presumably slowed as the system moved toward equilibrium.

3.2.2 Soil Mineralogy of the Batch Sorption Study

XRD analyses were conducted on the silt, sand, and clay fractions of the 3.0 M NaOH treatment at six contact times. The 0-day sample was put in contact with 3.0 M NaOH for 10 minutes prior to XRD analysis to evaluate whether any evaporites that might be present in the treated samples would remain during the preparation of the XRD mounts and thereby produce apparent differences between the untreated samples and treated samples that were not real. No evaporites were detected. A brief description of the minerals identified by the XRD analysis follows:

- Quartz, a silicate (SiO_2),
- Plagioclase, a series of Ca- and Na-containing feldspars [$(Ca,Na)Al_2Si_2O_8$, the pure Na end member is albite and the pure Ca end member is anorthite];
- Illite, a group of mica clay minerals with a general formula $KAl_2(SiAl)_4O_{10}(OH)_2$
- Muscovite, a dioctahedral mica with Al in the octahedral layer [$KAl_2(AlSi_3)O_{10}(OH)_2$],

- Smectite, expandable 2:1 layer clays [for these batch tests with Warden silt loam the following smectite was found [$Na_{0.33}(Al_{1.67}Mg_{0.33})(Si,Al)_4O_{10}(OH)_2$],
- Kaolinite, a 1:1 layer clay [$Al_4Si_4O_{10}(OH)_8$]
- Chlorite, a trioctahedral 2:1 layer clay [$(Mg^{2+},Fe^{2+,3+})_3(Si,Al)_4O_{10}(OH)_4$], and
- Amphibole, an inosilicate [$(Na,Ca)(Mg,Mn,Fe)_5Si_8O_{22}(OH)_2$].

XRD patterns of the 3.0 M NaOH-treated sand and silt fractions from the batch experiments are presented in Figure 3.38 and Figure 3.39, respectively. Tabulated semi-quantitative estimates of the mineral concentrations are presented in Tables 3.11 and 3.12 for the sand- and silt-sized fractions, respectively. These data do not provide any evidence of mineral dissolution, i.e., quartz, feldspar, muscovite, and amphibole resisted dissolution in the 3.0 M NaOH solution. The decrease in feldspar content in the silt fraction for the 10-day and 90-day treatments compared to the 0-, 180-, and 360-day treatments is probably related to variations in sample packing on the XRD mounts.

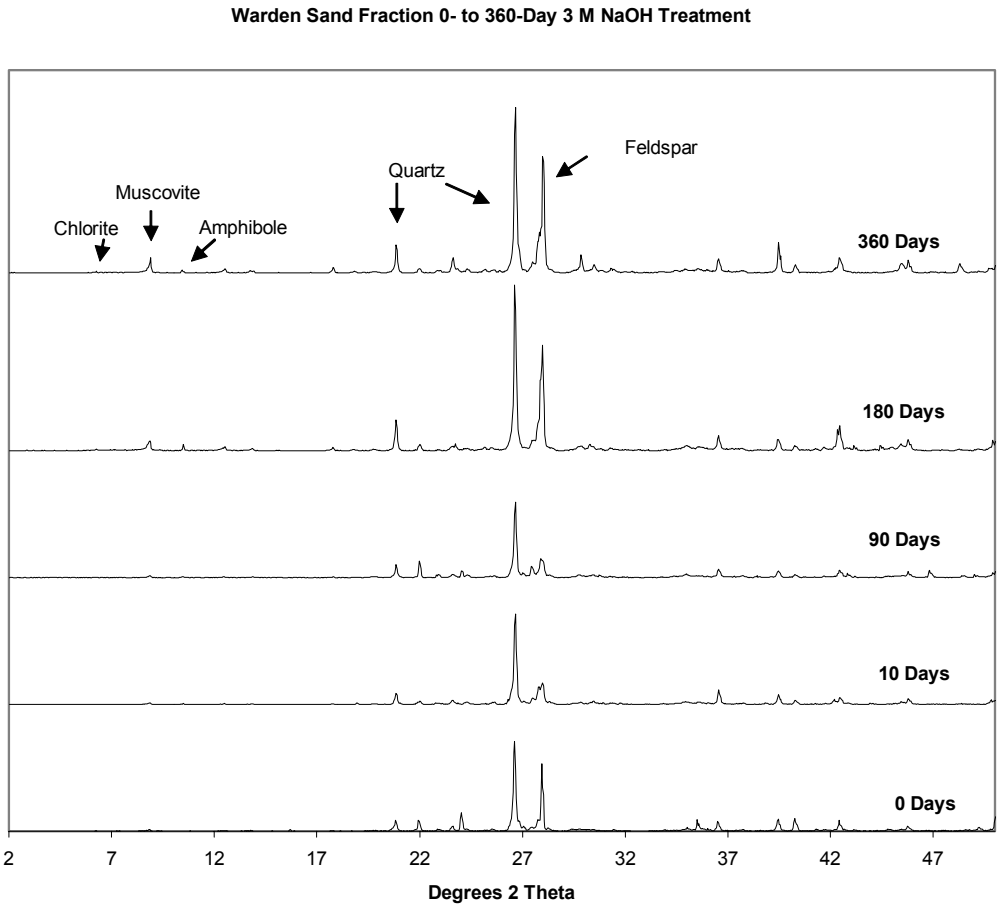

Figure 3.38. XRD Patterns From the Sand Fraction of the Warden Silt Loam 3.0 M NaOH Batch Experiment Scanned From 2 to 75° 2θ With Cu K_α.

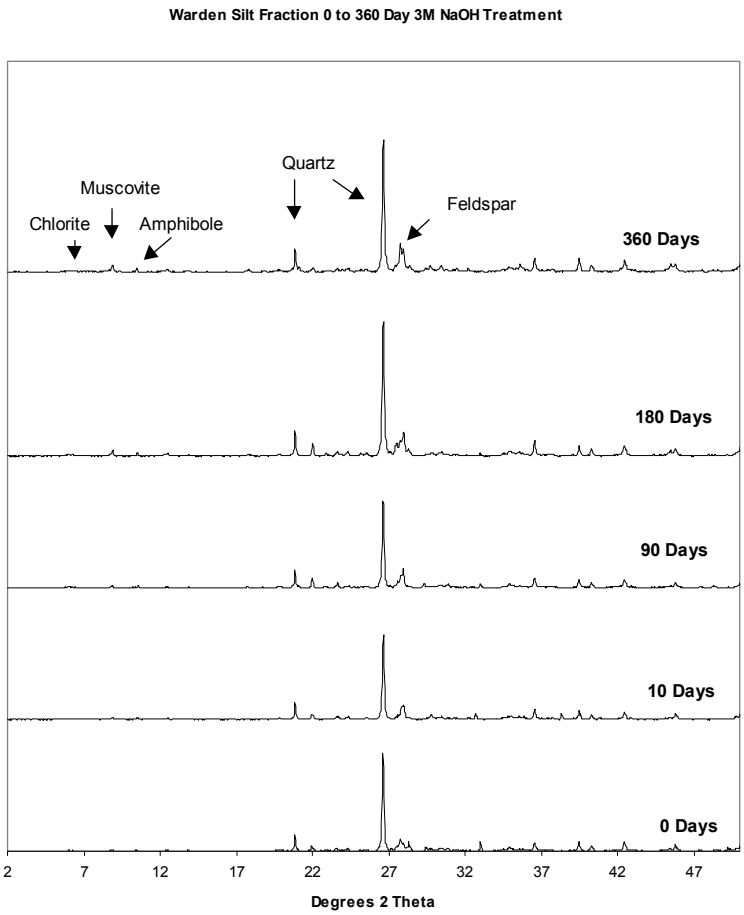

Figure 3.39. XRD Patterns From the Silt Fraction of the Warden Silt Loam 3.0 M NaOH Batch Experiment Scanned From 2 to 75° 2θ With Cu $K_{\alpha.}$

Table 3.11. Semi-Quantitative XRD Results (wt.%) for the Silt Fraction of the Warden Soil as a Function of Contact Time with 3.0 M NaOH

	Untreated	0 Days[a]	10 Days	90 Days	180 Days	360 Days
Quartz	85	80	75	75	75	75
Plagioclase	15	10	10	15	15	15
Muscovite	Tr[b]	Tr	Tr	Tr	< 5	< 5
Chlorite	Tr	Tr	1	Tr	Tr	Tr
Amphibole		Tr		Tr	Tr	Tr
Total	~100	~90	~85	~90	~95	~95

(a) 0-days treatment was put in contact with 3.0 M NaOH for 10 minutes.
(b) Tr-trace amounts detected by XRD analysis.

Table 3.12. Semi-Quantitative XRD Results (wt.%) for the Sand Fraction of the Warden Soil as a Function of Contact Time with 3.0 M NaOH

	Untreated	0 Days[(a)]	10 Days	90 Days	180 Days	360 Days
Quartz	65	55	80	80	55	55
Plagioclase	30	40	20	20	35	40
Muscovite	Tr[(b)]	Tr	Tr	Tr	< 5	< 5
Chlorite	Tr	Tr	Tr	Tr	Tr	Tr
Amphibole				Tr	< 5	Tr
Total	~95	~95	~100	~100	~100	~100

(a) 0-days treatment was put in contact with 3.0 M NaOH for 10 minutes.
(b) Tr-trace amounts detected by XRD analysis.

Because of the greater surface area and smaller particle size, significantly more changes in mineral weathering were expected in the clay fraction than in the silt or sand fractions of the Warden silt loam sediment. XRD tracings of the randomly mounted clay fraction are presented in Figure 3.40. These

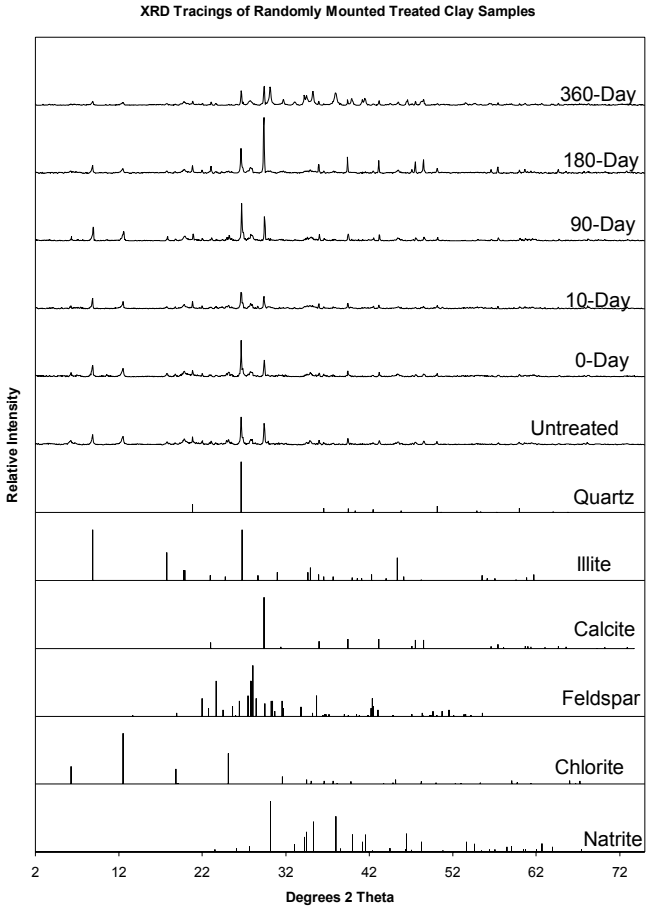

Figure 3.40. XRD-Tracings of the Randomly Mounted Clay Fraction from the Warden 3.0 M NaOH Batch Experiment, Scanned From 2 to 75° 2θ With Cu K_{α}.

tracings show large amounts of $CaCO_3$ precipitation starting with the 90-day treatment and Na_2CO_3 precipitation near the end of the 360-day treatment. It is also evident from these patterns that illite, chlorite, quartz, and feldspar are still present in the clay fraction of the 360-day treatment. Direct comparison of XRD tracings taken from the various treatments, however, is not valid. The carbonate formation in the treated sediments changes the mass absorption of the x-rays, thereby affecting the relative intensities of the characteristic mineral peaks. Removal of carbonates from the treated sediment, followed by the preparation of oriented mounts, allows for a better understanding of the relative mineral concentrations.

XRD patterns of the preferentially oriented, Mg^{2+}-saturated, ethylene glycol-solvated clay fractions are presented in Figure 3.41. Calcite ($CaCO_3$) and natrite (Na_2CO_3) were removed from the 10, 90, 180, and 360-day clay fractions prior to XRD analysis using dilute acetic acid-sodium actetate (pH=5). A small amount of calcite remained in the 3 M NaOH-treated 360-day sample after the carbonate removal treatment, as evidenced by the peak at 3.01Å (Figure 3.41). A lack of adequate sample prohibited the preparation of slides valid for semi-quantification. Additionally, the clay fraction was dried in an oven prior to sample preparation, altering the hydration properties of the clay and resulting in poor preferential orientation. It appeared that the illite and chlorite concentrations did not decrease significantly until 360 days of treatment at which point their reflections were about half their original intensity. Some of the decrease in peak intensity, however, may be due to the previously described lack of adequate sample and poor sample orientation, because TEM analysis of this sample revealed abundant illite and chlorite particles with unaltered morphologies and chemistries.

Smectite and kaolinite showed signs of significant dissolution in the 3.0 M NaOH treatment solution during the 360-day contact period. The intensity of the 001 smectite reflection (Figure 3.41) for the untreated sample was significantly larger than those in the 180- and 360-day treatments. Likewise, the 002 kaolinite reflection is present only in the early contact time patterns and is essentially absent from patterns from the later treatments (180 and 360 days). Neither mineral was detected by TEM analysis of the 360-day treated sediment. Additionally, the < 2-μm fraction from the 360-day treatment appeared to have a significant amount of gel-like material rich in Si and Al.

In summary, it appears that quartz, feldspar, amphibole, chlorite, and muscovite from the silt and sand fractions in the batch treatments resisted the caustic attack. In the clay fraction both XRD and TEM analysis suggest that illites (i.e., weathered muscovite) and chlorites were not greatly affected by the NaOH treatment. Large unaltered particles of both phases were observed by TEM in the 360-day treatment sample. Smectite and kaolinite were severely attacked and almost completely removed from the clay fraction after the 360-day batch treatment with 3.0 M NaOH.

Examples of SEM images taken of the sand fraction of the 3.0 M NaOH-treated and untreated Warden silt loam soil from the batch tests are presented in Appendix A, Figures A.6 through A.9. The plagioclase surface in the untreated soil was smooth with some slight undulation (Appendix A, Figure A.6). After only 90 days, it showed a significant amount of pitting, a result of dissolution. Increased pitting was observed after 180 days of treatment and by 360 days, the plagioclase surface had a precipitate coating with chemistry similar to a K-feldspar (based on EDX chemical composition data). This suggests that the solubility of K-feldspar was exceeded following 180 to 360 days of plagioclase dissolution.

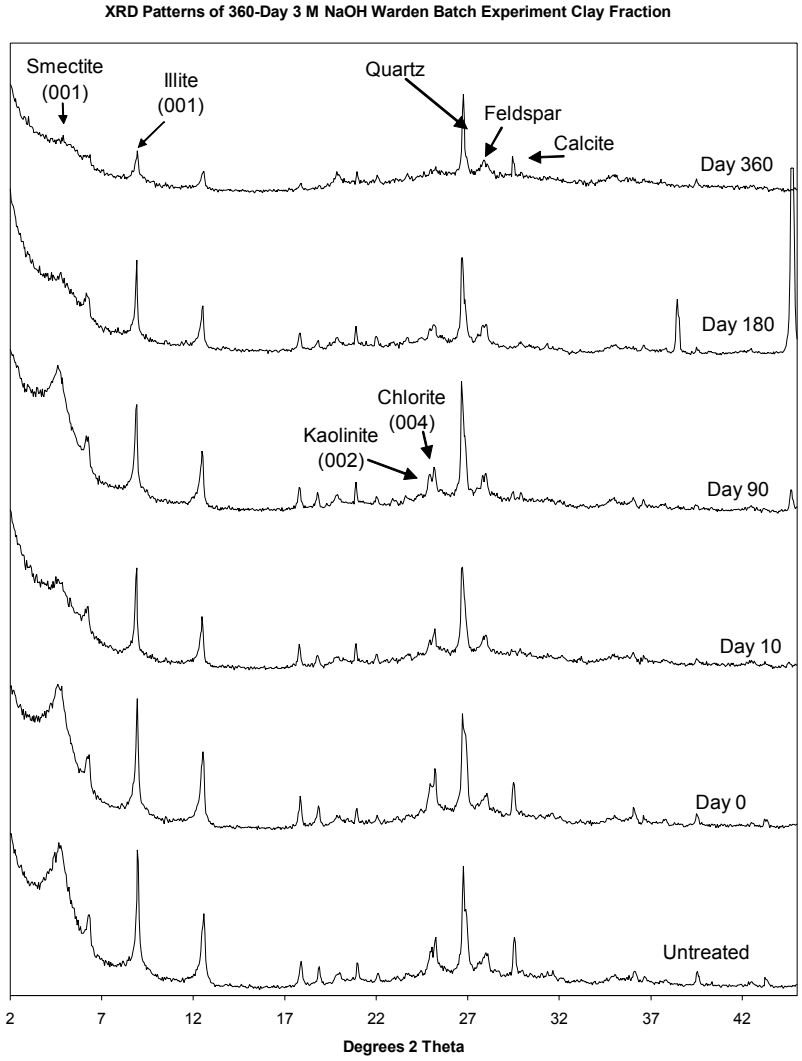

Figure 3.41. XRD Patterns Using Oriented Mounts of the Clay Fraction From the Warden 3.0 M NaOH Batch Experiment, Scanned From 2 to 45° 2θ With Cu K_{α}.

The K-feldspar surface in the untreated soil was smooth (Appendix A, Figure A.7). Like the plagioclase, K-feldspar showed significant pitting after only 90 days of treatment in 3.0 M NaOH. Further pitting was observed in the 180-day samples. Unlike the plagioclase, however, no coatings were found on the K-feldspar sample in the 360-day samples. Instead, the mineral sheets appeared to have separated. Identical observations were made for K-feldspar in the silt fraction of the Warden silt loam sediment that was contacted with 3.0 M NaOH caustic for different times (data not presented).

Quartz was covered with a precipitate with a chemical composition similar to K-feldspar after 90 days of caustic attack (Appendix A, Figure A.9). After 180 days, pitting on the quartz grains underneath the precipitate coating became increasingly evident. After 360 days, less precipitation was observed on the quartz, permitting more pitting of the quartz surface to be observed.

3.2.3 Aqueous Chemistry of the Batch Sorption Study

The chemical composition of the reacted batch solutions was determined at five times during the batch sorption experiments: 0 days (the treatment solution prior to contact with the soil), 10 days, 90 days, 180 days, and 360 days. The pH for the 0.03 M NaOH, 0.3 M NaOH, and 3.0 M NaOH treatment solutions after contact with the sediments versus time tended to remain fairly constant at 11.2, 12.7, and 13.4, respectively (not including the 0-day values) as shown in Figure 3.42. These batch-test pH values were about the same, or perhaps slightly less, than the pH values in the column effluents for the 0.3 and 3.0 M NaOH treatments (Section 3.1.2.4). No column tests were run with 0.03 M NaOH solution. For the 0.3 M NaOH treatment, the pH in the column study was ~13.0, whereas in the batch study it was ~12.7. In the 3.0 M NaOH treatment, the pH of the column study was ~13.5, whereas in the batch study it was ~13.4. Figure 3.42 shows that the pH of the reacting 0.03 M NaOH solution dropped from ~11 to ~9.5 between 180 and 360 days of contact.

Electrical conductivity (Figure 3.43), an indirect measure of ionic strength, did not change greatly in the reacted batch treatment solutions during the 360-day contact time, indicating that reactions with the Warden silt loam soil did not release or precipitate significant amounts of ions. No change in the electrical conductivity of the 0.03 M NaOH treatment was observed during the 360-day contact time suggesting that little dissolution occurred. For the stronger NaOH treatments (0.3 and 3 M), an initial increase in electrical conductivity was observed between 0 and 10 days; after 10 days the electrical conductivity remained constant. This suggests that during the first 10 days the Na^+ in the influent

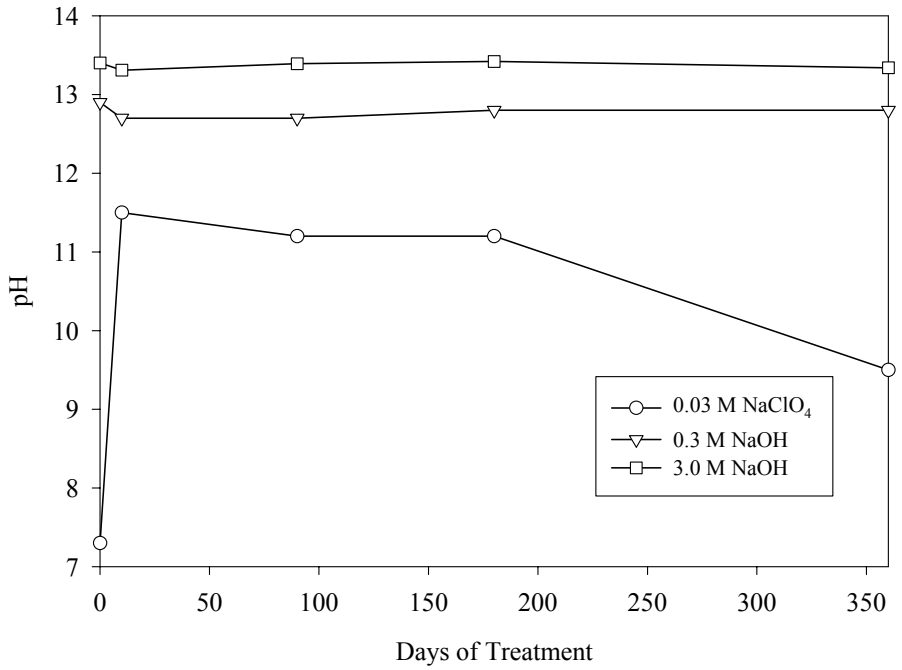

Figure 3.42. pH in the Warden Silt Loam Batch Study Solutions as a Function of Contact Time

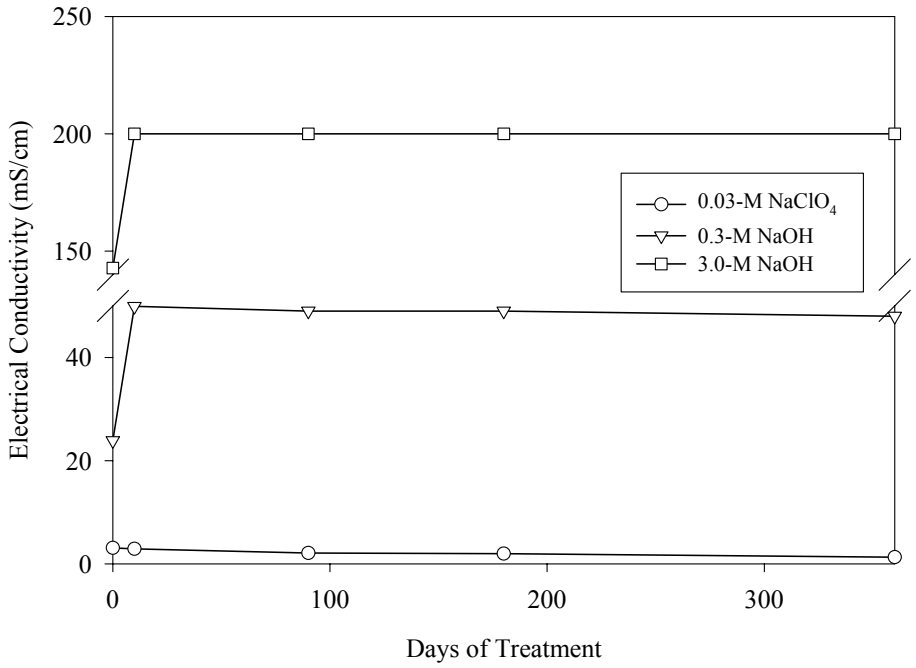

Figure 3.43. Electrical Conductivity in the Warden Silt Loan Batch Study Solutions as a Function of Contact Time

replaced multivalent ions from the mineral surfaces or that most of the dissolution occurred early in the tests or both. Constituent concentrations in the NaOH batch treatment solutions that increased during the first 10 days included Si, Al, and inorganic carbon.

For the 3.0 M NaOH batch treatment, aqueous Si and Al concentrations continued to increase during the 360-day contact time (see Figures 3.44 and 3.45). The two weaker caustic treatment effluents showed a moderate initial increase in aqueous Si and Al concentrations for the first 180 days, and then the concentrations tended to decrease slightly. As in the quartz sand and Warden silt loam column experiments, the Si-to-Al ratios in solution remained constant at about 4:1.

The reacted treatment solutions from the Warden silt loam batch tests had K concentrations that varied with time. For all three NaOH treatments, the initial solution appears to have contained K impurity in the NaOH reagents used to make the solutions. For the two weaker NaOH treatments there appears to have been a net loss of K as the sediment slurries reacted. For the 3 M NaOH treatment, there was additional K leached from the soil until 180 days of contact. Between 180 and 360 days of contact, the K concentration in the 3 M NaOH solution dropped significantly suggesting a K-bearing precipitate formed. The observed K concentrations in the column effluents (see Section 4.1.2.4, Figure 3.35) for the 0.03 M $NaClO_4$, 0.3 M NaOH, and 3.0 M NaOH treatments averaged about 3, 6, and 12 mg/L, respectively. These values are appreciably less than those shown in Figure 3.46. The extraordinarily high K values in the batch test solutions prior to contacting the sediments, suggests either some analytical problems or some significant contamination within the NaOH reagents used to make up the solutions.

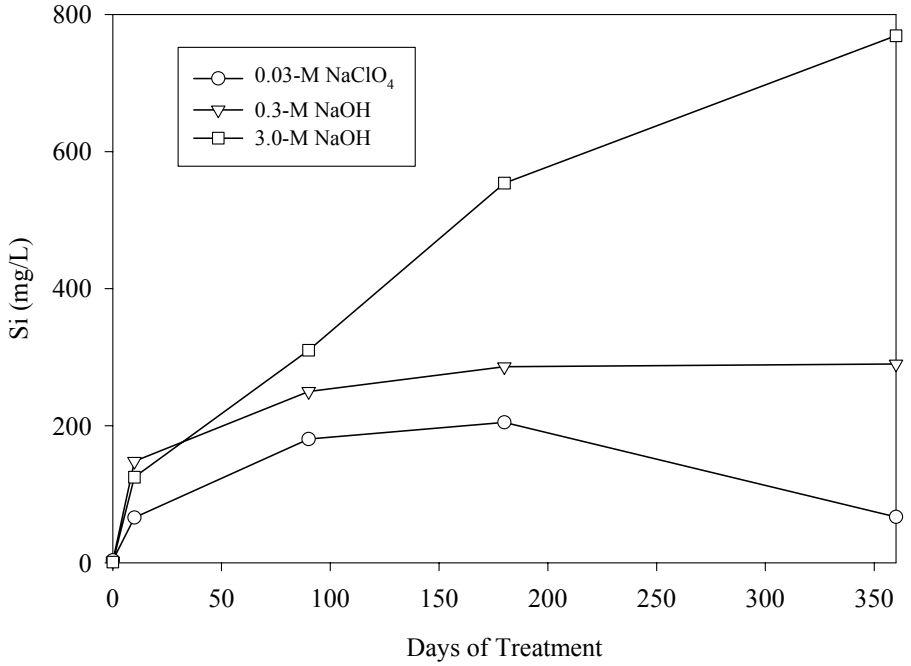

Figure 3.44. Aqueous Si Concentrations in the Warden Silt Loam Batch Study Solutions as a Function of Contact Time

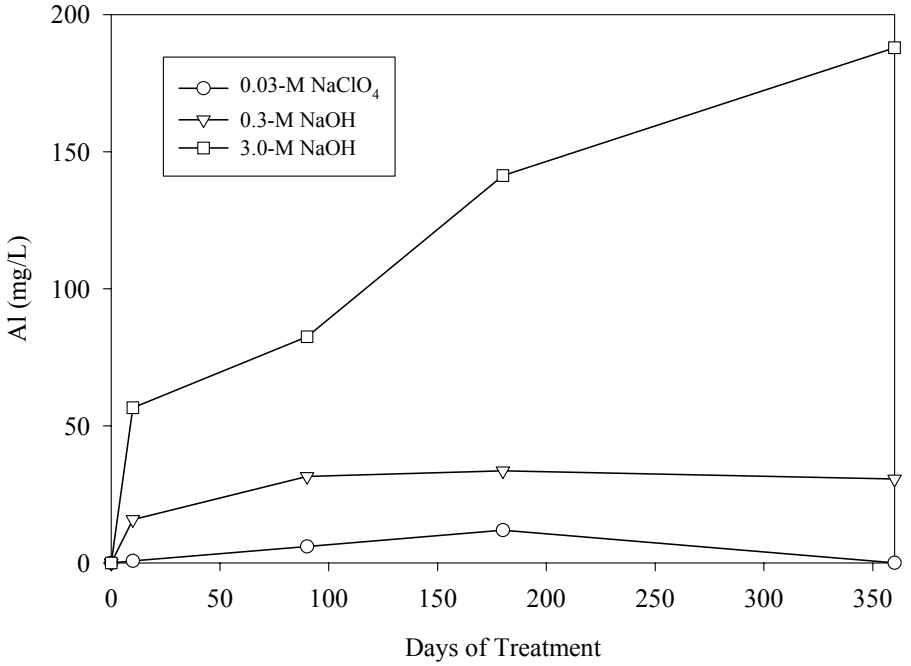

Figure 3.45. Aqueous Al Concentrations in the Warden Silt Loam Batch Study Solutions as a Function of Contact Time

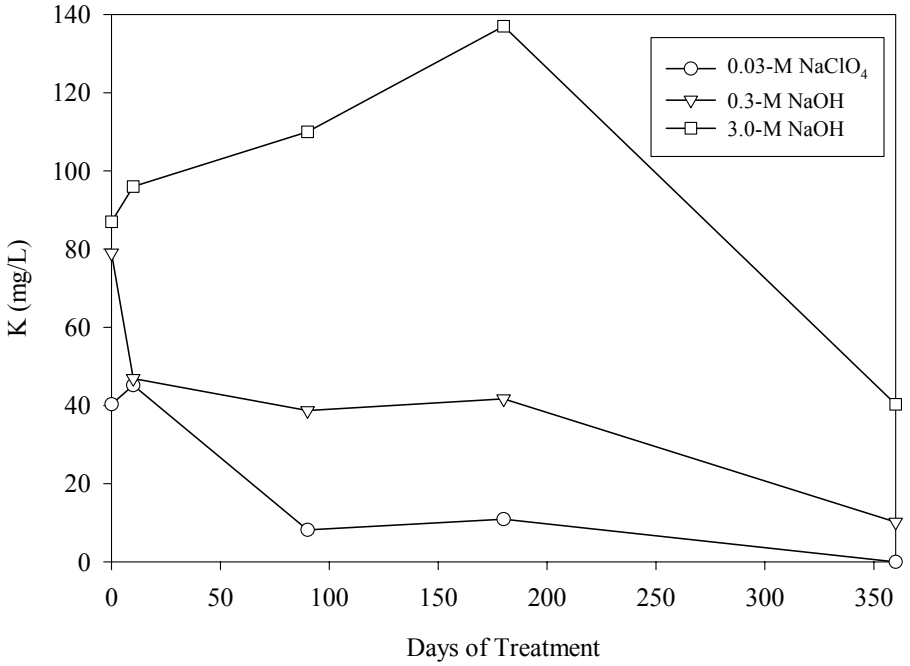

Figure 3.46. Aqueous K Concentrations in the Warden Silt Loam Batch Study Solutions as a Function of Contact Time

The total inorganic carbon concentrations for the 3.0 M NaOH treatment were about an order of magnitude greater than those for the 0.3 M NaOH treatment, which in turn were only slightly greater than those for the 0.03 M NaOH treatment as shown in Figure 3.47. The source of the carbon is likely CO_2 absorbed from the air into the caustic solutions.

3.2.4 Radionuclide Sorption of the Batch Sorption Study

After Warden silt loam samples had been treated with caustic solutions for periods of 0 to 360 days, the samples were equilibrated for 14 days with radiotraced caustic solutions. The soils and liquids were then separated and the radionuclide activity in the aqueous phase was determined by common counting methods (see Table 2.2). The decrease in the radionuclide concentration after contact with the treated soil was attributed to sorption. Importantly, the radionuclides were not in contact with the soils during the extended treatment period, only the last 14 days of contact. Thus, the sorption tests provide a measure of how the sorbing surface changed as a result of the three caustic treatments. Processes such as long-term radionuclide precipitation or co-precipitation during soil weathering were likely not captured by this methodology.

The 0-day-contact-time tests were included in this study to provide a measure of the competitive or ionic strength effects of Na in the treatment solutions on radionuclide sorption. The 0-day contact time tests involved no contact with NaOH but did include a 14-day contact period with radionuclide-spiked 0.03, 0.3, and 3.0 M $NaClO_4$ solutions. It was observed by SEM that the 0.03 M $NaClO_4$ treatment (and by inference the two higher concentrations) did not alter particle surfaces. Since the only difference between the NaOH and the $NaClO_4$ solutions are the anions (i.e., hydroxide vs. perchlorate), it was

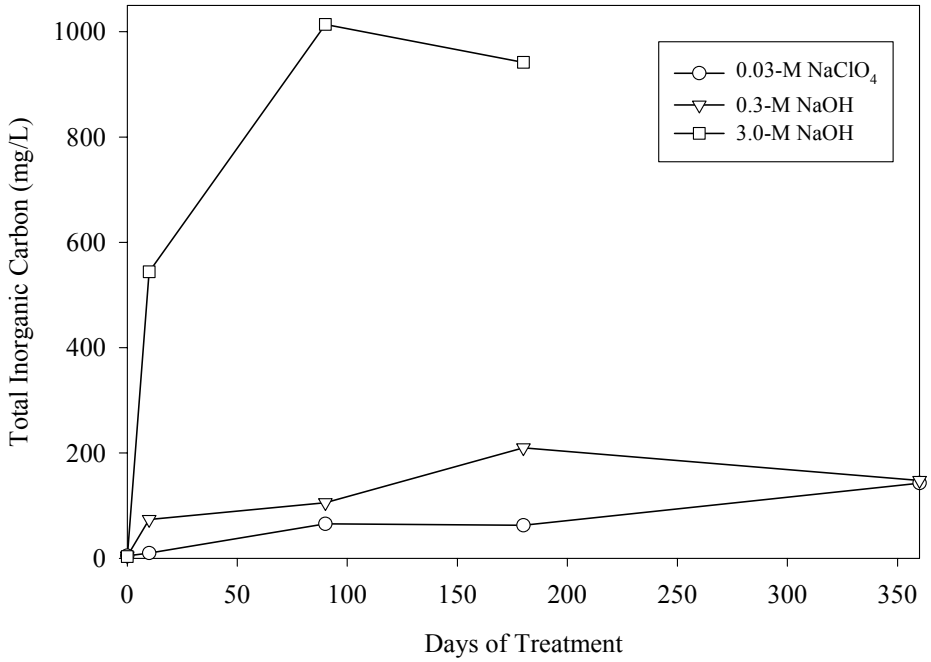

Figure 3.47. Total Aqueous Inorganic Carbon Concentrations (mg/L as C) in the Warden Silt Loam Batch Study Solutions as a Function of Contact Time

expected that the cation competition of Na in the two sets of solutions would be nearly identical. The perchlorate ion, however, was not expected to behave geochemically like the hydroxide ion. The perchlorate ion is not strongly attracted to particle surfaces and has many waters of hydration layers between it and the mineral surface (i.e., it forms an outer-sphere bond), whereas the hydroxide ion adsorbs directly to particle surfaces (i.e., it forms an inner-sphere bond). Thus, competitive effects of hydroxide ions on anionic radionuclide sorption were expected. Furthermore, hydroxide was expected to alter the pH-dependent charge in the soil by increasing the number of cationic sorption sites on any variably charged solid surfaces.

There was no systematic decrease in Cs K_d values as the molar concentration of $NaClO_4$ was increased (Contact Time = 0 days in Table 3.13). Stated differently, Na concentrations between 0.03 M and 3.0 M did not significantly compete with trace concentrations of Cs for sorption sites in the untreated soils. For the soils with 10-day contact times with caustic solutions, the Cs K_d values did not change significantly from the values for the perchlorate controls. Following 90 days of caustic attack, there was no overall change in the Cs K_d versus perchlorate controls, but there was a trend of increasing K_d values as the NaOH concentration increased. There are two possible explanations for the rise in K_d values as OH^- attack occurred. First, the interlayer sheets in some clays may have been expanded or opened up by the caustic attack thus exposing additional exchange sites. Second, Cs may have been co-precipitated with solids formed during the caustic attack.

Table 3.13. Cs and Sr Kd Values as a Function of Contact Time

Contact Time (Days)	Treatment	Cs K_d (mL/g)		Sr K_d (mL/g)	
		Average	Stdev.	Average	Stdev.
0	0.03 M $NaClO_4$	40,260	2205	124	3
	0.3 M $NaClO_4$	42,357	510	18	0
	3.0 M $NaClO_4$	38,085	910	1	1
10	0.03 M $NaClO_4$	39,097	3568	738	37
	0.3 M NaOH	35,229	6432	345	16
	3.0 M NaOH	41,610	1275	324	17
90	0.03 M $NaClO_4$	38,894	284	754	40
	0.3 M NaOH	41,788	1193	315	21
	3.0 M NaOH	43,323	2144	350	15
180	0.03 M $NaClO_4$	18,578	1522	1358	62
	0.3 M NaOH	4121	1316	575	38
	3.0 M NaOH	869	78	472	42
360	0.03 M $NaClO_4$	1558	1141	575	48
	0.3 M NaOH	3182	1649	237	41
	3.0 M NaOH	584	79	225	6

For the 180-day and 360-day treatments, the Cs K_d values decreased greatly for all treatments. One plausible explanation is that the available supply of exchange sites was depleted by the complete destruction or dissolution of the smectite clays, the most common source of surface exchange sites binding the Cs.

As expected for Hanford sediments (see K_d reviews by Kaplan and Serne 2000 and Cantrell et al. 2003), the Sr K_d values were appreciably less than the Cs K_d values (Table 3.13). The Sr K_d values in the control perchlorate solutions at time zero decreased appreciably as the molar strength of Na was increased (see data in Table 3.13 for contact time = 0 day). Under ambient groundwater conditions at the Hanford Site, Sr tends to sorb moderately to mineral surfaces via cation exchange processes. Thus, the degree to which it sorbs to surfaces is markedly influenced by the chemistry of the background solutions. For the longer contact times with the caustic solutions, the Sr K_d increased appreciably. These high K_d values likely reflect the formation of Sr-carbonate precipitates. The elevated pH levels for these tests (Figure 3.42) caused the dissolved inorganic carbon concentrations to also increase (Figure 3.47). Strontium, a chemical analog of Ca, readily forms precipitates (e.g., strontianite, $SrCO_3$) or co-precipitates with carbonate (e.g., calcite). The consistent decrease in Sr K_d values for the two higher concentrations at longer contact times with NaOH likely reflects the effects of increased dissolution of clays in the soil and increased competition for the remaining sorption sites in the high Na concentration solutions.

The Sr K_d value was significantly higher in the NaOH solutions than in the neutral pH perchlorate solutions regardless of the duration of the caustic attack. There was a consistent drop in the Sr K_d values between 180 and 360 days of caustic attack, likely caused by the near complete dissolution of smectite clays that are a major contributor to the cation exchange sites in the Hanford sediments. Nevertheless, the

Sr K_d values for OH^- solutions remained larger than those for the perchlorate solutions showing that Sr removal from high-pH solutions occurred despite the destruction of clay adsorption sites.

Sorption tests were performed for three radionuclides that exist primarily as anions in the Hanford subsurface: pertechnetate (TcO_4^-), selenate (SeO_4^{2-}), and iodide (I^-) (Table 3.14). For the 0-day perchlorate control tests, Se K_d values increased as the $NaClO_4$ concentrations increased. The cause for this is not known. For soils with contact times with NaOH > 0 days, no Se sorption was detected. It is known that oxyanions such as selenate are more stable in high pH solutions (see for example Rai and Serne 1978; EPA 1999a,b; Krupka and Serne 2002). Further, if the observed sorption of trace concentrations of selenate on the Warden silt loam from the neutral pH perchlorate solutions was caused by anion exchange onto the small mass of variably charged hydrous oxides surface sites that are positively charged at acidic to neutral pH, then these sites would be transformed to negatively charged sites in the caustic solutions. Thus any weakly bound selenate would be released from the variably charged hydrous oxide site. Finally, if there are any fixed-positive-charge sites in the Warden silt loam that are not sensitive to pH changes, then the sheer competition from adding OH^- ions may limit selenate adsorption. In the "far field" vadose zone in past performance projections (see Mann et al. 2001) some sorption has been allowed for selenate. Even if the caustic glass leachate completely dominates the entire vadose zone below the repository, such that there will be no sorption of selenate, the dilution and pH neutralization that will occur in the upper unconfined aquifer will allow selenate adsorption to occur onto the aquifer sediments. It is recommended that a future performance assessment sensitivity run be performed to address this point.

Table 3.14. Se, I, and Tc K_d Values as a Function of Contact Time

Contact Time (Days)	Treatment	Se K_d (mL/g)		I K_d (mL/g)		Tc K_d (mL/g)	
		Average	Stdev.	Average	Stdev.	Average	Stdev.
0	0.03 M $NaClO_4$	15	1	0	0	0	0
	0.3 M $NaClO_4$	18	2	0	0	0	0
	3.0 M $NaClO_4$	42	8	0	0	0	0
10	0.03 M $NaClO_4$	0	0	-1	0	0	0
	0.3 M NaOH	0	0	-1	0	0	0
	3.0 M NaOH	0	0	-1	0	0	0
90	0.03 M $NaClO_4$	0	0	-1	0	0	0
	0.3 M NaOH	0	0	-1	0	0	0
	3.0 M NaOH	0	0	-1	0	0	0
180	0.03 M $NaClO_4$	0	0	0	0	0	0
	0.3 M NaOH	0	0	0	0	0	0
	3.0 M NaOH	0	0	0	0	0	0
360	0.03 M $NaClO_4$	-1	0	-2	0	0	0
	0.3 M NaOH	-1	0	-2	0	0	0
	3.0 M NaOH	-1	0	-3	0	0	0

No iodine or technetium sorption was observed for the neutral-pH perchlorate or the high-pH NaOH solutions as a function of time or ionic strength. Thus we would not expect adsorption reactions to retard the migration of selenate, iodide, or pertechnetate from high pH and saline glass leachate percolating through the near-field ILAW vadose zone sediments. There, however, would be significant adsorption of ^{90}Sr, ^{137}Cs, and ^{135}Cs in the near-field. Further, as the pH of the glass leachate is neutralized by reactions with the vadose zone sediments, or certainly by the time vadose zone pore water reaches the water table, there would appear to be some adsorption potential for selenate (including ^{79}Se). There does not appear to be significant potential for the adsorption of iodide or pertechnetate in the near- or far-field Hanford vadose zone based on this work. There is evidence, however, that some minerals and sediments germane to the Hanford Site may be capable of adsorbing iodide (see Kaplan et al. 2000). There is also evidence that the weathering products that form in the glass (i.e., zeolites) can sequester these three anion species (I^-, SeO_4^{2-}, and TcO_4^-) via incorporation into crystal lattice sites or entrapment in the hollow internal structures that are present in most zeolites (see Mattigod et al. 2002 and McGrail et al. 2001).

4.0 Conclusions and Implications for the ILAW PA

The ILAW generated from the Hanford Site will be disposed of in a vitrified form. It is expected that leachate from the vitrified waste will have a high pH and a high ionic strength. Such solutions are known to dissolve silicate minerals and may have significant effects on radionuclide sorption to subsurface materials. These processes could impact the hydrology, mineralogy, radionuclide geochemistry, and physical properties of the near field. Collectively, these processes could greatly impact radionuclide mobility and therefore the performance assessment of the disposal site.

It is not known how the presence of a glass leachate will influence radionuclide mobility at the ILAW disposal site. The dissolution of minerals could decrease the hydraulic conductivity of the sediment if dissolved constituents re-precipitate downstream, or it could increase the hydraulic conductivity of the sediment if dissolved solutes flow downstream without re-precipitating in a limited subsurface region. Similarly, the presence of glass leachate could increase radionuclide mobility by increasing the number of ions competing for sorption sites and by dissolving the minerals that sorb the radionuclides, or it could decrease radionuclide mobility by promoting the co-precipitation of the radionuclides as immobile solids in the reaction products.

The objective of this study was to determine the influence of glass leachate on hydraulic, physical, mineralogical, and sorptive properties of Hanford sediments. Our approach was to put solutions of NaOH, a simplified surrogate for glass leachate, in contact with a quartz sand, a simplified surrogate of the Hanford subsurface sediment, and Warden soil, an actual Hanford sediment. Two studies were conducted: a column study consisting of experiments with quartz sand and Warden soil, and a batch sorption study with Warden soil. The soil or quartz sand were put in contact with the simplified glass leachate solution for varying time periods and changes in the hydraulic conductivity, porosity, bulk density, moisture retention characteristics, mineralogy, aqueous chemistry, and soil-radionuclide distribution coefficients (K_d's) were determined.

After passing 0.3 M and 3.0 M NaOH solutions through quartz sand columns for 194 days, some of the particles became brittle and there was an enrichment in darker particles. SEM and EDX analyses showed that the particles that had become brittle were primarily feldspars and the darker particles were likely ilmenite ($FeTiO_3$). Ilmenite is largely resistant to dissolution by NaOH, and the apparent increase in the dark particles in the quartz sand after contact with the NaOH was the result of the decreased concentration of other minerals, not the precipitation of additional ilmenite. After NaOH treatment, sieve analysis revealed that there was increased particle aggregation. The 0.3 M NaOH-treated sand had lower hydraulic conductivity and greater moisture retention than the control (a 0.03 M $NaClO_4$ treatment). The 3 M NaOH-treated quartz columns also had a small reduction in hydraulic conductivity but the moisture retention decreased versus applied pressure (opposite trend from the 0.3 M treatment). The cause for these different hydrologic responses between the 0.3 and 3.0 M NaOH treatments may be the greater amount of aggregation measured in the 3.0 M NaOH-treated sand and the existence of more precipitated gel coatings in the 0.3 M NaOH-treated sand. These Al and Si gel coatings may have trapped water in their amorphous structure thus causing the observed change in moisture retention properties.

Consequently, we do not suggest that the caustic attack changed the moisture retention properties as a result of dissolution-caused decreases in particle size distribution, one of our initial hypotheses for performing this work.

The NaOH treatments induced much more mineral dissolution and aggregation of residual particles in the Warden soil column experiment than in the Quartz sand column experiment. The 0.3 M NaOH-treated Warden silt loam sediment contained aggregates that could not be broken apart with water and gentle mechanical forces. The 3.0 M NaOH-treated Warden silt loam sediments contained more of these aggregates as well as a gel and several large void spaces within the soil column. Particle size distribution of the 0.3 M NaOH-treated soil was nearly identical to that of the control, contrary to the visual observation of increased aggregation. Particle size distribution of the 3.0 M NaOH-treated soil was very different from the control. There were almost no clay-sized particles remaining after caustic treatment compared to 4 wt.% clay-sized particles in the original sediment. The silt fraction of the 3.0 M NaOH treatment increased 17% with respect to the control; the percentage of almost all other size fractions, including the various sand fractions, decreased. That is, some sand-sized grains were made smaller and the clay-sized particles were either dissolved or agglomerated with other material to become larger.

The effects of the NaOH treatments on the Warden soil moisture retention characteristics were very similar to those observed in the quartz sand; namely, that there was more moisture retained by the 0.3 M NaOH-treated soil than the control and less moisture retained by the 3.0 M NaOH-treated soil than the control. All of the soil columns including the control columns showed significant decreases in hydraulic conductivity after 6 months of fluid percolation. Therefore, the drop in hydraulic conductivity was not caused solely by caustic attack. We later discovered that improper techniques and artifacts in the column apparatus caused most of the apparent decrease. Although our attempts to quantitatively measure changes in bulk density and porosity failed, visual and XMT observations suggested that numerous voids formed in the columns. In conclusion, although there were visual signs (e.g., aggregation of particles, voids in the columns, signs of gel coatings with 0.3 M NaOH treatment), we did not find clearly significant changes in hydraulic conductivity, overall porosity, and bulk density. The changes were either below our detection limits or there were flaws in our technique.

The 3.0 M NaOH-treated Warden soil from the column experiment had less kaolinite and chlorite and essentially no smectite remaining after the 194-day treatment. The concentration of illite did not appear to change. Quartz, feldspar, and calcite concentrations increased; quartz and feldspar because the proportion of other minerals decreased, and calcite as a result of calcite precipitating out of the elevated pH solutions. SEM images of the treated soil showed that feldspar particles became increasingly pitted as the molar strength of NaOH increased. Significant amounts of Si-Al gel-coatings were observed on albite, quartz, and plagioclase particles; fewer coatings were observed on orthoclase particles.

The chemical species found in the effluents from the Warden soil columns were very similar to those found in the effluents from the quartz sand columns; the concentrations of soluble Al, Si, Fe, K, and others, however, were much higher in the soil column effluents. The similarity in specific species was attributed to the fact that the quartz sand and the Warden soil were made up primarily of similar minerals (e.g., quartz, feldspar, and mica/illite). The differences in concentrations are attributed to the soils containing more amorphous (i.e., more soluble) material and smaller particles (i.e., more reactive surface

area) than the quartz sand. For both of the column experiments, dissolution in the first seven days was more rapid than in the remaining 187 days. Aqueous concentrations in the effluents from the constant flow experiments were highest in the first 7 days; aqueous concentrations of Si, Al, and K generally decreased over the remaining 187 days.

Appreciably more precipitation of reaction products took place during the 360-day batch experiment with the Warden soil than in the flow-through column tests. This was attributed to the batch experiment being a closed system where dissolved reaction products are not removed. The solution concentrations in the batch tests increased with time until back reactions caused precipitation of previously dissolved materials or new secondary phases. In the batch tests, caustic treatment also changed the particle size distribution of the soil by forming large sand-sized aggregates under all treatment conditions after 90 days of contact. There appears to be evidence of early diminution of medium sand-sized grains after 10 days of contact forming silt-sized particles. The silt size-fraction remained larger than the starting distribution throughout the testing period even as the large sand-sized aggregates formed at a slow rate for the caustic tests at 0.03 to 0.3 M NaOH. For the 3 M NaOH treatment the Warden silt loam large sand-sized aggregates are present after 90 days but the clay- and silt-sized fractions decrease after the first 10 days of contact. Between 10 and 180 days at 3 M NaOH caustic treatment, the fine sand sizes increase, likely as silt and clay particles are aggregated. The aggregates continue to grow into coarse sand-sized material between 90 and 360 days of contact.

The NaOH treatments in the soil batch experiment did not result in the dissolution of quartz, Na-feldspar, amphibole, chlorite, and muscovite in the silt and sand fractions. Fine-grained Ca-feldspar, however, showed evidence of dissolution. In the clay fraction, both XRD and TEM analysis suggest that illite and chlorite were not greatly affected by the NaOH treatments. Large unaltered particles of both minerals were observed using TEM on the 360-day-treated soil. Smectite and kaolinite were severely attacked and almost completely removed from the clay fraction after the 360-day 3 M NaOH caustic treatment. No mineralogy or SEM/TEM characterization was done of the 0.03 or 0.3 M NaOH batch treatments on the Warden silt loam.

Sorption tests were conducted with the soils from the batch sorption study. Cs K_d values were measured in soils treated for up to 360 days. The Cs K_d values were large in the perchlorate control solutions and did not change significantly over the Na solution concentration range of 0.03 to 3 M. After 10 days of caustic attack the Cs K_d values did not change appreciably. At 90 days of caustic treatment, there is still little change in the Cs K_d but it did increase as the NaOH content increased. After 180 and 360 days of caustic contact the Cs K_d dropped noticeably. One plausible explanation is the complete destruction of the smectite clays eliminated the most significant and common adsorbent in the soil.

Sr K_d values were quite sensitive to the ionic strength of the perchlorate control solutions and to some extent the NaOH treatments. The higher the Na concentration in solutions, the lower the Sr K_d. The Sr K_d increased dramatically when the pH of the system increased during the caustic treatments. This large increase in Sr K_d might reflect Sr co-precipitation with the calcium carbonate that forms. At long contact times with caustic, the Sr K_d drops some, perhaps because of destruction of the smectite clays, but the K_d still remains 4 to 100 times larger than for neutral pH conditions. At high Na concentrations and high pH, the Sr Kd remains much higher than for neutral pH with high Na concentrations. Thus the probable Sr co-precipitation process overshadows the adsorption processes that are quite sensitive to Na competition.

None of the anions (iodide [I^-], pertechnetate [TcO_4^-], or selenate [SeO_4]) sorbed to the caustic-treated soils. Selenate did show moderate adsorption onto the soil during the control tests in perchlorate solutions with neutral pH values. The Se K_d increased as the Na concentration increased in the neutral pH control solution ($NaClO_4$) suggesting that high ionic strength increases selenate adsorption.

In summary, these studies showed that under chemical conditions approaching the most caustic glass leachate conditions expected in the near field of the ILAW disposal site, approximated by 0.3 M NaOH, significant changes in mineralogy were observed. Under flowing conditions, some aggregation of solids was observed, likely from cementation via Al-Si gel or carbonate formation. The gels and amorphous precipitates increased the moisture retention characteristics but had only minor effects on the saturated hydraulic conductivity of the soil. Little change in Cs K_d values and a significant increase in Sr K_d values were measured for caustic-treated sediments. As the severity of the caustic treatment increased the Cs and, to a lesser extent, the Sr K_d values drop slightly with time. The slight drop might be caused by the near complete destruction of the smectite clays in the soil.

There was no observed adsorption of the anions iodide, selenate, and pertechnetate onto the caustic-treated sediments when the solutions remained at high pH values. In the "far field" vadose zone in past performance projections, some sorption has been allowed for selenate. Even if the caustic glass leachate completely dominates the entire vadose zone below the repository, such that there will be no sorption of selenate, the dilution and pH neutralization that will occur in the upper unconfined aquifer will allow selenate adsorption to occur onto the aquifer sediments. It is recommended that a future performance assessment sensitivity run be performed to address this point.

Since a majority of the dissolution and precipitation occurred within 7 days of contact with the caustic solution, future research on the dissolution aspects of caustic attack can be conducted over shorter durations but the subsequent re-precipitation processes and the re-incorporation of trace contaminants into secondary minerals and gels appear to occur over time periods that do not reach steady state within one year.

5.0 References

Amer, A. M. 2002. "Alkaline Pressure Leaching of Mechanically Activated Rosetta Ilmenite Concentrate." *Hydrometallurgy* 67:125–133.

American Society for Testing and Materials (ASTM). 1985. "Standard Test Method for Particle-Size Analysis of Soils. D 422-63 (1972)." *1985 Annual Book of ASTM Standards* Vol.04.08:117-127. American Society for Testing and Materials, Philadelphia, Pennsylvania.

American Society for Testing and Materials (ASTM). 1988. "Standard Test Method for Total and Organic Carbon in Water by High Temperature Oxidation and by Coulometric Detection." *1988 Annual Book of ASTM Standards.* American Society for Testing and Materials, West Conshohocken, Pennsylvania.

Amonette, J. E. 1994. Mineralogical Analysis of Soil Samples by X-Ray *Diffraction (XRD)*. JEA-3, Rev. 0, Pacific Northwest National Laboratory, Richland, Washington.

Blake, G. R., and K. H. Hartge. 1986. "Particle Density." In *Methods of Soil Analysis, Part 1, Physical and Mineralogy Methods*, ed. A. Klute, pp. 377-382. Soil Science Society of America, Madison, Wisconsin.

Brady, P. V., and J. V. Walther. 1989. "Controls on Silicate Dissolution Rates in Neutral and Basic pH Solutions at 25°C." *Geochim. Cosmochim. Acta* 53:2823-2830.

Cantrell, K. J., R. J. Serne, and G. V. Last. 2003. *Hanford Contaminant Distribution Coefficient Database and Users Guide*. PNNL-13895, Rev. 1, Pacific Northwest National Laboratory, Richland, Washington.

Casey, W. H., H. R. Westrich, G. W. Arnold, and J. F. Banfield. 1989. "The Surface Chemistry of Dissolving Labradorite Feldspar." *Geochim. Cosmochim. Acta* 53:821-832.

Casey, W. H., H. R. Westrich, and G. W. Arnold. 1988. "Surface Chemistry of Labradorite Feldspar Reacted with Aqueous Solutions at pH = 2, 3, and 12." *Geochim. Cosmochim. Acta* 52: 2795-2807.

de Andrade, J. B., G. S. Nunes, M. P. Veiga, A. C. Spinola Costa, S. L. C. Ferreira, A. M. M. Amorim, and S. T. Reis. 1997. "Spectrophotometric and Inductively Coupled Plasma Atomic Emission Sprectrophotometric Determination of Titanium in Ilmenites After Rapid Dissolution with Phosphoric Acid." *Talanta* 44:165-168.

Drees, L. R., L. P. Wilding, N. E. Smeck, and A. L. Senkayi. 1989. "Silica in Soils: Quartz and Disordered Silica Polymorphs." In *Minerals in Soil Environments*, 2nd ed., eds. J. B. Dixon and S. B. Week. Soil Science Society of America, Madison, Wisconsin.

Drever, J. I. 1973. "The Preparation of Oriented Clay Mineral Specimens for X-Ray Diffraction Analysis by a Filter Membrane Peel Technique." *Am. Mineral.* 58:553-554.

EPA. See U.S. Environmental Protection Agency.

Gee, G. W., and J. W. Bauder. 1986. "Particle-size Analysis." In *Methods of Soil Analysis, Part 1. Physical and Mineralogy Methods*, ed. A. Klute, pp. 383-411. Soil Science Society of America, Madison, Wisconsin.

Hillel, D. 1971. Soil and Water—Physical Principles and Processes. Academic Press, New York.

Holdren, G. R., and P. M. Speyer. 1987. "Reaction Rate-surface Area Relationships During the Early Stages of Weathering. II. Data on Eight Additional Feldspars." *Geochim. Cosmochim. Acta* 51:2311-2318.

Kaplan D. I., and R. J. Serne. 2000. *Geochemical Data Package for the Hanford Immobilized Low-Activity Tank Waste Performance Assessment (ILAW-PA)*. PNNL-13037, Rev. 1, Pacific Northwest National Laboratory, Richland, Washington.

Kaplan, D. I., K. E. Parker, and J. C. Ritter. 1998. Effects of Aging a Hanford Sediment and Quartz Sand with Sodium Hydroxide on Radionuclide Sorption Coefficients and Sediment Physical and Hydrological Properties: Final Report for Subtask 2a. PNNL-11965, Pacific Northwest National Laboratory, Richland, Washington.

Kaplan, D. I., R. J. Serne, K. E. Parker, and I. V. Kutnyakov. 2000. "Iodide Sorption to Subsurface Sediments and Illitic Minerals." *Environ. Sci. Technol.* 34:399-405.

Khaleel, R. 1999. Far-Field Hydrology Data Package for Immobilized Low-Activity Tank Waste Performance Assessment. HNF-4769, Rev. 1, Fluor Daniel Northwest, Inc., Richland, Washington.

Khaleel, R. and E. J. Freeman. 1995. *Variability and Scaling of Hydraulic Properties for 200 Area Soils, Hanford Site*. WHC-EP-0883, Westinghouse Hanford Company, Richland, Washington.

Klute, A. and C. Dirksen. 1986. "Hydraulic Conductivity and Diffusivity: Laboratory Methods," In *Methods of Soil Analysis, Part 1. Physical and Mineralogy Methods*, ed. A. Klute, pp. 687-734. Soil Science Society of America, Madison, Wisconsin.

Krupka, K. M. and R. J. Serne. 2002. Geochemical Factors Affecting the Behavior of Antimony, Cobalt, Europium, Technetium, and Uranium in Vadose Zone Sediments. PNNL-14126, Pacific Northwest National Laboratory, Richland, Washington.

Mann, F. M., K. C. Burgard, W. R. Root, R. J. Puigh, S. H. Finfrock, R. Khaleel, D. H. Bacon, E. J. Freeman, B. P. McGrail, S. K. Wurstner, and P. E. LaMont. 2001. *Hanford Immobilized Low-Activity Waste Performance Assessment: 2001 Version*. DOE/ORP-2000-24, Rev. 0, Office of River Protection, Richland, Washington.

Mattigod, S. V., R. J. Serne, B. P. McGrail, and V. L. Legore. 2002. "Radionuclide Incorporation in Secondary Crystalline Minerals From Chemical Weathering of Waste Glasses Radionuclides". *In MRS Proceedings,* vol. 713, pp. 597-604. Warrentown, Pennsylvania.

McGrail, B. P., D. H. Bacon, J. P. Icenhower, F. M. Mann, R. J. Puigh, H. T. Schaef, and S. V. Mattigod. 2001. "Near-Field Performance Assessment for a Low-Activity Waste Glass Disposal System: Laboratory Testing to Modeling Results." *J. Nucl. Mater.* 298:95-111.

McKinley J. P., S. A. Rawson, and D. G. Horton. 1986. "Form and Composition of Secondary Mineralization in Fractures in Columbia River Basalts." In *Microbeam Analysis – 1986*, ed. W. F. Chambers, pp. 127-130. San Francisco Press, Inc.

Meyer, P. D. and R. J. Serne. 1999. *Near-Field Hydrology Data Package for the Immobilized Low-Activity Waste 2001 Performance Assessment*. PNNL-13035, Pacific Northwest National Laboratory, Richland, Washington.

Moore, D. M. and R. C. Reynolds. 1989. X-Ray Diffraction and the Identification *and Analysis of Clay Minerals*, Oxford University Press, Oxford, United Kingdom.

Rafal, M., J. W. Berthold, N. C. Scrivner, and S. L. Grise. 1994. "Models for Electrolyte Solutions." In *Models for Thermodynamic and Phase Equilibria Calculations,* ed. S. I. Sandler, pp. 601-670. Marcel Dekker, Inc., New York.

Rai, D. and R. J. Serne. 1978. *Solid Phases and Solution Species of Different Elements in Geologic Environments.* PNL-2651, Pacific Northwest Laboratory, Richland, Washington.

Rhoades, J. D. 1996. "Salinity: Electrical Conductivity and Total Dissolved Solids." In *Methods of Soil Analysis, Part 3 – Chemical Methods,* ed. D. L. Sparks, pp. 417-436. Soil Science Society of America, Madison, Wisconsin.

Rockhold, M. L., M. J. Fayer, and P. R. Heller. 1993. *Physical and Hydraulic Properties of Sediments and Engineered Materials Associated with Grouted Double-Shell Tank Waste Disposal at Hanford*. PNL-8813, Pacific Northwest Laboratory, Richland, Washington.

Tardy, Y., and D. Nahon. 1985. "Geochemistry of Laterites, Stability of Al-Goethite, Al-Hematite, and Fe^{3+}- Kaolinite in Bauxites and Ferricretes: An Approach to the Mechanism of Concretion Formation." *Amer. J. Sci.* 285:865-903.

U.S. Environmental Protection Agency (EPA). 1999a. Understanding Variation in Partition Coefficient, K_d, Values: Volume I. The K_d Model, Methods of Measurement, and Application of Chemical Reaction Codes. EPA 402-R-99-04A, prepared for the U.S. Environmental Protection Agency, Washington, D.C. by Pacific Northwest National Laboratory, Richland, Washington.

U.S. Environmental Protection Agency (EPA). 1999b. Understanding Variation in Partition Coefficient, K_d, Values: Volume II. Review of Geochemistry and Available K_d Values for Cadmium, Cesium, Chromium, Lead, Plutonium, Radon, Strontium, Thorium, Tritium (^3H), and Uranium. EPA 402-R-99-004B, prepared for the U.S. Environmental Protection Agency, Washington, D.C. by Pacific Northwest National Laboratory, Richland, Washington.

Whittig, L. D., and W. R. Allardice. 1986. "X-Ray Diffraction Techniques." In *Methods of Soil Analysis, Part 1 Physical and Mineralogical Methods, Second Edition,* ed. A. Klute, pp. 331-362. Soil Science Society of America, Inc., Madison, Wisconsin.

Wieland, E., B. Wehrli, and W. Stumm. 1988. "The Coordination Chemistry of Weathering: III. A Generalization on the Dissolution Rates of Minerals." *Geochim. Cosmochim. Acta* 52:1969-1981.

Appendix A

Scanning Electron Microscope

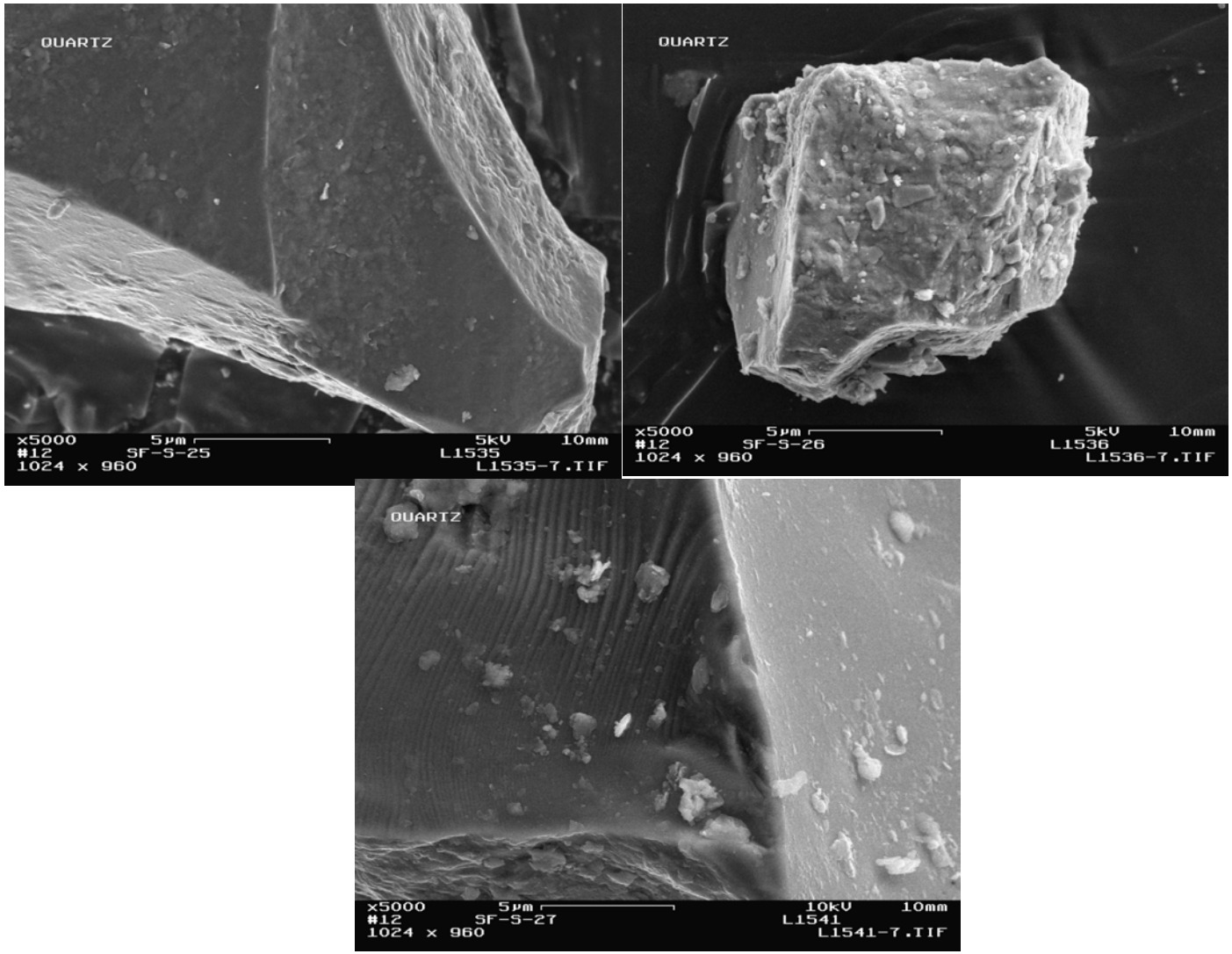

Figure A.1. Quartz (Silt Fraction) From Warden-Soil Column Experiments After 194 Days to Provide Examples of How Surface Roughness Changes with Treatments: Untreated (Top Left), 0.3 M NaOH Treatment (Top Right), and 3.0 M NaOH Treatment (Bottom)

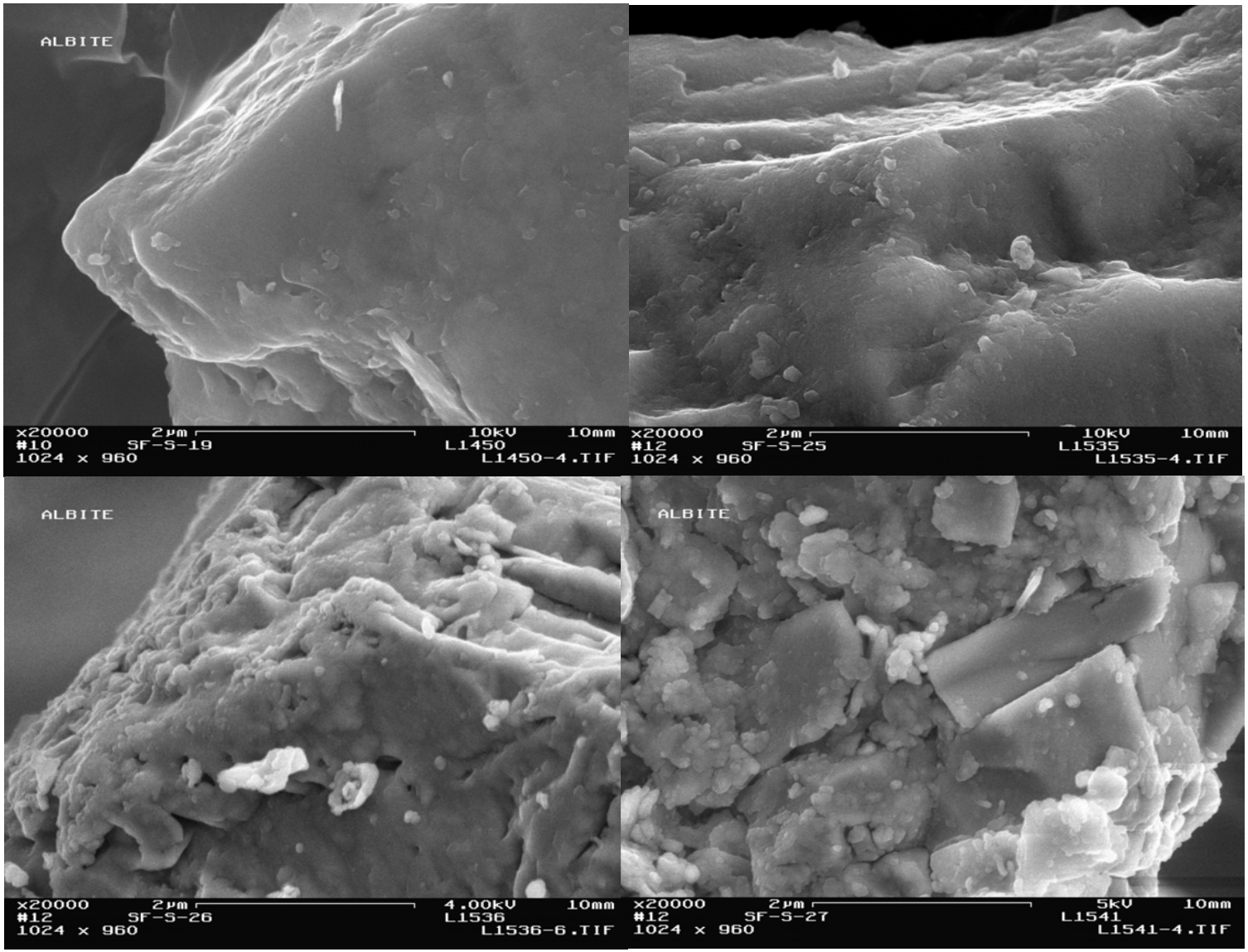

Figure A.2. Albite (Silt Fraction) From Warden-Soil Column Experiment After 194 Days: Untreated (Top Left), 0.03 M $NaClO_4$ Treatment (Top Right), 0.3 M NaOH Treatment (Bottom Left), and 3.0 M NaOH Treatment (Bottom Right)

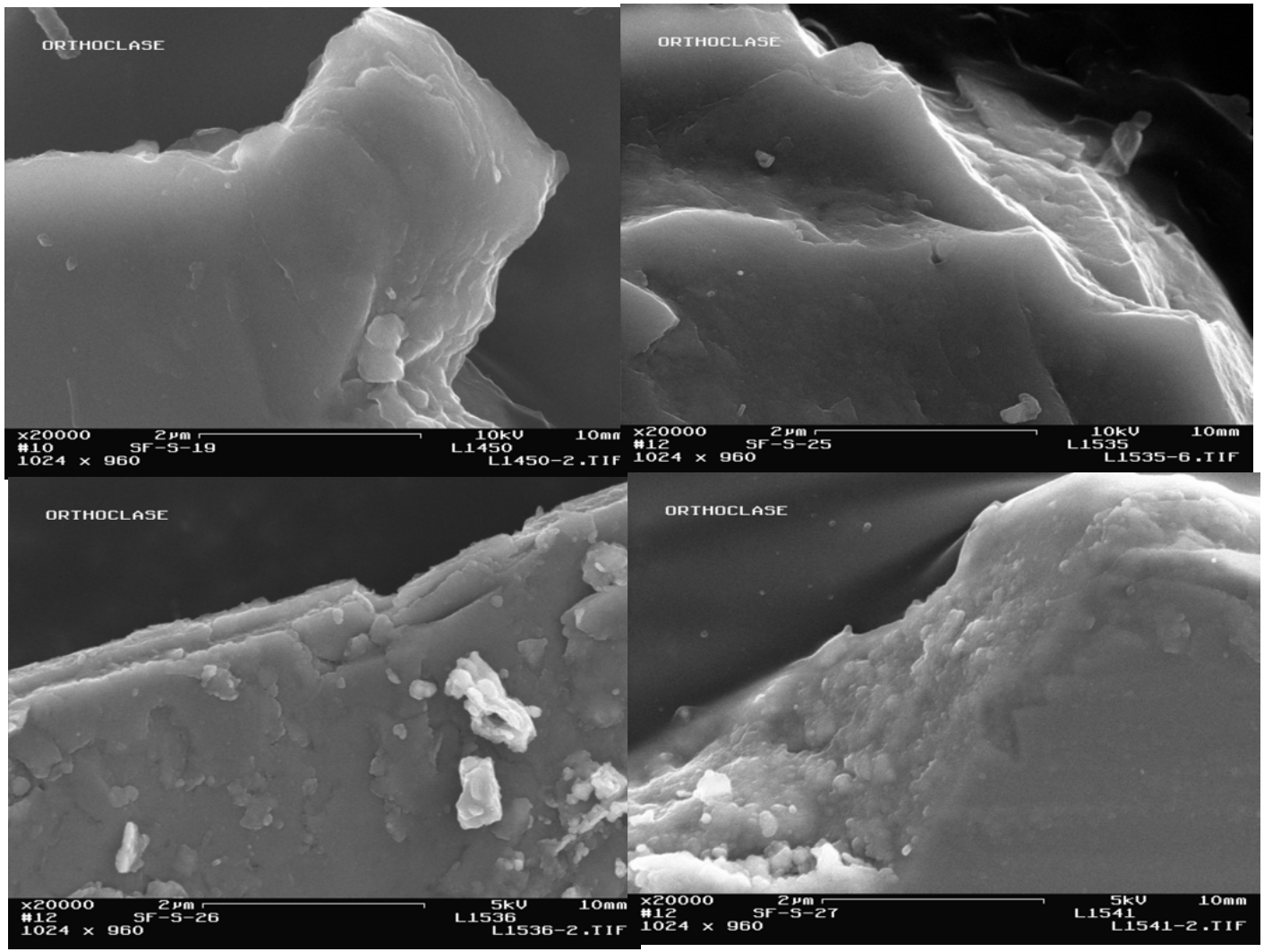

Figure A.3. Orthoclase (Silt Fraction) From Warden-Soil Column Experiment After 194 Days: Untreated (Top Left), 0.03 M $NaClO_4$ Treatment (Top Right), 0.3 M NaOH Treatment (Bottom Left), and 3.0 M NaOH Treatment (Bottom Right)

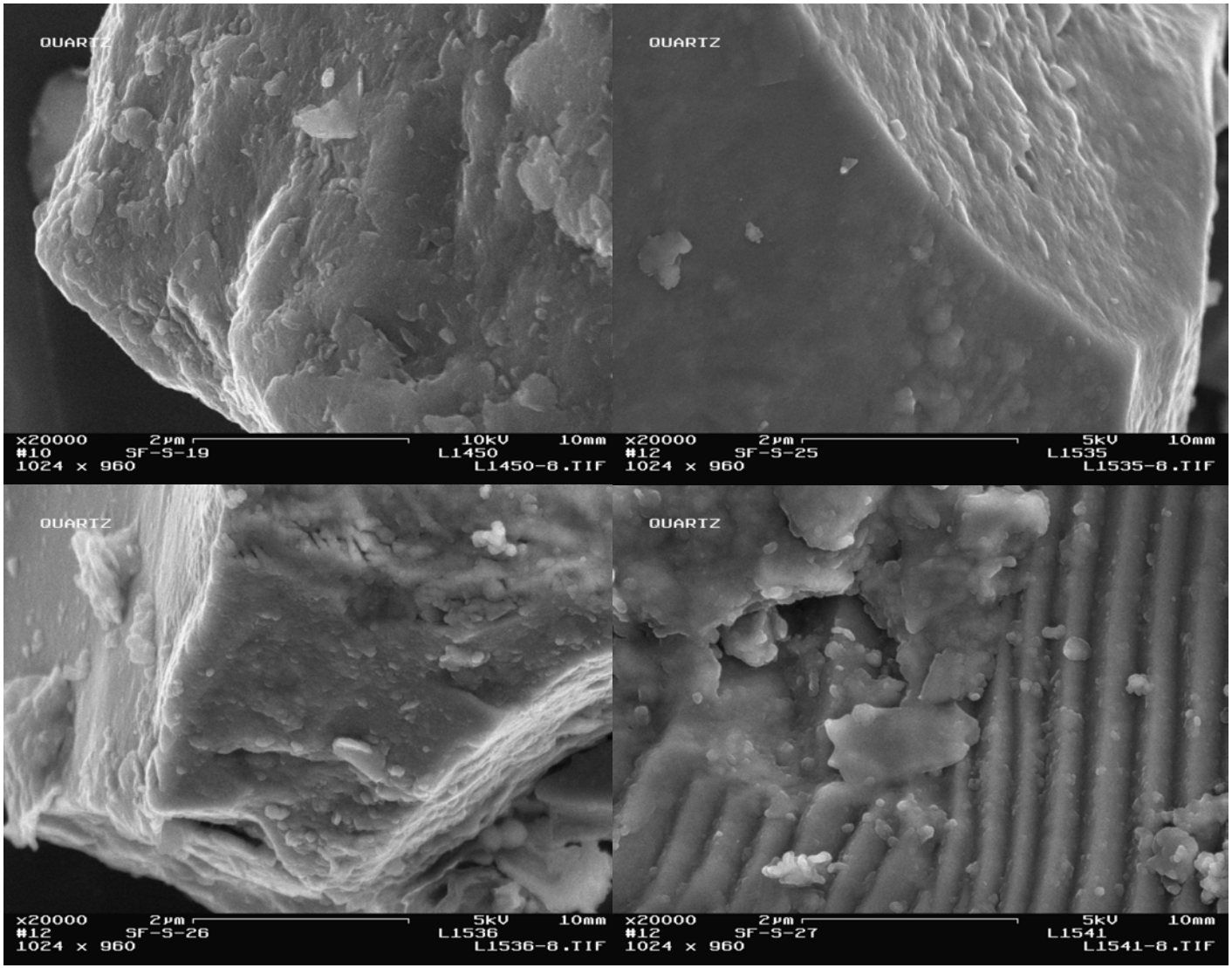

Figure A.4. Quartz (Silt Fraction) from Warden-Soil Column Experiment After 194 Days: Untreated (Top Left), 0.03 M $NaClO_4$ Treatment (Top Right), 0.3 M NaOH Treatment (Bottom Left), and 3.0 M NaOH Treatment (Bottom Right)

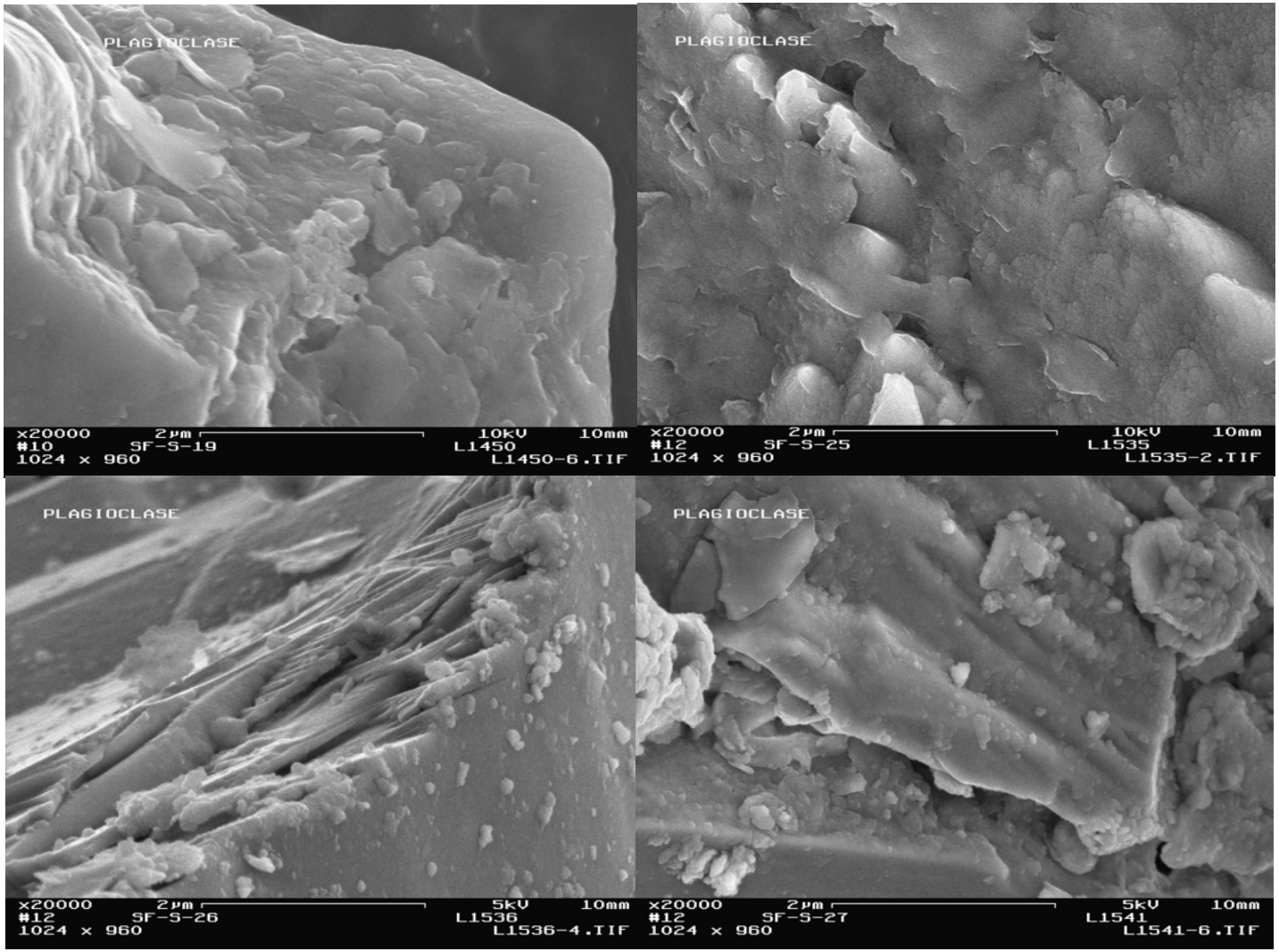

Figure A.5. Plagioclase (Silt Fraction) From the Warden-Soil Column Experiment After 194 Days: Untreated (Top Left), 0.03 M $NaClO_4$ Treatment (Top Right), 0.3 M NaOH Treatment (Bottom Left), and 3.0 M NaOH Treatment (Bottom Right)

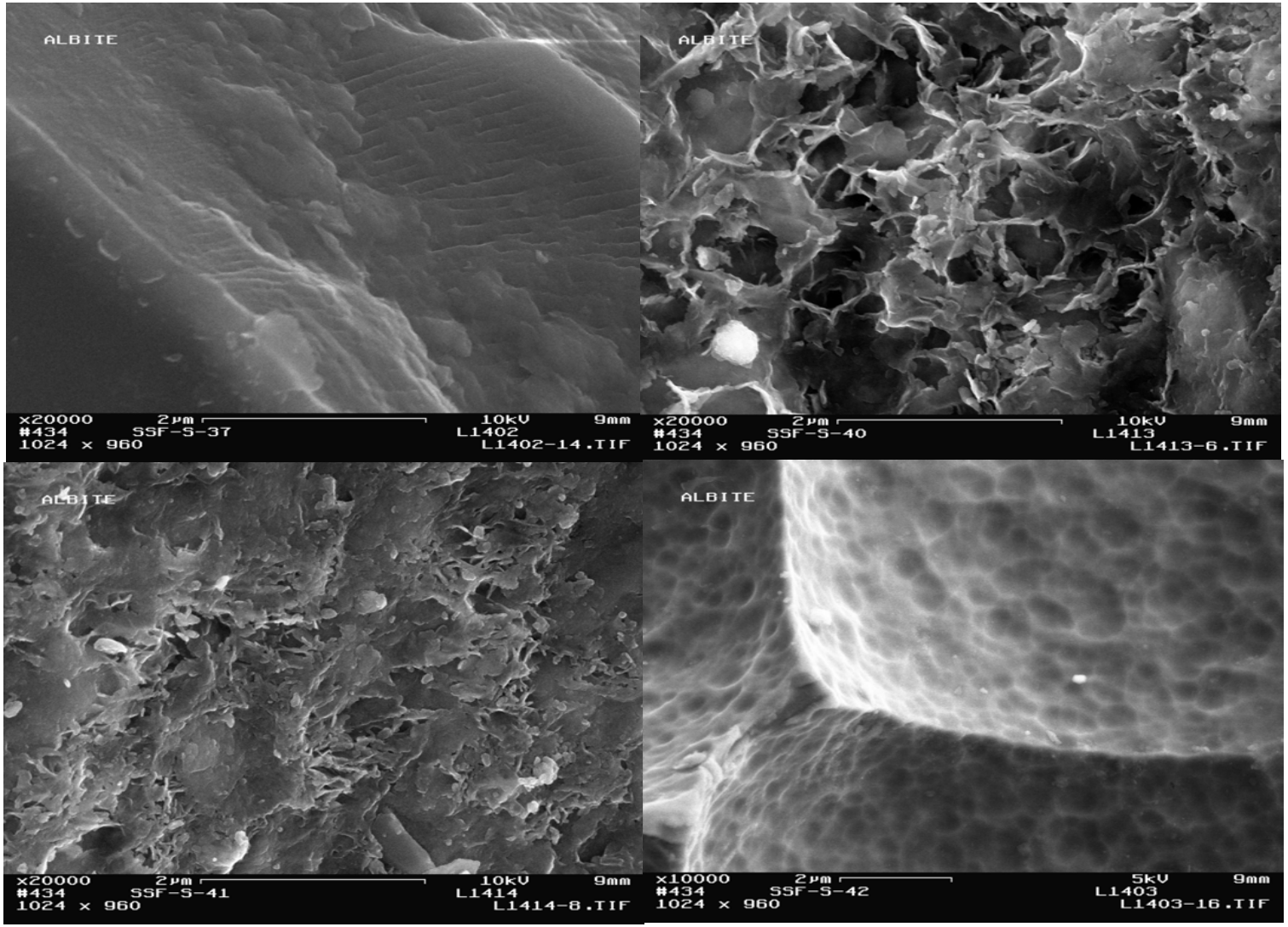

Figure A.6. Albite (Sand Fraction) from the 3.0 M NaOH Batch Treatment After 0 (Top Left), 90 (Top Right), 180 (Bottom Left), and 360 Days (Bottom Right)

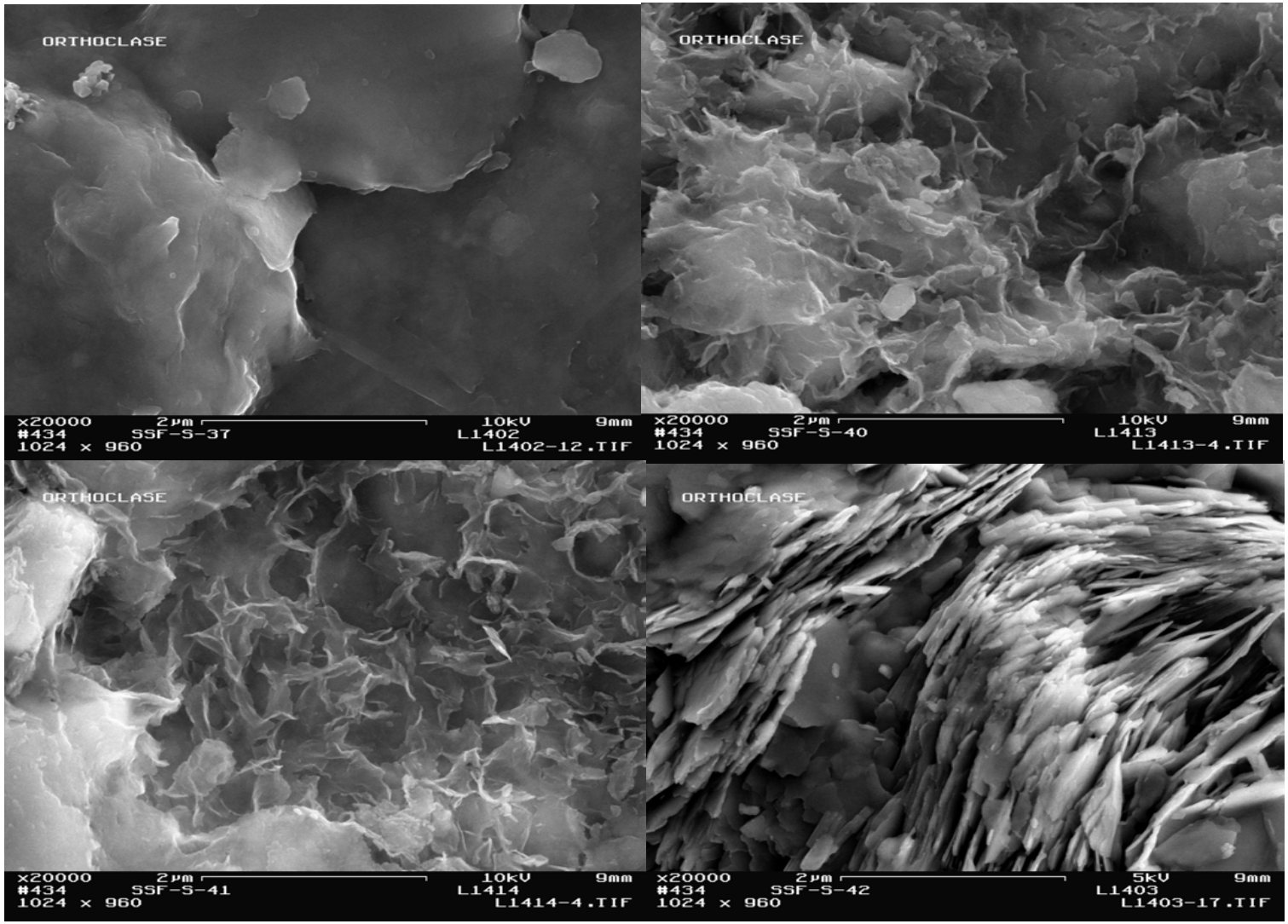

Figure A.7. Orthoclase (Sand Fraction) from the 3.0 M NaOH Batch Treatment After 0 (Top Left), 90 (Top Right), 180 (Bottom Left), and 360 Days (Bottom Right)

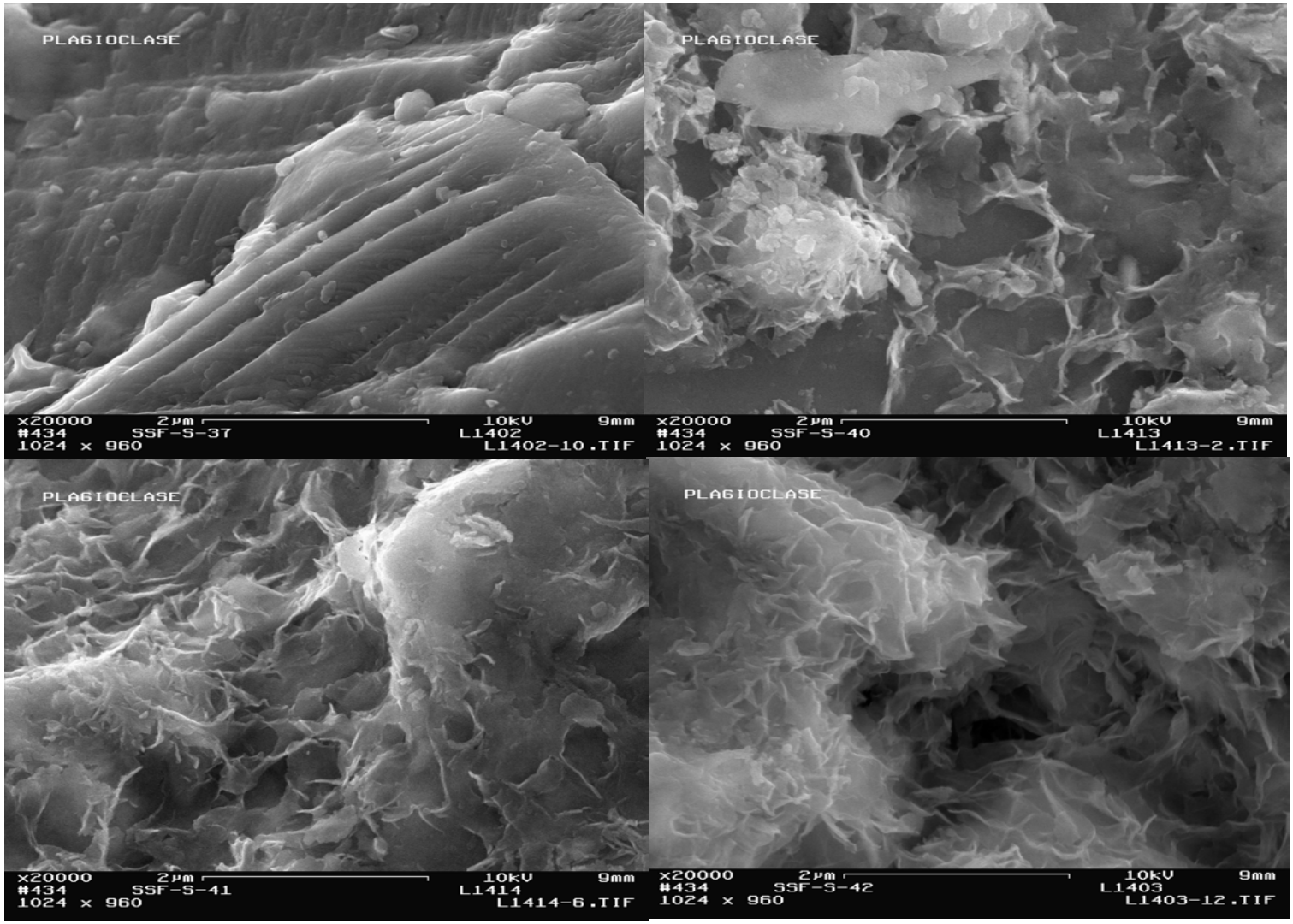

Figure A.8. Plagioclase (Sand Fraction) from the 3.0 M NaOH Batch Treatment After 0 (Top Left), 90 (Top Right), 180 (Bottom Left), and 360 Days (Bottom Right)

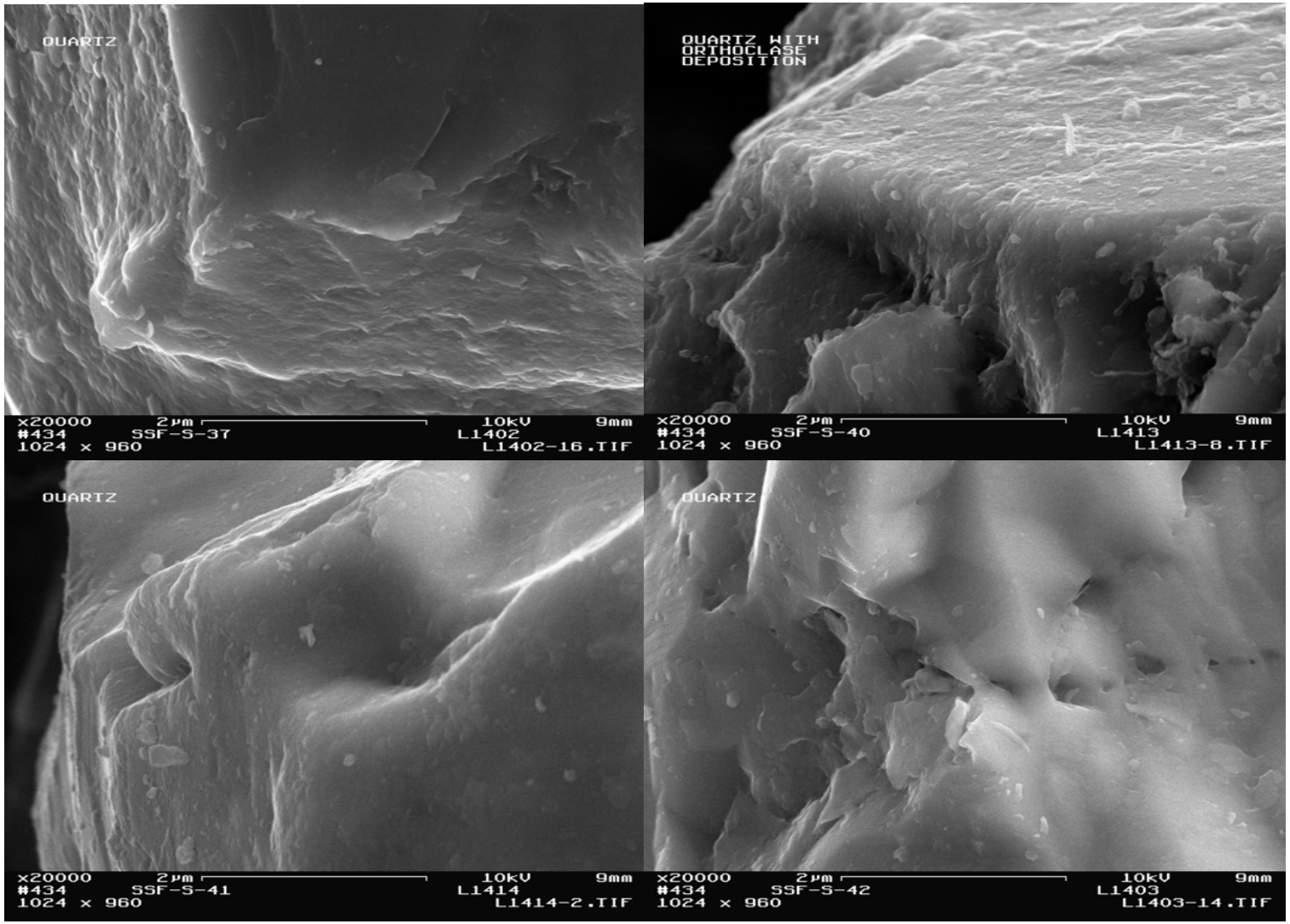

Figure A.9. Quartz (Sand Fraction) from the 3.0 M NaOH Batch Treatment After 0 (Top Left), 90 (Top Right), 180 (Bottom Left), and 360 Days (Bottom Right)

Distribution

No. of Copies

26 OFFSITE

Dr. Harry Babad
2540 Cordoba Court
Richland, WA 99352-1609

P. Brady
Geochemistry Department, 6118
Sandia National Laboratories
PO Box 5800
Albuquerque, NM 87185-0750

C. R. Bryan
Sandia National Laboratories
4100 National Parks Highway
Carlsbad, NM 88220

S. Carroll
Lawrence Livermore National Laboratory
Mail Stop L-219
Livermore, CA 94550

J. Chorover
Associate Professor – Environmental Chemistry
Department of Soil, Water and Environmental Science
Shantz 429, Building #38
University of Arizona
Tucson, AZ 85721-0038

D. A. Dunning
Oregon Office of Energy
625 Mariona St. N. E.
Salem, OR 97301-3742

No. of Copies

M. Flury
Department of Crop and Soil Sciences
Washington State University
Pullman, WA 99164

A. P. Gamerdinger
2122 E. Hawthorne
Tucson, AZ 85719

J. Harsh
Department of Crop and Soil Sciences
Washington State University
Johnson Hall -- Room 249
Pullman, WA 99164-6420

Dr. C. Johnston
Soil Chemistry and Mineralogy
1150 Lily Hall
Purdue University
West Lafayette, IN 47907-1150

Dr. D. I. Kaplan (5)
Westinghouse Savannah River Company
Bldg. 774-43A, Rm 215
Aiken, SC 29808

Dr. P. C. Lichtner
Los Alamos National Laboratory
PO Box 1663
Los Alamos, NM 87545

M. A. Mayes
Environmental Sciences Division
Oak Ridge National Laboratory
PO Box 2008
Oak Ridge, TN 37831-6038

No. of Copies

Dr. K. L. Nagy
Department of Earth and Environmental Sciences
University of Illinois at Chicago (MC-186)
845 West Taylor Street
Chicago, IL 60607-7059

H. Nitsche
Director, Center for Advanced Environmental and Nuclear Studies
Lawrence Berkeley National Laboratory
1 Cyclotron Road MS 70A-1150
Berkeley, CA 94720

P. Reed
U.S. Nuclear Regulatory Commission
Office of Nuclear Regulatory Research
Division of Systems Analysis and Regulatory Effectiveness
Radiation Protection, Environmental Risk and Waste Management Branch
Mail Stop: T9-F31
Washington, DC 20555-0001

D. Sherwood
Rivers Edge Environmental
1616 Riverside Drive
West Richland, WA 99353

C. I. Steefel
Lawrence Livermore National Laboratory
Earth & Environmental Sciences Directorate
Mail Stop L-204
PO Box 808
Livermore, CA 94551-9900

Dr. S. J. Traina, Director
Sierra Nevada Research Institute
University of California, Merced
PO Box 2039
Merced, CA 95344

No. of Copies

Dr. T. T. C. Vandergraaf
Atomic Energy of Canada, Limited
Whiteshell Nuclear Research Establishment
Pinawa, Manitoba ROE 1LO
Canada

Dr. J. Wan
Lawrence Berkeley National Laboratory
1 Cyclotron Rd. MS 70-0127A
Berkeley, CA 94720

W. A. Williams
US Department of Energy
Office of Environmental Restoration
EM-33
19901 Germantown Road
Germantown, MD 20874-1290

ONSITE

3	**DOE Office of River Protection**	
	C. A. Babel	H6-60
	P. E. LaMont	H6-60
	R. W. Lober	H6-60
5	**DOE Richland Operations Office**	
	J. P. Hanson	A5-13
	K. A. Kapsi	A5-13
	J. G. Morse	A6-38
	DOE Public Reading Room (2)	H2-53
11	**CH2M Hill Hanford Group, Inc.**	
	K. C. Burgard	L6-57
	M. P. Connelly	E6-35
	E. A. Fredenburg	H9-03
	T. E. Jones	E6-35
	A. J. Knepp	H6-60
	F. M. Mann (5)	E6-35
	G. Parsons	L6-75

No. of Copies		
2	**Environmental Protection Agency**	
	N. Ceto	B5-01
	M. L. Goldstein	B5-01
2	**Fluor Federal Services**	
	R. Khaleel	E6-17
	R. J. Puigh	E6-17
3	**Fluor Hanford, Inc.**	
	B. H. Ford	E6-35
	G. A. Jewel	A0-21
	M. I. Wood	H8-44
2	**Washington State Department of Ecology**	
	J. A. Caggiano	B5-18
	A. D. Huckaby	B5-18
48	**Pacific Northwest National Laboratory**	
	D. H. Bacon	K9-33
	C. F. Brown	P7-22
	W. J. Deutsch	K6-81
	M. J. Fayer	K9-33
	A. R. Felmy	K8-96
	M. D. Freshley	K9-33

No. of Copies		
	G. W. Gee	K9-33
	D. G. Horton	K6-81
	J. P. Icenhour	K6-81
	C. T. Kincaid	E6-35
	K. M. Krupka	K6-81
	C. W. Lindenmeier (2)	P7-22
	W. J. Martin	K6-81
	S. V. Mattigod	K6-81
	D. E. McCready	K8-93
	B. P. McGrail	K6-81
	P. D. Meyer (3)	BPO
	C. J. Murray	K6-81
	A. T. Owen (2)	K6-81
	K. E. Parker (2)	P7-22
	E. M. Pierce	K6-81
	S. P. Reidel	K6-81
	K. P. Saripalli	K6-81
	R. J. Serne (10)	P7-22
	H. T. Schaef (3)	K6-81
	W. Um	P7-22
	A. L. Ward	K9-33
	S. B. Yabusaki	K9-36
	J. S. Young	K8-93
	J. M. Zachara	K8-96
	Hanford Technical Library (2)	P8-55